STUDIES ON NEW LUMINESCENT POLYMERS FOR LUMINESCENT SOLAR CONCENTRATOR

By

KEE SHIN YIING

A master thesis submitted to the Department of Electrical and Electronic Engineering, Faculty of Engineering and Science,
Universiti Tunku Abdul Rahman,
in partial fulfillment of the requirements for the degree of
Master of Engineering Science
January 2014

ABSTRACT

STUDIES ON NEW LUMINESCENT POLYMERS FOR LUMINESCENT SOLAR CONCENTRATOR

Kee Shin Yiing

The Luminescent Solar Concentrator (LSC) is made up of a polymer plate (host matrix) that contains luminescent dye with solar cells attached to its edges. The luminescent dye absorbs sunlight and re-emits light at random direction. Part of the emitted light is trapped within the plate and transported by internal total reflection to the small-area solar cells at the edges.

In this study, two types of luminescent dyes - commercially available and laboratory synthesized dyes are used. The commercially available dyes are Polyfluorene-Vinylene (PFV) and Polyfluorene-Vinylene Copolymer (PFV Copolymer) while laboratory synthesized dye is polymerizable naphthalimide dye – 4-butylamino-N-allyl-1.8-naphthalimide. Rhodamine 6G dye is used as a reference luminescent material because of its high luminescent quantum efficiency. It is also used to copolymerize with polymerizable naphthalimide dye to form multiple-dye PMMA LSC. The results show that the LSC with PFV copolymer dye and the multiple dye of polymerizable naphthalimide dye

to Rhodamine 6G dye ratio of 2:1 have higher emission irradiance and longer lifetime than Rhodamine 6G dye.

Besides, LSC is constructed using 3 different polymer host matrices - poly(methyl methacrylate) (PMMA), epoxy and unsaturated polyester (UP). The results show that epoxy can become a good host matrix for LSC. Large amount of micro-voids that scatter the incident light can be formed in the epoxy LSC. So, its emission irradiance is higher than the LSC made by other host matrices even though the same dye is used. Moreover, epoxy LSC also has the highest short circuit current density and power conversion efficiency. The photo-stability of epoxy LSC with micro-voids scattering is also higher than that of PMMA and unsaturated polyester LSC.

In summary, various LSCs are constructed to conduct experiments that evaluate the performance of different dyes and host matrices. In addition, analysis and discussion of results are carried out with some recommendations of high performance LSC. Lastly, proposal of future work are also suggested.

PUBLICATIONS

Based on the work of this thesis, a few papers have been published or submitted as shown in table below:

No	Category	Title	Publisher	status
1	Book chapter	Chapter Title: Recent Research and Development of luminescent solar concentrator (Book title: Solar Cell Nanotechnology)	Wiley & Sons, pp. 271-292, 2013.	Published
2	Journal	Design and Evaluation of Passive Concentrator and Reflector Systems for Bifacial Solar Panel on a Highly Cloudy Region	Renewable Energy, Vol. 63, pp.415-425, Mar. 2014	Published
3	Journal	Use of Polyfluorene-Vinylene Dyes and Microvoids in Luminescent Solar Concentrators for the Improvement of Emission and Photostability	Science Direct: Renewable Energy	Submitted

ACKNOWLEDGEMENTS

I would like to thank my supervisor Ir. Dr. Lim Yun Seng and my co-supervisor Prof. Dr. Ewe Hong Tat for their direction, assistance, and guidance. In particular, Ir. Dr. Lim Yun Seng's numerous recommendations and suggestions have been invaluable for the project.

I also wish to thank Mr. Lo Chin Kim, who has taught me knowledge on all the measurement setup. Special thanks must also go to Mr. Saravanan a/l Sivasangaran, Mr. Lee Meng Keong, Mr. Ho Chan Cheong and all the lab officers for their assistance in the laboratory.

Last but not least, I offer my deepest regards and blessings to all of those who supported me in any respect during the completion of the project.

APPROVAL SHEET

This dissertation/thesis entitled "**STUDIES ON NEW LUMINESCENT POLYMERS FOR LUMINESCENT SOLAR CONCENTRATOR**" was prepared by KEE SHIN YIING and submitted as partial fulfillment of the requirements for the degree of Master of Engineering Science at Universiti Tunku Abdul Rahman.

Approved by:

_____

(Ir. Dr. LIM YUN SENG) Date:……..
Professor/Supervisor
Department of Electrical and Electronic Engineering
Faculty of Engineering and Science
Universiti Tunku Abdul Rahman

_____

(Prof. Dr. EWE HONG TAT) Date:……..
Professor/Co-supervisor
Department of Internet Engineering and Computer Science
Faculty of Engineering and Science
Universiti Tunku Abdul Rahman

FACULTY OF ENGINEERING AND SCIENCE

UNIVERSITI TUNKU ABDUL RAHMAN

Date: _____

SUBMISSION OF THESIS

It is hereby certified that **KEE SHIN YIING** (ID No: **12UEM01374**) has completed this thesis entitled "STUDIES ON NEW LUMINESCENT POLYMERS FOR LUMINESCENT SOLAR CONCENTRATOR" under the supervision of Ir. Dr. LIM YUN SENG (Supervisor) from the Department of Electrical and Electronic Engineering, Faculty of Engineering and Science, and Prof. Dr. EWE HONG TAT (Co-Supervisor) from the Department of Internet Engineering and Computer Science, Faculty of Engineering and Science.

I understand that University will upload softcopy of my thesis in pdf format into UTAR Institutional Repository, which may be made accessible to UTAR community and public.

Yours truly,

_____

(KEE SHIN YIING)

DECLARATION

I Kee Shin Yiing hereby declare that the dissertation/thesis is based on my original work except for quotations and citations which have been duly acknowledged. I also declare that it has not been previously or concurrently submitted for any other degree at UTAR or other institutions.

_____

(KEE SHIN YIING)

Date_____

TABLE OF CONTENTS

LIST OF TABLES

LIST OF FIGURES

LIST OF SYMBOLS / ABBREVIATIONS

λ	Wavelength of the incident radiation
α	Absorption coefficient (cm^{-1})
A_{cell}	Total surface area of solar cells attached to the LSC sides (m^2)
A_{top}	Top surface area of LSC (m^2)
A-SI	Amorphous silicon solar cell
AIBN	Azobisisobutyronitrile
Al_2O_3	Aluminium oxide
ATR-FTIR	Attenuated total reflectance - Fourier transform infrared spectroscopy
C=C	Carbon double bond carbon
CF_{Jsc}	Short circuit current concentration factor
C-H bond	Carbon-hydrogen bond

=C-H str.	Double bond carbon single bond hydrogen
C-O bond	Carbon-oxygen bond
C=O str.	Carbon double bond oxygen stretching (carbonyl)
CdS	Cadmium sulfide
CdSe	Cadmium selenide
CdTe	Cadmium telluride solar cell
CIGS	Copper indium gallium selenide solar cell
CSE_N	Cumulative solar energy on day N (Jm^{-2})
D_a	Dark spectrum counts
πD_p	Circumference of a scatterers
DMSO	Dimethylsulfoxide
E_r	Normalized irradiance spectrum
ESI-MS	Electrospray ionization- Mass spectrometry
$[Eu(phen)_2]CI_3$	Europium phenanthroline complex

FF	Fill factor of solar cell
G_{geom}	Geometric Gain
GaAs	Gallium arsenide solar cell
HALS	Hindered Amine Light Stabilizers
$I_{em}(\lambda)$	Emission spectral irradiance of LSC ($Wm^{-2}nm^{-1}$)
I_{sc}	Short circuit current of solar cell (A)
$I_{solar(n)}$	Solar irradiance on day n (Wm^{-2})
lnP	Indium phosphide solar cell
IR	Infrared
I-V response	Current-voltage response
J_{sc}	Short circuit current density
$J_{sc(ref)}$	Reference short circuit current density (Am^{-2})
LC	Liquid chromatography
LC/MS	Liquid chromatography mass spectrometry

LR	Lumogen F Red
LSC	Luminescent solar concentrator
MMA	Methyl methacrylate
Mono-Si	Mono-crystalline silicon solar cell
MS	Mass spectrometry
Multi-Si	Multi-crystalline silicon solar cell
NH str.	Amine stretching
OLSC	Organic luminescent solar concentrator
P_{in}	Light power input to solar cell (W)
P_{lamp}	Light source irradiance (Wm^{-2})
P_{out}	Electrical power output of solar cell (W)
PCE	Power conversion efficiency (%)
PFV	Polyfluorene-Vinylene
PFV copolymer	Polyfluorene-Vinylene Copolymer

PMMA	Poly(methyl methacrylate)
PPV	Poly(p-phenylenevinylene)
PVA	Polyvinylacetate
PVC	Polyvinyl chloride
QDs	Quantum dots
Q-TOF	Quadrupole time of fight
R_a	Reference spectrum counts
Red F	Red polyfluorene
Rh6G	Rhodamine 6G
S_a	Incident light that pass through the LSC (counts)
S_e	Emission spectrum (counts)
SiO_2	Silicon oxide
SR(λ)	Spectral response of solar cell ($AW^{-1}nm^{-1}$)
T	Optical transmission

$t_{1(n)}$	The time when the sunlight exposure begins on day n (s)
$t_{2(n)}$	The time when the sunlight exposure ends on day n (s)
UP	Unsaturated polyester
UV	Ultraviolet
UV-vis	Ultraviolet-visible
V_{oc}	Open circuit voltage of solar cell (V)
ZnS	Zinc Sulfide

CHAPTER 1

INTRODUCTION

A Luminescent Solar Concentrator (LSC) is a transparent plate that contains a luminescent specimen with mirrors and solar cells attached to its edges as shown in Figure 1.1. Luminescent dye absorbs any incoming sunlight and then re-emits at random directions (Lim et al. 2012). Since the refractive index of the transparent polymer plate is much higher than that of the external medium, a large proportion of the emitted light is trapped within the plate and transported by the total internal reflection to the edges, where it is absorbed by small-area solar cells (Samini et al. 2009; Teh et al. 2009). Lastly, the solar cells will convert the trapped luminescent emission into electricity.

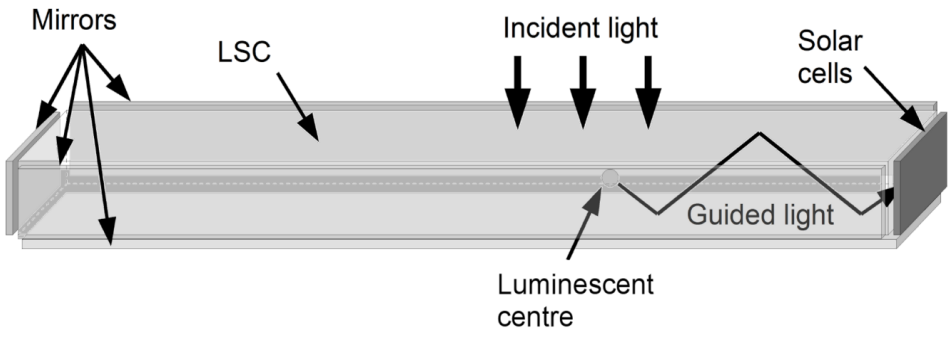

Figure 1.1 Construction of LSC

The advantage of LSC is that it can concentrate the direct and diffuse sunlight into a small area of solar cells without using any tracking and cooling

systems because its large surface area allows solar heat to be dispersed across the surface. Therefore, it can reduce the cost and improve the efficiency of the building integrated photovoltaic system.

Several types of luminescent materials have been used in LSC, such as laser dyes or organic dyes, semiconductor quantum dots (Barnham et al. 2000), rare earth materials (Werts et al. 1997), and semiconducting polymers (Sholin et al. 2007). Organic dyes are commonly used in LSC because they have high quantum efficiency, re-emitting about 90% of the energy fed into LSC. Examples of the dyes used in the early development of luminescent solar concentrators are Rhodamine 6G and Coumarin 6 (Meredith 1983).

However, many studies have already been carried out on organic dyes and prove that organic dye has relatively large self-absorption of the dye's emission and short lifetime. Therefore, polymerizable dyes such as polymerizable naphthalimide dyes can be an alternative dye in LSC. Polymerizable dyes contain unsaturated bonds which could be used in the copolymerization process with polymer. In these copolymers, the chromogenic of dyes are included along the polymer chain so they have excellent fastness properties against heat, washing, rubbing and light (Panah et al. 2010).

Besides, discovery of new luminescent materials is necessary to keep the innovation development of LSC. Commercial available Polyfluorene-Vinylene (PFV) and its copolymer dye are the potential new dyes that are

worth to be studied because they have manufacturer-reported peak emission wavelengths of 507 nm and 522 nm respectively. Their peak emission wavelengths are in the range of high silicon solar cell external quantum efficiency – 500 nm-900 nm (Green et al. 2012).

The compatibility of dyes in host matrix also affects the dye's emission and lifetime. In general, the Poly(methyl methacrylate) (PMMA) (Sark et al. 2008; Soti et al. 1996; Earp et al. 2004; Currie et al. 2008; Slooff et al. 2008; Rowan et al. 2007) and glasses (Kinderman et al. 2007; Bomm et al. 2011; Bomm et al. 2010; Kastelijn et al. 2009; Drake et al. 1982) are the standard host matrices for LSC. In this study, PMMA as well as two more alternative host matrices, namely unsaturated polyester and epoxy, are used to be the host of LSC.

The objectives of my research are:

1. To study the efficiency of new luminescent dyes in LSC,
2. To study and evaluate the performance of different commercially available polymer host matrices for LSC,
3. To analyze and verify the photo-stability of LSC with different concentration of dyes in different host matrices.

The layout of this thesis is presented in the following.

In chapter 2, a brief review of LSC and its materials are introduced.

In chapter 3, chemicals and the mold fabrication process are described. The procedures on the dye synthesis and construction of LSC sample are presented in details. The experiment set up and instruments used for the measurement of the LSC samples are also presented.

In chapter 4, the results of PMMA luminescent solar concentrators with different dyes – PFV, PFV copolymer, Rh6G and synthesis polymerizable dye- in different concentrations are presented and discussed. The characteristics of the synthesized polymerizable dyes are determined by using attenuated total reflectance - fourier transform infrared spectroscopy (ATR-FTIR) and mass spectrometry (MS). The absorptions and emissions of all LSCs are measured. Besides, their emission irradiances are determined to identify which dyes produce the maximum emission irradiance.

In chapter 5, the studies on the LSCs containing PFV and PFV copolymer are described. The absorption coefficients and emissions of LSCs with different matrix are studied in that chapter. Micro-voids scattering in epoxy LSC and the effect of micro-voids concentration to scattering intensity are described as well.

In chapter 6, the performance of LSC integrated with various solar cells is evaluated. The short circuit current densities, power conversion efficiencies and the photo-degradation rates of PMMA LSC, unsaturated polyester LSC and epoxy LSC were presented in details.

The last chapter contains the conclusion of this thesis as well as some recommendations for future work.

CHAPTER 2

LITERATURE REVIEW

A Luminescent Solar Concentrator (LSC) basically consists of a transparent plate that contains luminescent dyes with solar cells attached to its edges. The transparent plate is usually a glass (Kinderman et al. 2007; Bomm et al. 2011; Bomm et al. 2010; Kastelijn et al. 2009; Drake et al. 1982) or PMMA plate (Sark et al. 2008; Soti et al. 1996; Earp et al. 2004; Currie et al. 2008; Slooff et al. 2008; Rowan et al. 2007). Luminescent dye absorbs any incoming sunlight and then re-emits at random direction (Lim et al. 2012). A large proportion of the emitted light will be trapped within the plate and transported by total internal reflection to the edges, where it is absorbed by small-area solar cells (Samini et al. 2009; Teh et al. 2009).

In this chapter, the LSCs and commonly used luminescent dyes are reviewed. The novel organic dye such as polymerizable naphthalimide dye, Polyfluorene-Vinylene (PFV) and PFV copolymer dye that have not been used in LSC before, are also studied to identify the potential of these luminescent dyes for LSC. Besides, recent development of unsaturated polyester and epoxy as the host matrices in LSC has also been reviewed in this chapter.

2.1 Luminescent Solar Concentrator (LSC)

In 1973, Lerner constructed the first solar concentrator system based on a solution of laser dye between two glass plates, but finally his ideas were rejected (Hermann 1982). Three years later in 1976, Weber and Lambe published the first paper on the topic of a luminescent solar concentrator (Weber & Lambe 1976). The paper describes a planar solar concentrator that was constructed using a luminescent medium (rare earth doped glasses and organic dyes) to absorb radiation and collect the light via the total internal reflection. The results show that the medium strongly absorbs a portion of light from the solar spectrum and then emits it at longer wavelengths.

In 1977, Zewail and Terry Cole published a paper in the Journal of Optics Letters describing a new type of energy cascade concentrator that was used to reduce the cost of silicon in solar electricity system and to alleviate the tracking problem (Meredith 1983). Basically, the flat sheet of PMMA was doped with several dyes. They are spectrally matched so that radiation emitted by one kind of dye can be almost completely absorbed by another, producing a cascade in which short-wavelength solar radiation is transformed to longer, more usable wavelengths for solar cells.

After that, this topic gained popularity very quickly with much research efforts being carried out to study luminescent concentrator for solar application, until its further development was hindered by poor performance of luminescent materials (Hermann 1982).

In recent years, there has been a renewed interest in LSC due to the new development in luminescent materials, matrix materials, new theoretical insights and a strong drive to make solar energy cheaper by using the solar spectrum more efficiently. Materials such as photonic layers (Rau et al. 2005) and liquid crystal (Debije et al. 2007) have also been used to reduce the losses in the LSC and further improve the its efficiency.

Therefore, there are 4 main criteria that should be met by the LSC materials to overcome the challenges faced in LSC development, (Rowan et al. 2008):

4. Absorption of all wavelengths < 950 nm with high absorption coefficients and an emission peak near wavelength of 1000 nm.
5. Minimum re-absorption losses due to overlap of absorption and emission spectra.
6. Near-unity fluorescence quantum yield.
7. Long-term stability under the exposure of sunlight.

2.2 Common Luminescent Dyes Used in LSC

The common luminescent dyes used in LSC are laser dyes or organic dyes, semiconductor quantum dots, rare earth materials and semiconducting polymers. Their dye properties and application were described in details in this section.

2.2.1 Organic Dyes

The organic dyes used in the early development of luminescent solar concentrators are Rhodamine 6G and Coumarin 6 because they are widely available and have well characterized properties (Meredith 1983). For example, luminescent quantum yield of Rhodamine 6G is 98% and it is ideally suited to be used in LSC. In recent year, a few more commercial available important organic dyes were introduced to be used in LSC. They are listed in Table 2.1 with their corresponding absorption, emission peak wavelengths and luminescent yield (Sark et al. 2008) .

The advantages of using organic dyes are their availability in a wide range of colours and also their extremely high luminescence (Sark et al. 2008). Besides, organic dyes also can be easily dissolved in a wide range of organic polymers, such as poly(methyl methacryate) (PMMA), which are then casted into sheet form (Wilson 2010).

Table 2.1 Overview of the organic dyes with the corresponding absorption, emission peak wavelengths and luminescent yields

Commercial dye name	Chemical structure	Absorption λmax (nm)	Emission λmax (nm)	Luminescence quantum yield (%)
Makrolex fluorescent red G	Coumarin	520	600	87
Lumogen F Blue 650	Naphthalimide	377	411	>80
Lumogen F Violet 570	Naphthalimide	378	413	94
Lumogen F Yellow 083	Perylene	476	490	91
Lumogen F Yellow 170	Perylene	505	528	>90
Lumogen F Orange 240	Perylene	524	539	99
S13	Perylene	526	534	100
Lumogen F Red 305	Perylene	578	613	98

However, organic dyes have relatively large self-absorption of the dyes emission because they have an overlap of absorption and emission spectra. The re-absorption increases the probability that a photon is lost by non-radiative decay of the dye molecule. Besides, organic dye typically has an absorption bandwidth of only 100 nm (Wilson 2010) . The lifetime of organic dye is also short because the organic dye in LSC degrades rapidly after exposing to sunlight for several weeks (Drake et al. 1982).

Several research efforts were carried out to maximize the LSC performance. Sah et al. added 5-10% of dimethylsulfoxide (DMSO) to the PMMA host matrix because the DMSO could stabilize the excited state, lowering its energy and cause the emission spectrum to have a red-shift of 50-100 nm (Sah et al. 1980). Overall, it reduces the spectral overlap and the degree of re-absorption.

Another research team, Richard & McIntosh constructed a multiple-dye PMMA LSC using Lumogen series of organic dyes manufactured by BASF (Ludwigshafen, Germanay). Multiple dyes with different absorption range were incorporated into the same sheet to increase the overall absorption. Besides, the photons in multiple dye system were absorbed and re-emitted by successively longer wavelength dye, creating a cascade effect where any absorbed photon passing through the chain of dyes and was emitted by the longest-wavelength dye where its emission was more usable by solar cell (Richards & McIntosh 2006). The maximum efficiency at 4.4% has been reported for this multiple dye LSC.

The most recent development of organic dye is the synthesis of a new organic dye, perylene, with a high Stoke's shift of 300 meV (Sanguineti et al. 2013). The LSC doped with the new organic dye has fluorescent quantum efficiency of 70% with high chemical and photochemical stability. The quantum yield in the LSC is very high due to the completely separated absorption and emission peaks.

The effort to maximize the performance of LSC is not limited only on the improvement of organic dye properties, but also on scatterer effect in LSC. Filatov et al. investigated the luminescent spectra and excitation spectra of Rh6G in polyvinylacetate (PVA) matrix with embedded fine-dispersed particles of silicon oxide (SiO_2) and aluminium oxide (Al_2O_3). The presence of scatterers, such as SiO_2 and Al_2O_3, in LSCs increased the amount of incoming light trapped in LSC and hence reduced the escape cone losses. Depending on the sizes of the scatterers, the incoming light with different wavelengths was scattered to different directions and then the scattered light propagated to the edges of LSCs through the total internal reflection, as described in the paper (Filatov et al. 2003). Besides, Debijie et al. also studied the scatterer effect in LSC. They added white scattering layers to the bottom side of the luminescent solar concentrator which was made up of a polycarbonate sheet waveguide containing 35 ppm of Lumogen red 305. It was found that a rear scatterer separated from the waveguide by an air gap resulted in 37%-50% increase of energy output from the waveguides (Debije et al. 2009).

The photo-stability of organic dye is also a key factor that determines the performance of LSC. A study showed that the dyes can last for only a few weeks under solar illumination (Drake et al. 1982). But after a few years, Seybold and Wagenblast reported that the BASF-developed Lumogen F range of dyes had high quantum yields and better photo-stability, and they appeared to last for many years (Seybold & Wagenblast 1989).

Some studies show that the degradation rate of organic dyes in polymer matrix is influenced by the minor compounds, which are present in the LSCs such as remaining unpolymerized monomer, stabilizer, initiator and other additives (Sark et al. 2008). Recently, another study was carried out to study on the photo-degradation mechanism of a perylene-based thin-film organic luminescent solar concentrator (OLSC). By exposing the OLSC to the sunlight in the presence of oxygen, substantial changes to the molecular structure of the organic dye were noticed. Such changes were identified by means of photoluminescence, UV–vis and FTIR spectroscopy. The potential degradation mechanism in the dye molecule could therefore be proposed. These findings provided an important insight to the photo-degradation mechanism of perylene-based OLSC devices. As a result, various establishing ideas to prolong the lifespan of OLSC could be developed. The use of radical scavenging molecules was one of the options for maintaining the photo-stability of the dyes. Hindered Amine Light Stabilizers (HALS) could be used to scavenge radicals generated during the sunlight exposure. In addition, protective films with refractive index similar to that of the polymer matrix could be used to minimize the molecular damages (Griffini et al. 2013).

2.2.2 Quantum Dots

Nano crystals of inorganic compound, or more commonly known as quantum dots, have been doped in PMMA to produce luminescent solar concentrators. The advantages of using quantum dots over organic dyes are their ability to sustain its emission longer than organic dyes when they were

exposed to ultra violet light. Besides, the specific emission wavelengths in the solar spectrum can be tuned from 850 nm to 1900 nm by choosing the appropriate size of the quantum dots (Du et al. 2002; Mićić et al. 1997).

However, the optical efficiency and the concentration factor of the quantum dot solar concentrators are restricted by the low luminescent quantum efficiency of the quantum dots and the large re-absorption loss. Their luminescent quantum efficiency is about 80%, lower than 100% for organic dyes (Peng et al. 1997). Moreover, the preparation of good quality acrylic plates containing the quantum dots by polymerization is more complicated than those using organic dyes because the quantum dots are passivated by hydrophobic ligands, which causes the quantum dots to form turbid dispersions in the hydrophilic monomer such as MMA. The luminescence of hydrophobic quantum dots in hydrophilic media is quenched as a consequence of the formation of agglomerates which reduces the quantum yield (Sark et al. 2008).

In year 2008, Reda embedded a luminescent quantum dot – cadmium sulfide (CdS) in thin film by sol-gel spin coating on silica matrix to study and control the optical properties of the quantum dot solar concentrator. The CdS crystallite structure in the silica matrix was hexagonal and that the size of the CdS crystallites was 3.5-6.5 nm. Their sizes increased with rising annealing temperature. A red-shift in the absorption and emission spectra was observed in the nanocrystalline CdS-doped silica by increasing the annealing temperature from 373 K to 673 K in order to increase the particle size. The photo-stability of CdS-based solar concentrators was examined after 4 weeks of exposure to

sunlight. The results showed that the absorption loss increased after the sunlight exposure and that the quantum dots were sensitive to oxygen and sunlight. Besides, it was also showed that the sample annealed at lower temperature increased the emission at the edges of luminescent solar concentrator (Reda 2008).

Another research team, Kennedy et al. studied on the optical efficiency and concentration factor of a single-plate quantum dot solar concentrator using near infra-red (NIR) emitting quantum dots in year 2009. The results showed that the re-absorption losses could account for 58% and 57% of incident photons being absorbed in LSC if it contained commercially available green and orange visible-emitting quantum dots, respectively. However, if the near infra-red emitting quantum dot was used in the LSC, the re-absorption loss could be reduced to 43% of incident photons. Its optical efficiency was higher than those of the green and orange quantum dot solar concentrator (Kennedy et al. 2009).

Besides, the development of multiple dyes quantum dot LSC has also been reported. Hyldahl et al. constructed the luminescent solar concentrators made of the combined quantum dots, namely CdSe cores and ZnS shells in year 2009. The emission intensity and photo-stability of the combined quantum dot solar concentrators were assessed and compared with that of the luminescent solar concentrator containing the organic dye, Lumogen F Red 300 (LR). The measured fluorescence quantum yields of the combined quantum dots were lower than that of LR. However, the photo-degradation rate

of the quantum dot LSC was approximately 5 times slower than the LR LSC under the same sunlight exposure. The photo-degradation of the quantum dot LSC's absorption completely recovered during a prolonged dark cycle (Hyldahl et al. 2009).

Another new development is the multishell quantum dot LSC. Bomm et al. synthesized and characterized the CdSe core and multishell quantum dots which were embedded in a polymer matrix, namely poly(lauryl methacrylate-co-ethylene glycol dimethacrylate) in year 2011. The inorganic shells of the quantum dots consist of 2 monolayers of CdS, 3 monolayers of $Cd_{0.5}Zn_{0.5}S$ and 2 layers of ZnS. The multiple layers of shells were able to avoid agglomeration of the nanocrystals. The results showed that the inorganic fluorophores were stable under intense illumination over long periods of time. The LSC had a final quantum yield of 45% and an overall power conversion efficiency of 2.8% (Bomm et al. 2011).

Recently, another research team, Chandra et al. enhanced the fluorescence of CdSe/ZnS core-shell quantum dots (QDs) in LSC by adding gold nanoparticles (Au NPs). In the optimal concentration of Au NPs, a maximum quantum efficiency of 53% is achieved for the particular QD/Au NP composite (Chandra et al. 2012).

2.2.3 Rare Earth

Rare-earth (lanthanide) ion such as Yb^{3+} and Nd^{3+} were used in the early development of LSC because of their high quantum yield and excellent photo-stability (Friedman 1981; Reisfeld & Kalisky 1981). Rare earth complex was then synthesized to increase the absorption coefficient and reduce the amount of rare-earth ion required. Besides, some researchers also complexed the ion with several different ligands that have different absorption ranges to extend its absorption range (Wilson 2010).

Rare earth elements such as Europium (III) complex, Ytterbium (III), Neodymium (III) and Erbium (III) chelates have been used as luminescence materials in PMMA luminescent solar concentrator. Rare earth complexes are attractive because of their large Stoke's shifts, narrow emission bandwidths and excellent photo-stability (Jiu et al. 2006).

Jeżowska-Trzebiatowska et al studied the luminescent solar concentrators using neodymium and chromium doubly doped on the specially made lithium aluminium phosphate glass (Jeżowska-Trzebiatowska et al. 1986). The dependence of the light concentration coefficient versus dopant concentration and attenuation of the guided light in the LSC were studied. The best results showed that a 0.25 m^2 triangular plate LSC receives 8-fold concentrated power at the edge, equivalent to 30 W. The light concentration efficiency was estimated to be 3% for the 1 m^2 rectangular solar concentrator containing chromium and neodymiun.

In year 2000, Machida et al prepared a uniform and transparent solar concentrators by having quartz plates dip coated by organically modified-silicates (ormosil) solutions together with europium phenanthroline complex, $[Eu(phen)_2]CI_3$. The ormosil solutions were derived from tetraethoxysilane and diethoxydiphenylsilane. The characteristics of the luminescent solar concentrators coupled with crystalline solar cells were studied. The results showed that the solar cell power outputs were increased by 10-15% as compared with the values of uncoated LSC. This is because the ormosil solution mixed with $[Eu(phen)_2]CI_3$ converts ultraviolent radiation to the high red emission to be utilized by the solar cells for power generation (Machida et al. 2000). Recently, Wu et al. also constructed a solar concentrator with minimum self-absorption loss and maximum geometric gain by doping a rare earth complex, $Eu(TTA)_3Phen$, into a polymer optical fiber (Wu et al. 2010).

2.2.4 Semiconducting Polymer

Semiconducting polymers are originally developed for the light emitting diode industry. They often have very high quantum yields and long lifetime. When polymers are excited, they undergo a change in structural conformation, which increase the Stoke's shift and may thus reduce re-absorption losses (Peeters et al. 2011). Furthermore, the width of their absorption and emission bands can be tuned by controlling the chain lengths.

Sholin et al. studied the efficiency of LSCs consisting of semiconducting polymers in liquid encased in glass and compared with that of

organic dyes and quantum dots. The results suggested that commercially available quantum dots may not be the viable LSC dyes because of their large absorption/emission band overlaps and relatively low quantum yields. Materials such as red polyfluorene (Red F) demonstrated that semiconducting polymers with high quantum yield and small absorption/emission band overlap are good candidates for LSCs (Sholin et al. 2007).

2.3 Progress in Organic Luminescent Dye

There are number of luminescent dyes that have not been used in LSC. Polymerizable naphthalimide dye, PFV and PFV copolymer are some of these dyes. Their properties and initial application are described in detail in the following sections.

2.3.1 Polymerizable Naphthalimide Dye

The polymerizable naphthalimide dyes are commonly used in light emitting diodes (Bouché et al. 1996; Morgado et al. 1998; Zhu et al. 1998), liquid crystals for utilization in electro-optical device (Wolarz et al. 1992; Grabchev et al. 2000) and ion probes (Cosnard & Wintgens 1998). However, they have never been used in LSC before.

Synthesis of some polymerizable naphthalimide dyes such as 4-methylamino or ethylamino-N-allyl-1,8-naphthalimide had been reported

(Konstantinova et al. 1993; Bojinov & Konstantinova 2002). The presence of various alkylamino groups on 4-substitued can affect the fluorescent characteristics. Besides, it was also reported that the derivatives of 4-amino-1,8-naphthalimide contain an unsaturated group, which could be used in copolymerization with vinyl monomer. This has a good resistance to wet treatment and solvent (Konstantinova et al. 1993).

Moreover, researchers also found that the polymerizable naphthalimide can be copolymerized with rhodamine dye. Tian et al. reported that the naphthalimide moieties can act as a good energy pumping antenna and an internal photostabilizer for rhodamine molecule. The results showed that the lasing efficiency, thermal stability and photo-stability of these copolymers increase greatly (Tian et al. 2000).

In year 2001, two novel highly fluorescent polymerizable naphthalimide dye, 4-alkylamino-N-allyl-1,8-naphthalimide dye were synthesized and their basic photo-physical properties have been determined. They are 4-butylamino-N-allyl-1,8-naphthalimide and 4-hexylamino-N-allyl-1,8-naphthalimide. These two dyes exhibit intense yellow-green color when they are copolymer with styrene polymer chain. The peak absorption wavelengths for these two dyes are 415-416 nm and the peak emission wavelengths are 498-500 nm. Besides, the results also showed that 90-92% of the dyes were chemically bonded to form styrene polymer chain (Grabchev et al. 2001). This implies that the dyes are suitable for production of colored fluorescent copolymers.

Another research team, Panah et al. synthesized and characterized 2 fluorescent polymerizable naphthalimide dyes: 4-propylamino-N-allyl-1,8-naphthalimide and 4-butylamino-N-allyl-1,8-naphthalimide. After that, they copolymerized these two types of dyes with poly(methyl methacrylate) (PMMA) by bulk process. The results showed that the emission of these two copolymers occurred in the wavelength of 511-512 nm. The luminescent quantum efficiency for 4-propylamino-N-allyl-1,8-naphthalimide and 4-butylamino-N-allyl-1,8-naphthalimide are 70% and 89%, respectively. Besides, the dyes were involved in the polymerization process: they were about 97%-99% covalently bonded along the polymer chain, giving fluorescent copolymeric side-groups (Panah et al. 2010). In these copolymers, the chromogenic of dyes are included along the polymer chain so they have excellent fastness properties against heat, washing, rubbing and light.

2.3.2 PFV Homo-polymer and PFV Copolymer

Polyfluorene-Vinylene (PFV) is a derivative class of light emitting poly (p-phenylenevinylene), also known as PPV. PPV and its derivates are classified as conjugated polymers with high photoluminescence efficiency, excellent charge transport ability, and film forming property (Burroughes et al. 1990; Zheng et al. 1999; Wu et al. 2004).

These conjugated polymers could emit different color lights from blue to red regions by modifying the chemical structure in the main chain or on the side chain. Therefore, they are commonly used as light emitting diode and

polymer light emitting diode materials (Burroughes et al. 1990; Gustafsson et al. 1992). However, there is currently no publication reporting their application in LSC.

In year 2003, Hwang et al. synthesized poly(9,9-di-n-octylfluorenyl-2,7-vinylene) (PFV), and its copolymer, poly[(9,9-di-n-octylfluorenyl-2,7-vinylene)-co-(1,4-phenylenevinylene)]s to improve electroluminescence device performance. They found that the polymer electroluminescent devices constructed from the PFV copolymer, poly(FV-co-PV)s showed 10 times higher efficiency than the devices constructed from the PFV homopolymer. Both the PFV and its copolymer showed their peak absorption and band edge at around 419 nm and 490 nm respectively. The peak emission wavelength of PFV and its copolymer are approximately 465 nm (Hwang et al. 2003).

Another research team, Jin et al. synthesized and characterized novel PPV derivatives, which are poly(9,9-di-n-octylfluorenyl-2,7-vinylene) poly(FV) and its copolymer, poly(9,9-di-n-octylfluorenyl-2,7-vinylene)-co-{2-methoxy-5-(2-ethylhehexyloxy)-1,4-phenylenevinylene}] poly(FV-co-MEHPV) with various feed ratios of MEH-PPV. Both poly(FV) and its copolymers have high molecular weight, high thermal stability and applicability for LEDs. The resulting electroluminescent polymers showed high thermal stability up to 415°C. The peak electroluminescent emission wavelengths of poly(FV) and poly(FV-co-MEHPV) were at 507 and 585 nm respectively, which correspond to greenish-blue and orange-red. Overall, poly(FV-co-MEHPV) improved the device performance of LED. The

luminescent efficiency of poly(FV-co-MEHPV) was much higher than that of pure MEH-PPV and poly(FV) (Jin et al. 2003).

Since PFV and its copolymer were already commonly used in light emitting diode and the results showed that these conjugated polymer have high photo-luminescent, they have potential to be used as novel luminescent materials in LSC. Furthermore, the commercially available PFV and its co-polymer from Sigma Aldrich have manufacturer-reported peak emission wavelengths of 507 nm and 522 nm respectively. Their peak emission wavelengths are in the range of high silicon solar cell external quantum efficiency – 500 nm to 900 nm (Green et al. 2012). .

2.4 Polymer Matrix

The polymer matrix is the host material of LSC which serves as a medium for doping the luminescent materials. The material of polymer matrix will influence the optical properties and performance of LSC.

In this research study, the standard host matrix, PMMA and two other alternative host matrices: unsaturated polyester and epoxy are used to construct the media of LSC. The characteristics of these 3 polymer matrices are discussed in the following.

2.4.1 Poly(Methyl Methacrylate) (PMMA)

Poly(methyl methacrylate) is the most common host material for LSC, also known as PMMA, Plexiglass, Lucite or simply “acrylic”. This material was used by many researchers in the early development of LSC (Weber & Lambe 1976; Goetzberger 1978; Goetzberger & Schirmer 1979; Batchelder 1982; Drake et al. 1982; Goetzberger & Greube 1977). In recent years, there are many more researchers who used PMMA as the host matrix for LSC construction (Sark et al. 2008; Soti et al. 1996; Earp et al. 2004; Currie et al. 2008; Slooff et al. 2008; Rowan et al. 2007).

The main advantages of PMMA are its low cost, high refractive index and high optical clarity (Bakr et al. 1999; Mansour et al. 2005; Kinderman et al. 2007). Besides, the dyes can be dissolved easily in the monomer of PMMA prior to polymerization. The photo-stability of PMMA is high and the lifetime can be up to 17 years (Rainhart & Schimmel Jr. 1975; Hermann 1982).

However, there are a few disadvantages of using PMMA. The photo-stability of luminescent dye in PMMA deteriorates very rapidly because the required additives react negatively with luminescent dye or by the presence of monomer residue due to incomplete polymerization (Kinderman et al. 2007).

Another disadvantage of using PMMA is that it has peak absorption wavelength above 700nm even though it has good optical transparency in the

visible region of the spectrum. This phenomena is caused by harmonic and overtones of the C-H and C-O bond vibrations in the molecule (Ballato et al. 2004). The host absorption loss therefore become significant if the emission wavelength of luminescent dye is above 700 nm.

2.4.2 Unsaturated Polyester (UP)

Unsaturated polyester (UP) is a class of polymer containing reoccurring -C(=O)-O- group in the main chain. They are generally prepared from saturated or unsaturated dibasic acids, which are condensed with dihydric alcohols. Mostly, styrene is used to cross link polyester background with a vinyl monomer to form a three dimensional structure (Haq 2007). The catalyst to initiate the cross-linking reaction is generally organic peroxide such as methyl ethyl ketone peroxide.

The main advantages of unsaturated polyester are its low production costs and simple fabrication technique (Andjelkovic et al. 2009). Besides, the curing process of unsaturated polyester is fast and easy to control. This is because unsaturated polyester can cured under room temperature via free radical polymerization mechanism.

Since unsaturated polyester has so many advantages, it becomes one of the most important thermoset materials used in composites industry for the preparation of moulding compounds, laminate, coating, and adhesives

(Andjelkovic et al. 2009). Since it was invented, unsaturated polyester have made significant structural and performance advances (Fink 2005), resulted in its broader application in automotive, building construction, and marine industries.

In year 2012, unsaturated polyester was introduced to be the host matrix for LSC for the first time. Lim et al. blended unsaturated polyester with MMA to enhance the optical properties of LSC by modifying the chemical structure during polymerization. They reported that the photo-degradation of organic dye during curing process can be minimized because it was cured under room temperature instead of ultraviolet curing. The UP has double bonds in its structure that form a three dimensional structure during polymerization process, hence making its mechanical strength to be high and thus the LSC is suitable to be installed on roofs, windows or walls. Besides, the results also showed that mixing unsaturated polyester with 5% MMA concentration can optimize the cross-linkage of the polymers. The emission from the edge of LSC dropped about 0.4% after 500 hour heat treatment (Lim et al. 2012). These results again proved that unsaturated polyester LSC possess the ability to maintain its absorbance and transmittance of light over a period of heat treatment.

2.4.3 Epoxy

Epoxy, also known as polyepoxide is a class of reactive polymer containing epoxy groups capable of becoming a thermoset form. Epoxy is

cheap and has excellent optical clarity, high refractive index and high transparency with peak absorption range at UV region, i.e. low absorbance in the range of dye emission and solar cell absorption (Daram et al. 2011). These properties make the epoxy to be a potential host matrix for LSC.

The epoxy covers a broad range of application such as adhesives, bonding, construction materials (flooring and paving), composites, laminates, coating, moulding, and textile finishing. Recently, it has been developed to be used in aero and spacecraft industry (Bhatnagar 1993).

In year 2007, Gallagher et al. constructed a quantum dot solar concentrator using different host materials such as Alumilite, Biothan, Plexit 55, Crystal clear 200, Water clear 781, Water clear 782 and epoxy resin. The results showed that the plexit 55 and epoxy have the highest overall emission intensities. The epoxy retained 77.5% of integrated emission compared to the reference sample. Furthermore, it exhibited around 30% lower absorption in the visible region than plexit 55 (Gallagher et al. 2007).

Another research team, Daram et al improved the performance of solar cell using epoxy plate doped with Rhodamine 6G dye. They prepared the LSC plates in different thickness and concentration of Rhodamine 6G dye. The optical properties of dye-doped and undoped epoxy and its applicability in solar cell were studied. The results showed that LSC plate with 4.5 mm

thickness at $5x10^{-5}$ mol/L dye concentration gave the highest conversion power efficiency of solar cell (Daram et al. 2011).

2.5 Summary

In this chapter, the LSC development has been reviewed. The 4 main categories of commonly used luminescent dyes in LSC were discussed: organic dyes, quantum dots, rare earth materials and semiconducting polymer. Besides, the progress of novel organic luminescent materials that haven't been used in LSC - polymerizable dye, PFV and PFV copolymer - has also been reviewed. Their properties and application in other fields were presented in details. Furthermore, polymer matrix materials were reviewed in this chapter as well because host matrices also play an important role in the performance of LSC. The standard host matrix, PMMA and other 2 more alternative, unsaturated polyester and epoxy were discussed in term of their advantages and applications.

CHAPTER 3

MATERIALS AND METHODOLOGY

This chapter details the main experimental materials and techniques used in this study, including commercially available luminescent dyes, polymerizable dye, host materials, construction of LSC, and measurement setup.

3.1 Luminescent Dyes

Organic luminescent dyes are used in this study. They are divided into two main categories, which are commercially available luminescent dye and polymerizable dye. Commercially available luminescent dyes was purchased directly from the chemical company while the polymerizable dye was synthesized by using the methods described in the publication (Panah et al. 2010) because this dye is not commercially available in the market yet.

3.1.1 Commercially Available Luminescent Dye

Three commercially available luminescent dyes are used to construct LSC as listed in Table 3.1 with their labels and company names. Their chemical structures are shown in Figure 3.1.

Table 3.1 Commercially available luminescent dyes used in LSC

No	Dye	Label	Company
1	Rhodamine 6G (dye content ~95%,)	Rh6G	Sigma Aldrich
2	Poly(9,9-di-(2-ethylhexyl)-9H-fluorene-2,7-vinylene)	PFV	Sigma Aldrich
3	Poly((9,9-di-(2-ethylhexyl)-9H-fluorene-2,7-vinylene)-co-(1-methoxy-4-(2-ethylhexyloxy)-2,5-(phenylenevinylene)) -- 90:10 mole ratio	PFV Co-Polymer	Sigma Aldrich

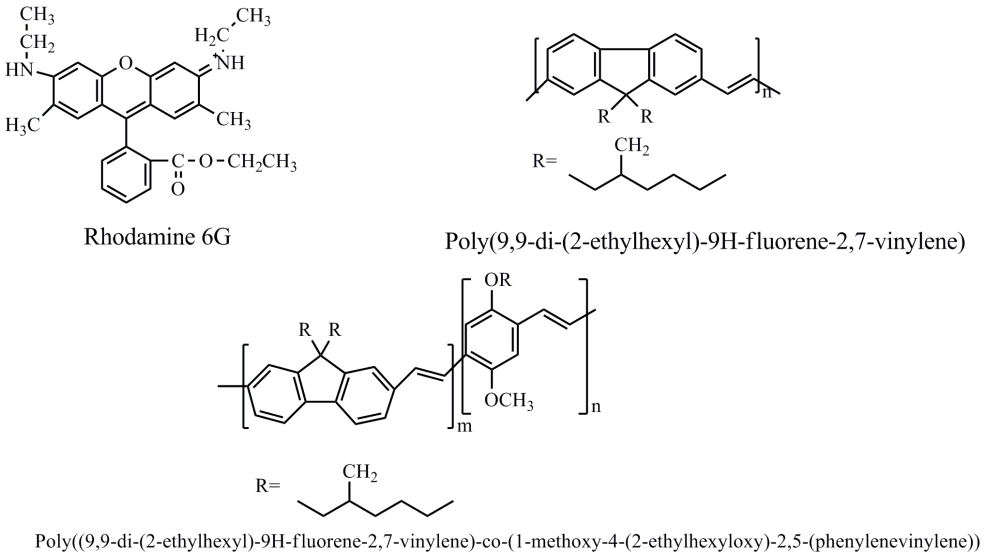

Figure 3.1 Chemical structures of three commercially available dyes

3.1.2 Synthesis of Polymerizable Dye (4-butylamino-N-allyl-1,8-naphthalimide)

The polymerizable dye, namely 4-butylamino-N-allyl-1,8-naphthalimide was synthesized in the laboratory by using the published methods. The polymerizable dye was then characterized using Attenuated Total

Reflectance Fourier Transform Infrared Spectroscopy (ATR-FTIR) and Mass Spectrometry (MS).

3.1.2.1 Materials and Methodology for the Synthesis of Polymerizable Dye

There are four stages to synthesize polymerizable dye, namely 4-butylamino-N-allyl-1,8-naphthalimide. The products obtained in one stage is used in the next stage. The final product is obtained in the last stage.

The first stage is the synthesis of 5-bromoacenaphthene. A solution of N-bromosuccinimide (18 g) in dimethylformamide (50 mL) was added to a suspension of acenaphthene (15.4 g) in dimethylformamide (50 mL) at room temperature. The solution was then mixed for 2 hours. After that, the solution was poured into 1.5 L of cold water and filtered to obtain crude product. The crude product was recrystallized from ethanol to give 5-bromoacenaphthene.

The second stage is the oxidation of product from the first stage. The product 5-bromoacenaphthene (2 g) was mixed with potassium dichromate (7.6g) in glacial acetic acid (200mL). The reaction mixture was heated under reflux for 2.5 hours. After that, the solvent was evaporated, and then the chromium salt was dissolved using boiling water and removed from the residue. The white crude product was recrystallized from glacial acetic acid to give 4-bromo-1,8-naphthalic anhydride white needle precipitate.

In the third stage, the product from the second stage, namely 4-Bromo-1,8-naphthalic anhydride (2.8 g), was dispersed in ethanol (50 mL), and allylamine (0.8 mL) was added at 55°C. The solution was heated under reflux for 3-4 hours and then cooled to room temperature. Finally, the product in this stage - 4-Bromo-N-allyl-1,8-naphthalimide was separated from the mixture by filtration, then washed with water and dried at 30 °C.

In the final stage, the product from the third stage, namely 4-Bromo-*N*-allyl-1,8-naphthalimide (2 g), was mixed with butylamine (6.2 mL) and dissolved in dimethulsulphoxide (17 mL). The solution was stirred at 80 °C overnight. The resulting solution was then poured into ice (50 g). The final product is 4-butylamino-N-allyl-1,8-naphthalimide yellow powder precipitate.

3.1.2.2 Characterization of Polymerizable Dye

The polymerizable dye - 4-butylamino-N-allyl-1,8-naphthalimide dye was characterized by Attenuated Total Reflectance Fourier Transform Infrared Spectroscopy (ATR-FTIR) and Mass Spectrometry (MS).

3.1.2.2.1 ATR-FTIR

The ATR-FTIR instrument used in this study is Thermo Scientific Nicolet iS10 as shown in Figure 3.2. Attenuated Total Reflectance (ATR) is a useful sampling accessory that virtually eliminates the need of sample

preparation. Therefore, it can make the sampling faster and improve sample-to-sample reproducibility.

The function of Fourier Transform Infrared Spectroscopy (FTIR) is to determine the structural information of a molecule. Absorption of the same type of bond is often found in certain small portions of the vibrational infrared region. Therefore, a small range of absorption wave number can be defined for a particular type of bond. Outside this range, the absorption is usually due to some other type of bond. Besides, the resemblance of two substances can be determined by comparing their infrared spectrum. If both their spectra have the same absorption peaks, then in most cases the two substances will be identical (Pavia et al. 2000).

Figure 3.2 Thermo Scientific Nicolet iS10 ATR-FTIR

3.1.2.2.2 MS

The MS instrument used in this study is Agilent Technologies 6520 Accurate-Mass quadrupole time-of-flight (Q-TOF) liquid chromatography/mass spectrometry (LC/MS) as shown in Figure 3.3. The sample in this study was directly injected to the MS without passing through the liquid chromatography (LC) for separation.

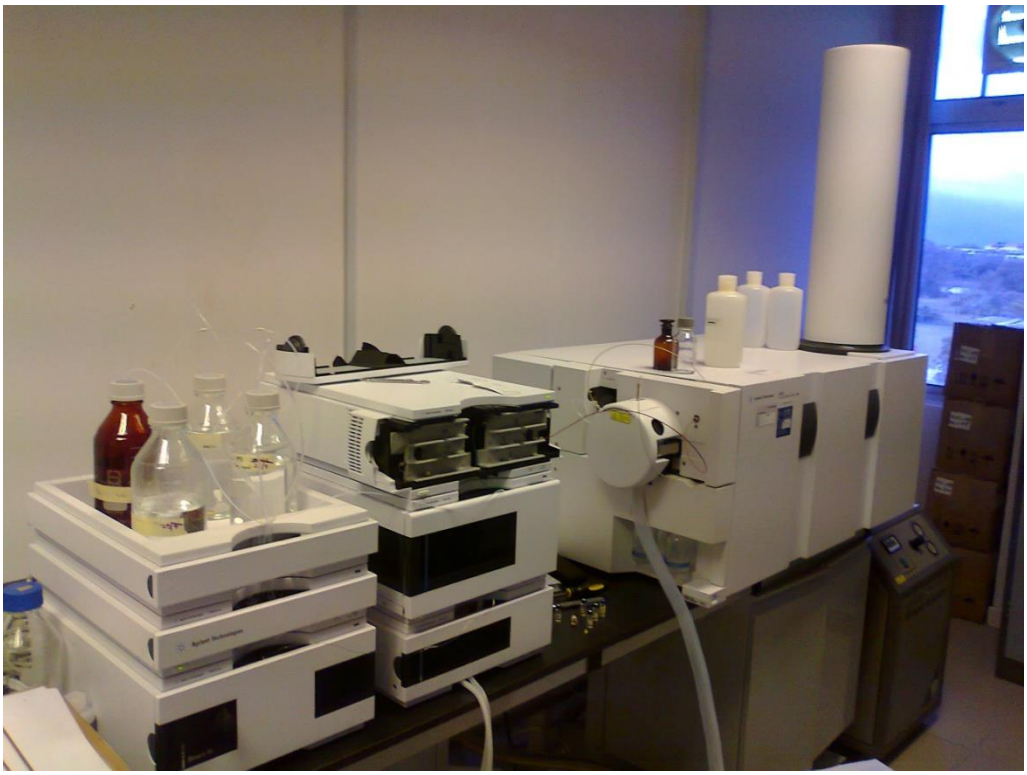

Figure 3.3 Agilent Technologies 6520 Accurate Mass Q-TOF LC/MS

The MS instrument is electrospray ionization mass spectrometry (ESI-MS). This technique produce ions from macromolecule by the addition of a hydrogen cation and denoted $[M+H]^+$. The resulting ions, called molecular ions, are then accelerated, sent through magnetic field, and detected. Without

any fragmentation, *m/e* ratio that corresponds to the molecular ion can be used to determine the molecular weight of the sample molecule (Pavia et al. 2000).

Furthermore, modern MS instrument is generally equipped with a computer that can be used to collect, process and display the mass spectral data. The computer can compare the mass spectral data it has obtained with the spectra in library database. The output of such a library search is a list of possible compounds having molecular weight of the sample and their molecular formulas.

3.2 Host Materials

Three types of commercially available polymer were used as host materials in this study. They are poly(methyl methacrylate), unsaturated polyester and epoxy. Their monomer/resin, initiator/hardener and co-polymer are listed in Table 3.2.

Table 3.2 Monomer, initiator and co-polymer for the 3 types of polymer host materials

No	Polymer host material	Monomer/resin	Initiator/hardener	Co-polymer
1	Poly(methyl methacrylate)	Pre-polymerised poly(methyl methacrylate) syrup (Asia Poly)	Azobisisobutyronitrile or AIBN	-
2	Unsaturated polyester	Reversol P-9133 unsaturated polyester resin (Synthomer)	Butanox M-50 (Akzo Nobel)	Methyl methacrylate (Sigma Aldrich)
3	Epoxy	D.E.R. 331 epoxy resin (Dow Chemical)	Jointmine 905-3S (Yun Teh)	-

3.3 Construction of LSC

The materials and methodology for LSC construction are discussed in this section. The mould design and the fabrication methodology are the main key factors that determine the quality of LSC.

3.3.1 Mould Design

Two types of moulds are designed for different matrices of LSC. The PMMA glass mould is for PMMA cell casting method because it can produce a LSC with better optical clarity (Ashby & Johnson 2010). This design follows the mould design for cell casting method in the industry, which is sealed

properly during the polymerization process in a water bath. Another mould design is for unsaturated polyester and epoxy LSC. The purpose of the design is to cast unsaturated polyester and epoxy LSC in cuvette size that can fit into the cuvette holder in the measurement setup.

3.3.1.1 PMMA Glass Mould

The materials used to construct PMMA LSC mould are two pieces of heat-resistance polished glass plate, one silicon gasket and four clamps. The mould was prepared by separating the two pieces of glass plate with silicon gasket around the edges. The glass plates were then held together by the spring loaded clamps so that the plates could be compressed together as the reacting mixture shrank during the polymerization process (Sadek et al. 2011). The glass mould design is illustrated in Figure 3.4.

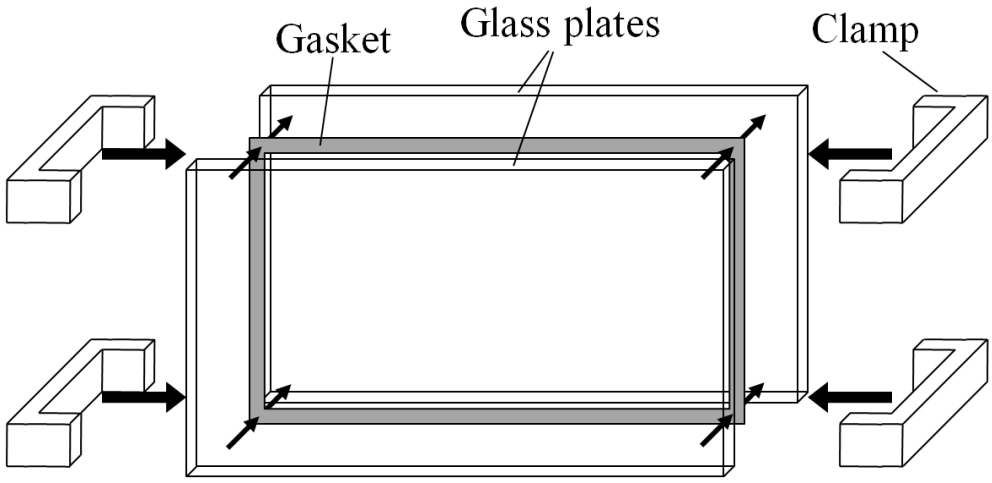

Figure 3.4 Illustration of assembled glass mould for casting PMMA LSC

3.3.1.2 Unsaturated Polyester and Epoxy Mould

The materials used to construct unsaturated polyester and epoxy LSC are two pieces of steel plate, four pieces of PVC block, one PVC sheet, two clamps and super glue. These materials are readily available in the market.

The dimension of mould was first printed on the transparent PVC sheet and the mould was cut accurately according to the desired shape as shown in Figure 3.5. The PVC sheet was then folded and assembled using super glue. The mould was designed with an open top so that the mixture of polymer resin could be poured from the top. PVC blocks were put at two sides of the mould to maintain its shape. After that, the steel plates were put at another two sides of the mould and held by clamps as shown in Figure 3.6.

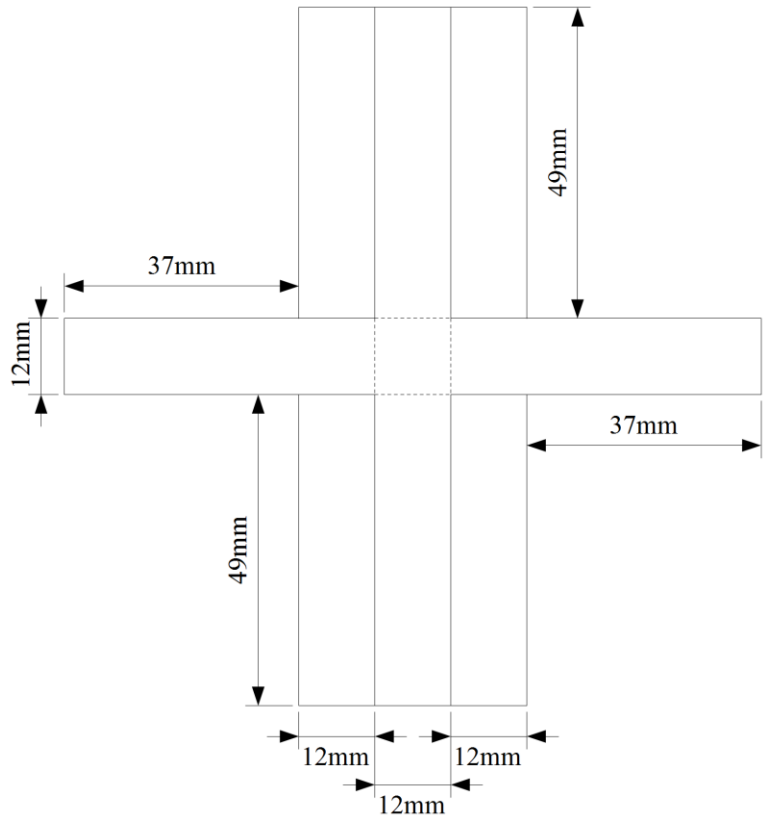

Figure 3.5 Dimension of mould in millimetre, mm. The dotted line indicates folding line and solid line indicates cutting line

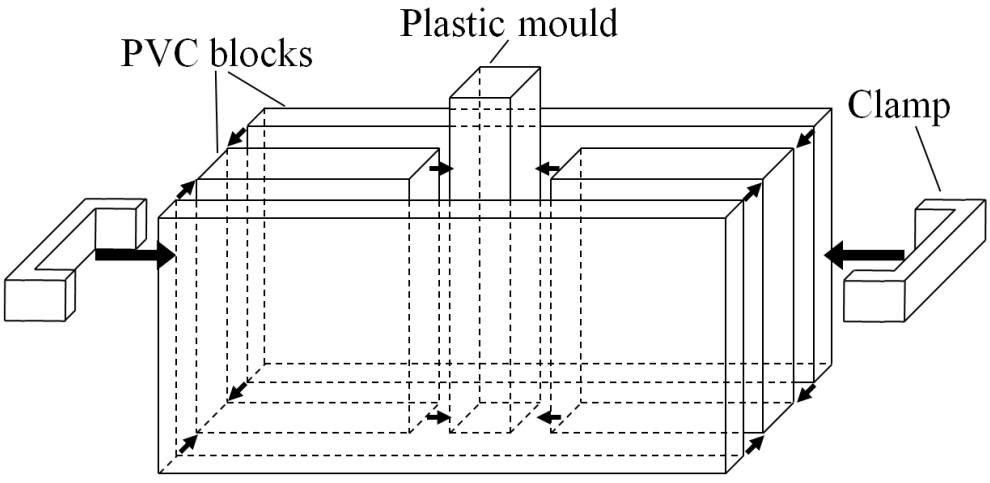

Figure 3.6 Assembled mould ready to cast UP and epoxy LSC

3.3.2 LSC Sample Fabrication

In this section, the materials and methodology for fabricating poly(methyl methacrylate), unsaturated polyester and epoxy LSC are discussed in details. A few parameters such as the amount of initiator, curing temperature and curing time are determined in order to produce a good quality LSC. All of the LSC pictures are shown in Appendix A.

Pre-polymerised poly(methyl methacrylate) syrup was used to cast a number of LSCs with Azobisisobutyronitrile or AIBN as the initiator. An appropriate amount of PMMA syrup, dye and approximately 0.05% of AIBN are added and weighed in a beaker. The mixture was stirred until the dye was dispersed evenly within the mixture. The mixture was then poured into a glass mould through a small opening at the gasket. The glass mould design was illustrated in Figure 3.4. After pouring in the syrup, the opening was closed and sealed by silicone sealant. The glass plates were held together by spring-loaded clamps so that the plates would close up as the reacting mixture shrank during the polymerization process. The glass mould was then put vertically into water bath and cured at 55 °C for 10 hours. After the polymerization process, it was placed in an oven at 80 °C for 4 hours to relieve the internal stress of the LSC. This process is known as annealing. Finally, it was slowly cooled down to room temperature and the LSC was then taken out from glass mould. The methodology for PMMA LSC casting is summarized in Figure 3.7.

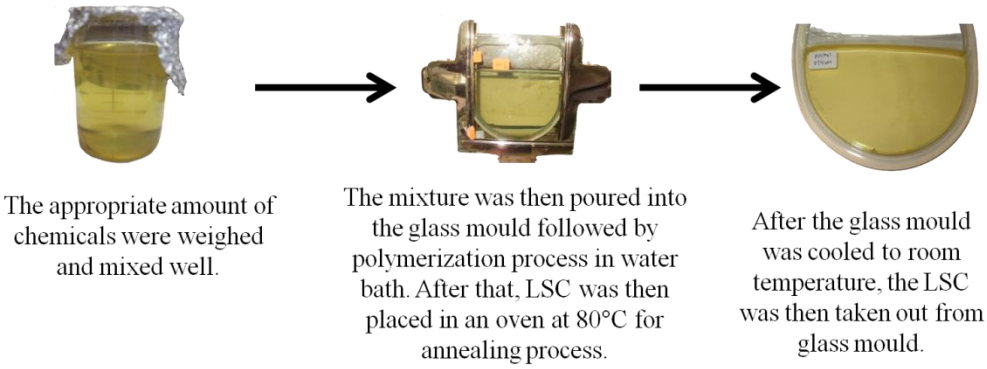

Figure 3.7 PMMA LSC casting

3.3.2.1 Unsaturated Polyester (UP) LSC

Reversol P-9133 unsaturated polyester resin was used to cast several LSCs with Butanox M-50 as the hardener and methyl methacrylate as the co-polymer. An appropriate amount of methyl methacrylate, unsaturated polyester resin and dye were weighed in a container. The mixture was stirred until the dye was dispersed evenly within the mixture. Next, the hardener methyl ethyl ketone peroxide (Butanox M-50) was added into the mixture before it was poured into a mould. The mould design is shown in Figure 3.6. The mixing weight ratio of unsaturated polyester and Butanox M-50 is 100:1. After that, the unsaturated polyester LSC was then left to cure at room temperature. The methodology for UP LSC casting is summarized in Figure 3.8.

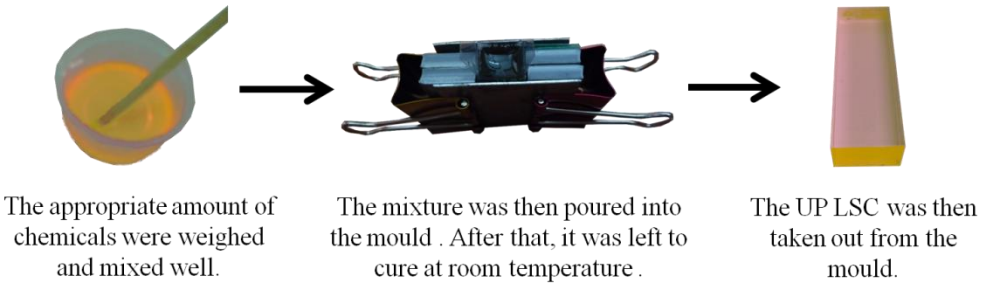

Figure 3.8 UP LSC casting

3.3.2.2 Epoxy LSC

D.E.R. 331 epoxy resin was used to cast several LSCs with Jointmine 905-3S as the hardener. An appropriate amount of D.E.R. 331 epoxy resin and dyes were weighed in a container. The mixture was stirred until dyes were dispersed evenly within the mixture. Then, the hardener, Jointmine 905-3S, was added into the mixture before it was poured into a mould shown in Figure 3.6. The epoxy LSCs were casted using the same moulds as that of UP LSCs. The mixing weight ratio of D.E.R. 331 Epoxy Resin and Jointmine 905-3S is 2:1. After this, the epoxy LSC was then left to cure at room temperature. The methodology for epoxy LSC casting can be summarized as Figure 3.9.

A large amount of micro-voids were formed in epoxy LSCs. This is because epoxy has high viscosity that makes it easier to trap micro-voids during casting process (Latorre et al. 2002). It is found that the amount of micro-voids trapped in the resin depends on the duration of stirring. We have also demonstrated that the formation of micro-voids is controllable by using a vacuum pump to withdraw the micro-voids during casting process. These two

are used to control the amount of micro-voids formed in the resin. Several epoxy LSCs with different amount of micro-voids were created and examined under Meiji Techno MT4300L-NDC3200 PRO biological microscope. The micro-void images were captured and their sizes were measured using VIS Plus imaging software.

The appropriate amount of chemicals were weighed and mixed well.

The mixture was then poured into the mould . After that, it was left to cure at room temperature .

The epoxy LSC was then taken out from the mould.A

Figure 3.9 Epoxy LSC casting

3.4 Measurement Setup

All the LSC were cut into the dimension of 7.5 mm×12 mm×35 mm to fit into a cuvette holder and polished for the measurement. The measurement setup and devices are described in detail in this section.

3.4.1 Absorption and Emission Setup

The measurement devices for absorption and emission measurements are Mikropack HL-2000-FHSA tungsten halogen light source and Ocean Optics USB4000 Spectrometer. The setups for absorption and emission measurements are as shown in Figure 3.10

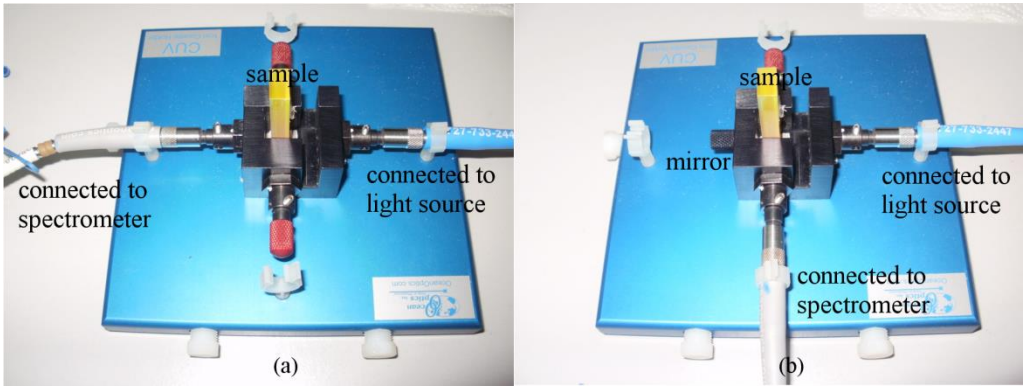

Figure 3.10 Experiment setup for (a) absorption and (b) emission measurement

Before starting the absorption measurement, dark spectrum and reference spectrum was stored. The dark spectrum, D_a (counts) was measured by blocking the incident light from entering the spectrometer; the reference spectrum, R_a (counts) was measured without any sample inside the cuvette holder. After that, the LSC was put into the cuvette holder. The amount of incident light that pass through the LSC, S_a (counts) was measured by the spectrometer. Optical transmission, T (%) was calculated as the percentage of incident light that transmit through the sample, $T = (S_a-D_a) / (R_a-D_a) \times 100\%$. Lastly, the absorption coefficient, α (cm^{-1}) was calculated from the optical transmission $\alpha = - \ln(T/100) / L$, where L (cm) is the sample thickness.

In emission measurement, the dark spectrum, D_e (counts) was stored in the same way as that in absorption measurement. The emission setup is different from the absorption setup. In emission setup, a small mirror was placed opposite to the illuminated sample surface to reflect the incident light back to the sample. The emission spectrum S_e (counts) was collected at the direction 90° to the incident light direction. The compensated emission

spectrum (S_e-D_e) was then calibrated using a calibration curve pre-determined by measuring a light source (S_r-D_r) with known normalized irradiance spectrum (E_r): calibrated emission spectrum = (S_e-D_e) / (S_r-D_r) × E_r. The measurement unit of emission spectrum is in spectral irradiance ($Wm^{-2}nm^{-1}$).

3.4.2 Setup for LSC Degradation

All the selected LSC samples were exposed to sunlight for 30 days. Eppley Precision Spectral Pyranometer was placed next to the LSC samples to measure the incoming solar irradiance (W/m^2) at one second intervals. The solar irradiance was recorded via National Instrument USB-6009. The setup for LSC degradation experiment is shown in Figure 3.11.

Figure 3.11 Setup for LSC degradation

After exposing the LSCs under the sunlight for one day, the samples were then collected back to measure their absorption and emission spectra in a dark room. The emission spectra were then used to calculate their emission irradiance.

The total amount of solar energy received by the LSC samples was calculated by integrating the solar irradiance over the period of sun exposure in each day. The photo-stability of the dyes can be studied by plotting the emission irradiances of the LSCs against the total amount of solar energy received by the LSC samples during the sunlight exposure.

3.4.3 Setup for Power Conversion Efficiency Measurement

LSCs were selected to calcuate their power conversion efficiency. The setup for the measurement is a diffuse reflector – white paper on top of a mirror - was put on the bottom of the LSC sample. The LSC was separated from the reflector by small pieces of paper at the 4 corners of LSC to create air gap between them. Solar simulator was used as the light source with AM1.5G spectrum. The emission irradiance was measured from the side of the LSC using Avantes spectrometer calibrated for irradiance measurement via fiber optics connected to a cosine corrector. The setup for power conversion efficiency measurement is shown in Figure 3.12.

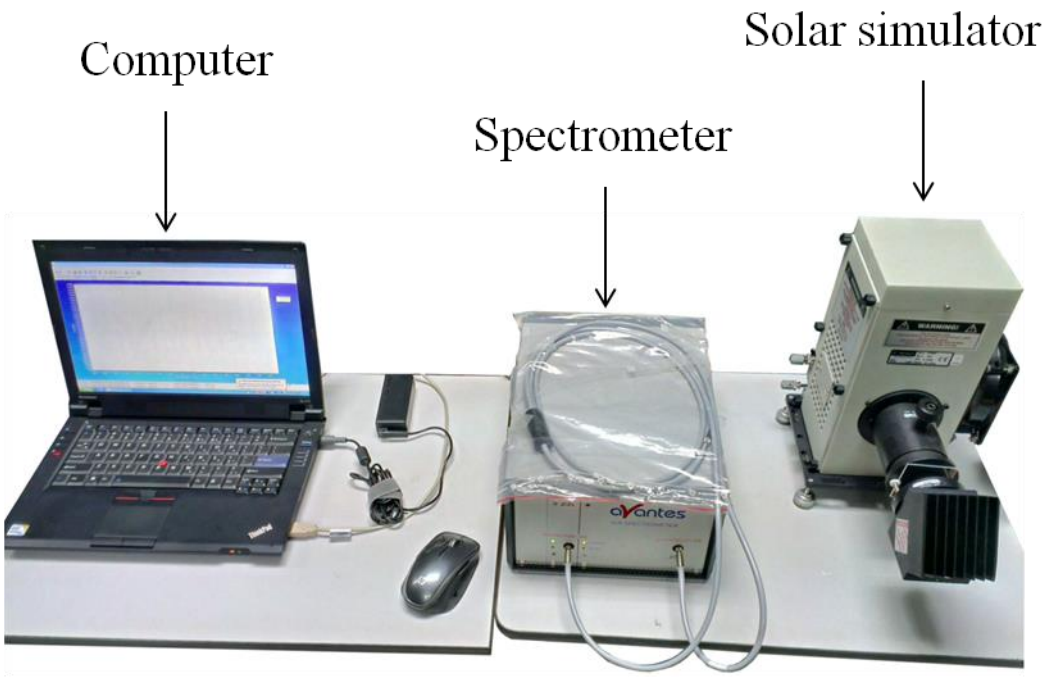

Figure 3.12 Setup for power conversion efficiency measurement

Power conversion efficiency was calculated as P_{out} / P_{in} = (I_{sc} V_{oc} FF) / (P_{lamp} A_{top}), where P_{lamp} is the light source irradiance (W/m^2), A_{top} is the top surface area of LSC (m), I_{sc} is the short circuit current (A), V_{oc} is the open circuit voltage (V) and FF is the fill-factor. The short circuit current (I_{sc}) was calculated by multiplying the short circuit current density (J_{sc}) to the area of the side to which the solar cell was mounted (A_{cell}). The power conversion efficiency was calculated by assuming that the I-V response of the device can be approximated by the substraction of the dark current from the short circuit current.

3.5 Summary

In this chapter, an introduction of the commercially available luminescent dyes and host materials are given. They were purchased from chemical companies and used as received. The methodology to synthesize polymerizable dye and construct LSC is also presented in details. The polymerizable naphthalimide dye was synthesis in the laboratory, using the published method. All LSCs were constructed in the laboratory. Besides, the mould designs and also the parameters of fabrication have been described. The measurement setup for absorption, emission, LSC degradation and power conversion efficiency measurement were also described.

CHAPTER 4

RESULT AND DISCUSSION FOR PMMA LUMINESCENT SOLAR CONCENTRATOR

This chapter begins with the introduction and characterisation of luminescent materials. The measurement results for absorption and emission of PMMA LSC with different dyes and concentrations are presented, followed by the optimum concentrations for every dye. The absorption and emission of PMMA LSC with different dyes in their optimum concentrations are compared with those of PMMA LSC with reference dye, Rhodamine 6G. The dye that has the highest emission irradiance and suitable to be used in LSC was identified from the results.

4.1 Luminescent Dyes

The luminescent dyes used to construct PMMA LSC are shown in Table 4.1. As mentioned earlier in chapter 3, all the dyes are commercially available except for the polymerizable naphthalimide dye - 4-butylamino-N-allyl-1,8-naphthalimide.

.

Table 4.1 PMMA LSC with different dyes

No	Dye	Label
1	Rhodamine 6G	Rh6G
2	Poly(9,9-di-(2-ethylhexyl)-9H-fluorene-2,7-vinylene)	PFV
3	Poly((9,9-di-(2-ethylhexyl)-9H-fluorene-2,7-vinylene)-co-(1-methoxy-4-(2-ethylhexyloxy)-2,5-(phenylenevinylene)) -- 90:10 mole ratio	PFV Co-Polymer
4	4-butylamino-N-allyl-1,8-naphthalimide	Naph
5	Mixture of Rhodamine 6G and 4-butylamino-N-allyl-1,8-naphthalimide	Rh6G + Naph

4.2 Characterisation of Luminescent Dye Synthesized in the Laboratory

The polymerizable naphthalimide dye (4-butylamino-N-allyl-1,8-naphthalimide) was produced in the laboratory and its structure was characterised using Attenuated Total Reflectance - Fourier Transform Infrared Spectroscopy (ATR-FTIR) and Mass Spectrometry (MS).

4.2.1 FTIR-ATR Spectrum of Polymerizable Naphthalimide dye

4-butylamino-N-allyl-1,8-naphthalimide powder was examined using ATR-FTIR to determine the functional group. The IR spectrum is shown in Appendix B. Characteristic peaks in certain wavenumbers represent certain functional group in the compound as shown in Table 4.2.

Table 4.2 Characteristic wavenumber for 4-butylamino-N-allyl-1,8-naphthalimide

Wavenumbers (cm^{-1})	Functional group
1567.78	C=C
1629.14, 1679.58	C=O str. Carbonyl
3077.34	=C-H str.
3374.08	NH str

The chemical structure of 4-butylamino-N-allyl-1,8-naphthalimide is shown in Figure 4.1. The absorption peak that occurs at the wavenumber of 1567.78 cm^{-1} represents the stretching of carbon double bond in alkene. The two peaks occurred at 1629.14 cm^{-1} and 1679.58 cm^{-1} are assigned to carbonyl stretching. Another absorption peak at 3077.34 cm^{-1} is assigned as sp^2 C-H stretching. Besides, a sharp absorption peak occurs at 3374.08 cm^{-1} represents N-H stretching.

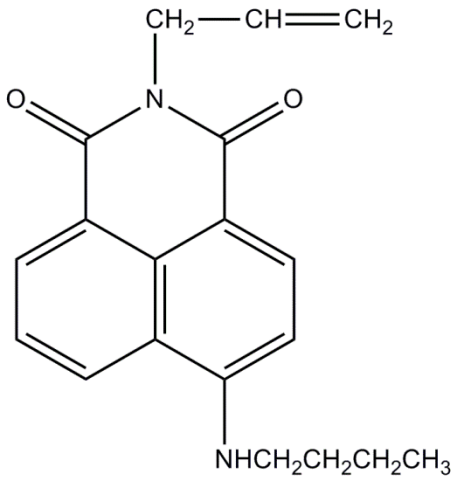

Figure 4.1 Chemical structure of 4-butylamino-N-allyl-1,8-naphthalimide

Beside those signification peaks listed in Table 4.2, aromatic ring also has carbon double bond stretching bands that usually appear between 1600 cm^{-1} and 1450 cm^{-1}. It also has a strong, sharp peak at 700 cm^{-1} – 800 cm^{-1}.

Comparing the IR spectrum with that from the journal (Panah et al. 2010), most of the measured absorption peaks coincide with the absorption peaks of the spectrum shown in the journal. The wavenumbers of absorption peaks differ from the published values by negligible values. Therefore, the IR spectrum proves that the synthesized powder is 4-butylamino-N-allyl-1,8-naphthalimide.

4.2.2 MS Spectrum of Polymerizable Naphthalimide Dye

The luminescent polymerizable naphthalimide dye - 4-butylamino-N-allyl-1,8-naphthalimide was examined using ESI-MS to determine its molecular weight. The ESI-MS spectrum is shown in Appendix C

The ESI-MS spectrum of 4-butylamino-N-allyl-1,8-naphthalimide shows $(M+H)^+$ at m/z 309.1592 with the molecular formula $C_{19}H_{20}N_2O_2$. After deducting the mass of a proton in the $(M+H)^+$ ion, the molecular mass of the compound was found to be 308.1519, which agree with the calculated molecular mass 308.3810. The compound was also found to be present in the spectrum at m/z 310.1636, which occurred most probably due to ionization with hydrogen isotope in the $(M+H)^+$ ion.

4.3 PMMA LSC with Polymerizable Naphthalimide Dye

LSCs presented in this section were constructed by doping the polymerizable naphthalimide dye - 4-butylamino-N-allyl-1,8-naphthalimide - in PMMA matrix as shown in Figure 4.2. They were casted in different concentrations to find out the optimum concentration that provided the highest emission irradiance. Their absorption and emission spectra are reported in the following subsections.

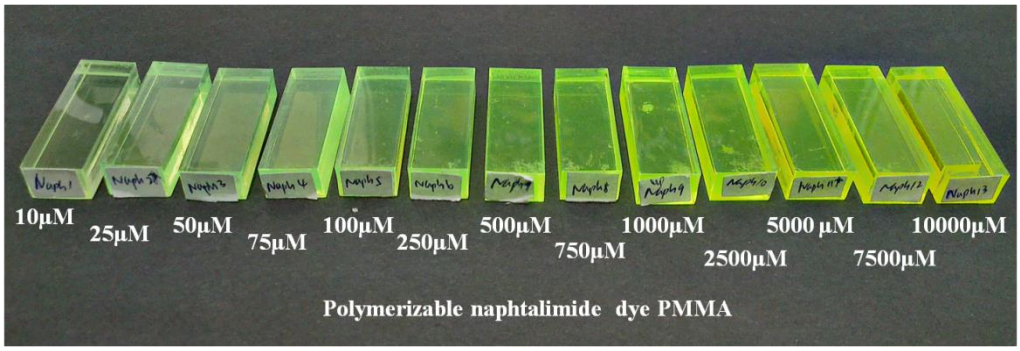

Figure 4.2 PMMA LSC with polymerizable naphthalimide dye

4.3.1 Absorption, Emission and Stoke's shift

The absorption and emission spectra of the LSCs that were measured in the laboratory using spectrometer are shown in Figure 4.3 and Figure 4.4 respectively. Only 4 dye concentrations are shown in the figures: 10 µM, 100 µM, 1000 µM, and 10000 µM, so that changes in the spectra shapes between LSCs with increasing dye concentrations can be clearly observed. Both the absorption and emission spectra of LSC with the same dye concentration are

put together in Figure 4.5 to compare their shapes. Absorption and emission wavelengths of all the LSCs together with their Stoke's shift are listed in Table 4.3.

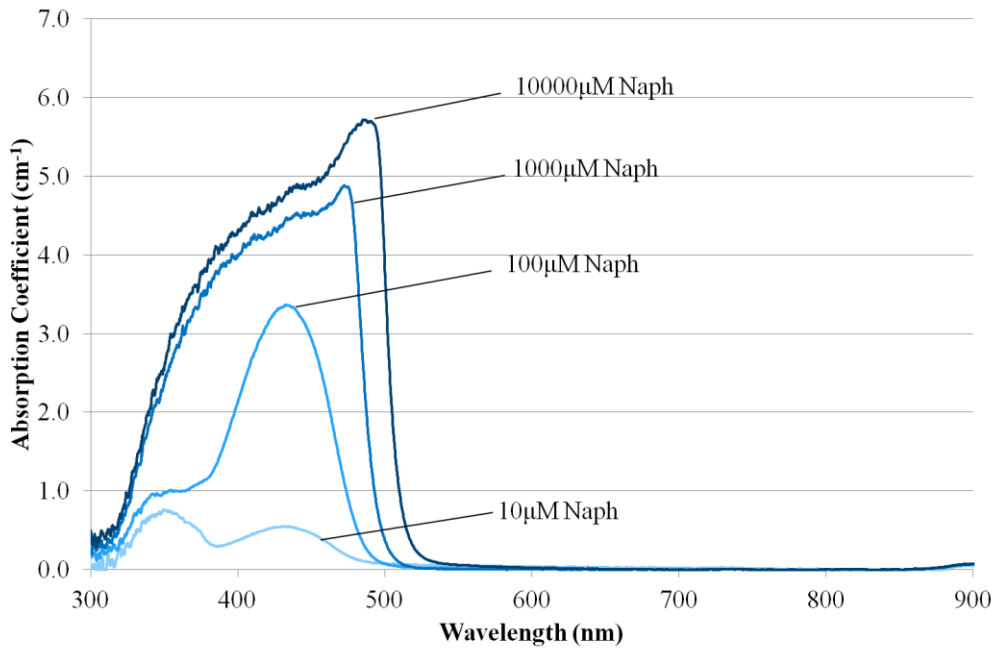

Figure 4.3 Absorption spectrum of PMMA LSC with 4-butylamino-N-allyl-1,8-naphthalimide dye in different concentrations

Figure 4.3 shows that the peak absorption coefficient increases with the dye concentration. The absorption peak wavelength at around 430 nm is observed for LSC with dye concentration in the order of 10 µM to 100 µM which is contributed from dye monomer, while broader absorption peak with longer absorption peak wavelength is found for that with higher dye concentration which is contributed by both the dye monomers and its aggregates.

The dye monomers form loosely bound dye polymers, or its aggregates and therefore this affects the shape of the absorption spectrum (Scheibe 1937). When the dye concentration is higher, more dye monomers will form aggregates, or in other words, the aggregates have higher concentration and therefore higher absorption. Contribution from the aggregates absorption becomes higher and higher, eventually their absorption becomes more significant than that from the dye monomers.

Similar to the observation for Rh6G dye in (Arbeloa et al. 2010), both J-aggregates and H-aggregates of dyes are formed in the LSC at higher concentration (1000 μM and 10000 μM). The J-aggregates have narrow absorption peak and a longer absorption peak wavelength, as compared to the monomer absorption peak. They have high luminescent quantum efficiency and small Stoke's shift. The H-aggregates, on the other hand, have a shorter absorption peak wavelength but low luminescence (Würthner et al. 2011). Therefore, the net effects are that the absorption spectrum becomes broader as the concentration increases as shown in Figure 4.3.

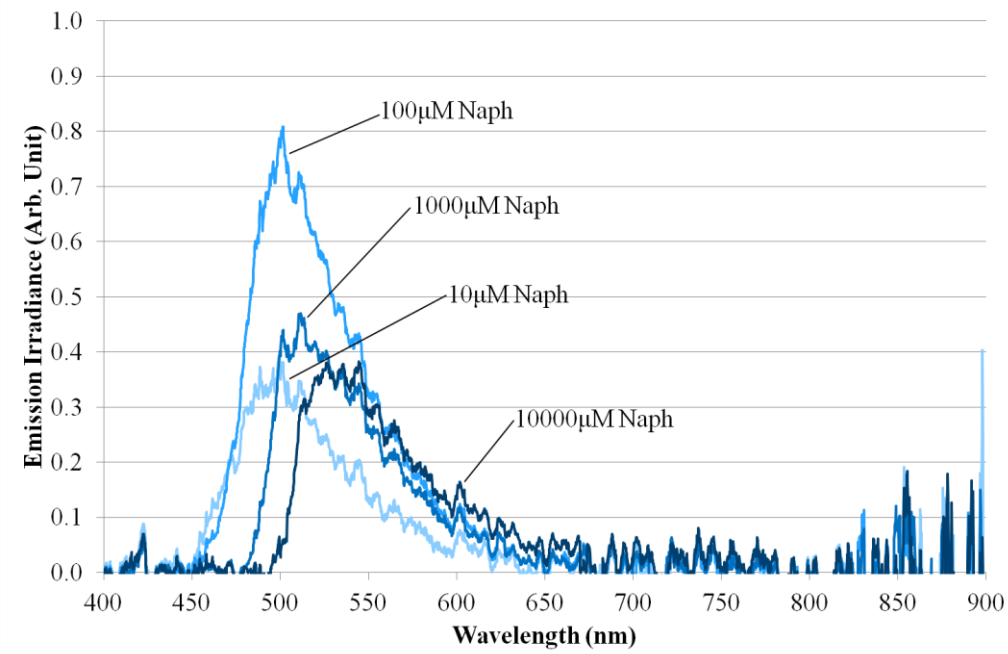

Figure 4.4 Emission spectrum of PMMA LSC with 4-butylamino-N-allyl-1,8-naphthalimide dye in different concentrations

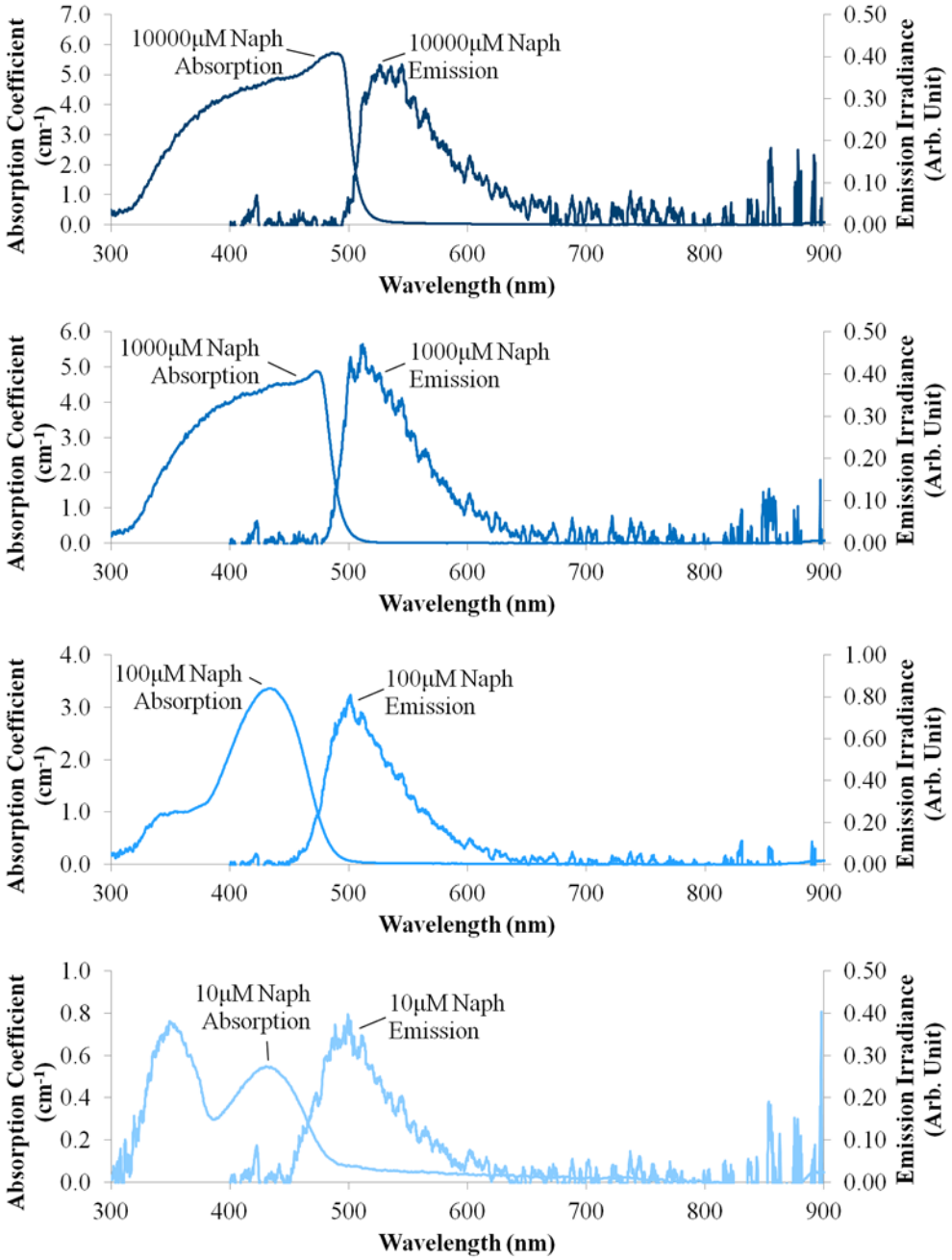

Figure 4.5 Absorption and emission spectrum of PMMA LSC with 4-butylamino-N-allyl-1,8-naphthalimide dye

From Figure 4.4, LSC with dye concentration of 100 μM gives the highest emission with emission peak at 499.40 nm while both LSCs with dye concentrations of 10 μM and 10000 μM give the lowest emissions. With increasing dye concentration, the emission peak with increasing intensity at

around 500 nm is observed at dye concentration in the order of 10 μM to 100μM. The increase in emission intensity in this case is simply due to the increase in dye concentration or number of dye molecules available to absorb incident light and then emit the luminescence. However, it is not the case at higher concentration despite the increase in number of dye molecules due to the formation of dye aggregates.

As shown in Figure 4.4 and Figure 4.5, the emission peak wavelengths shift to longer wavelengths with concentration higher than 1000 μM. This is caused by the process of re-absorption and re-emission of dye molecules. Since the long wavelength side of absorption spectrum overlaps with the short wavelength side of emission spectrum, the luminescence from a dye molecule is re-absorbed by another dye molecule that subsequently re-emits it at longer wavelength. The effect of this process becomes more significant at high concentration since more dye molecules are available for it. Therefore, the emission peak is shifted to a longer wavelength (Kurian et al. 2002; Bindhu & Harilal 2001).

However, the shift in emission peak wavelength is smaller than that in absorption peak wavelength and the emission peak intensity decreases with concentration higher than 1000 μM. This is because of the formation of both J-aggregates and H-aggregates at high concentration. The high-luminescence J-aggregates emit luminescence with small Stoke's shift, i.e. small difference between its absorption and emission peak wavelength (Würthner et al. 2011), therefore slows down the red-shift in overall emission peak; Formation of the

low-luminescence H-aggregates reduce the relative amount of high-luminescence monomers and J-aggregates, therefore suppress the overall emission intensity.

Table 4.3 Absorption and emission wavelength for PMMA LSC with 4-butylamino-N-allyl-1,8-naphthalimide dye in different concentration

Dye Concentration (μM)	Absorption peak wavelength (nm)	Emission peak wavelength (nm)	Stoke's shift (nm)
10	430.51	499.40	68.89
25	430.10	499.40	69.30
50	431.96	501.43	69.47
75	432.17	499.40	67.23
100	431.96	501.63	69.67
250	439.62	501.43	61.81
500	463.92	510.32	46.40
750	470.27	511.54	41.27
1000	472.32	511.54	39.22
2500	481.30	511.54	30.24
5000	486.40	525.83	39.43
7500	489.45	525.83	36.38
10000	485.58	525.83	40.25

From Table 4.3, the absorption peak wavelengths for the lowest dye concentration (10 μM) and the highest dye concentration (10000 μM) are

430.51 nm and 485.58 nm, respectively. While their emission peak wavelengths are 499.40 nm and 525.83 nm respectively. Therefore, both their absorption and emission peak wavelength shift to a longer wavelength when the dye concentration is increased. The red-shift of both the absorption and emission spectra can be observed in Figure 4.5 as well.

Smaller Stoke's shift of the dye at dye concentration higher than 1000μM, which is caused by red-shift in absorption peak and emission from J-aggregates with small Stoke's shift, contributes to higher re-absorption loss. High re-absorption loss due to small Stoke's shift is another factor that contributes to the reduction in emission intensity (Rowan et al. 2008).

4.3.2 Emission Irradiance and Optimum Concentration

Emission spectra of PMMA LSCs with 4-butylamino-N-allyl-1,8-naphthalimide dye in different concentrations were measured using a spectrometer. The emission irradiances were determined by integrating the area under emission spectra. It is a more accurate assessment of emission intensity as compared to the value of emission peak intensity. Comparing the emission irradiances, as shown in Figure 4.6, the optimum dye concentration that provides the highest emission irradiance can be determined. The optimum dye concentration for PMMA LSC with 4-butylamino-N-allyl-1,8-naphthalimide dye is found to be 75 μM.

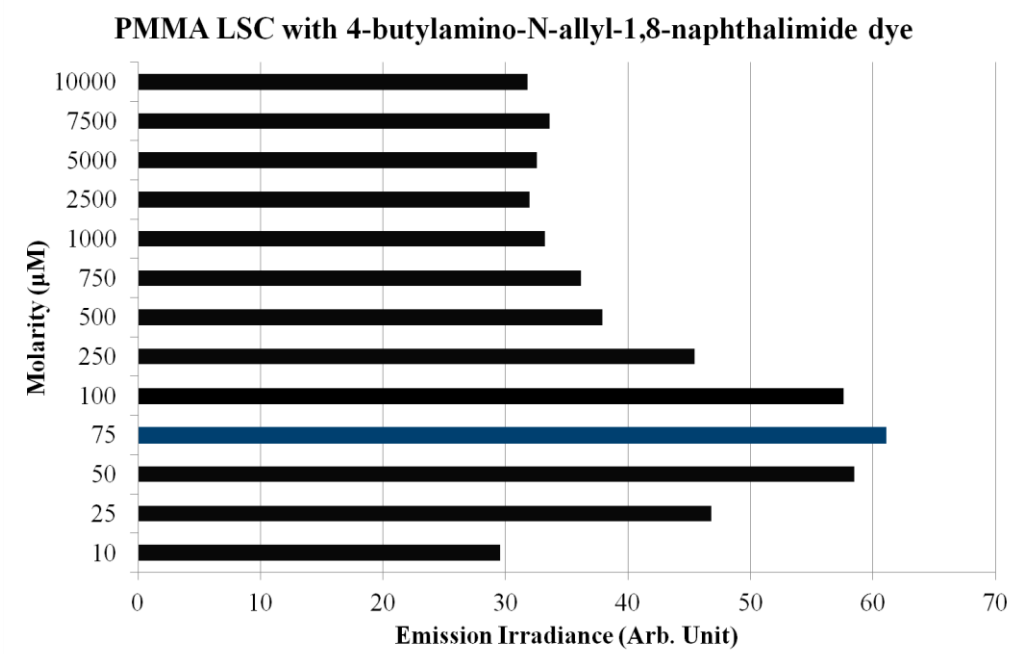

Figure 4.6 Emission irradiance of PMMA LSC with 4-butylamino-N-allyl-1,8-naphthalimide dye in different concentration

The emission irradiance of LSC increases with the rise of dye concentration until a maximum point and then decreases with further increase in the dye concentration. The decrease in emission irradiance at higher dye concentration beyond the optimum concentration is due to the process of re-absorption and re-emission with smaller Stoke's shift and the formation of dye aggregates, as explained in Section 4.3.1.

4.4 Multiple-dye PMMA LSC with Polymerizable Naphthalimide Dye and Rhodamine 6G

A number of LSCs were constructed in this project by doping multiple dye – polymerizable naphthalimide (4-butylamino-N-allyl-1,8-naphthalimide) and Rhodamine 6G in PMMA matrix with different molar ratios as shown in

Figure 4.7. These multiple-dye LSCs were casted in different molar ratios to find out the optimum ratio that provides the highest emission irradiance. Their absorption and emission spectra are reported in the following subsections. The molar ratio of multiple-dye PMMA LSCs were varied by changing the concentration of naphthalimide dye only where the concentration of Rhodamine 6G was made constant at 37.5 μM for all LSCs in this section. Constant Rhodamine 6G concentration at 37.5 μM was used because it was determined to be the optimum Rh6G concentration for unsaturated polyester LSC in (Lim et al. 2012).

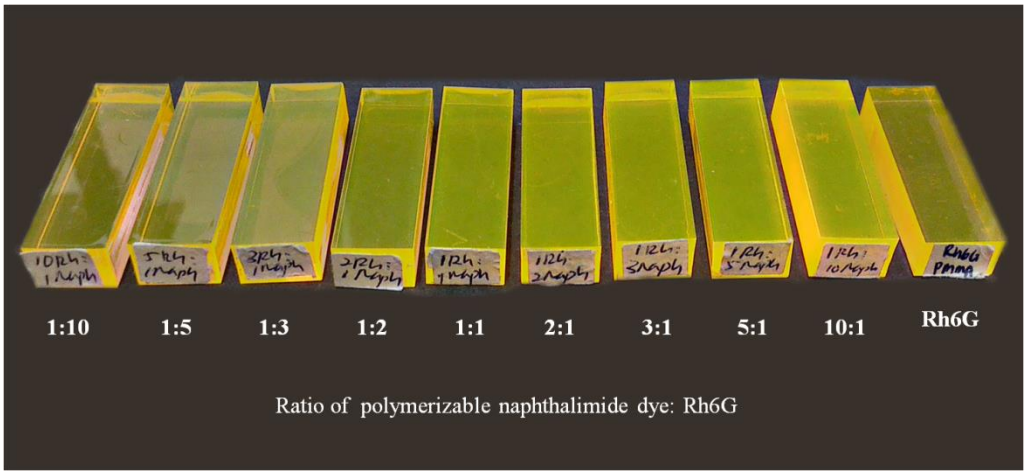

Figure 4.7 Multiple-dye PMMA LSC with polymerizable naphtahlimide dye and Rhodamine 6G in different ratio

4.4.1 Absorption, Emission and Stoke's shift

The absorption and emission spectra of the LSCs that were measured in the laboratory using spectrometer are shown in Figure 4.8 and Figure 4.9 respectively. Only 3 molar ratios of polymerizable naphthalimide to Rhodamine 6G are shown in the figures: 1:10, 2:1 and 10:1, together with a single dye Rhodamine 6G LSC so that changes in the spectra shapes between LSCs with increasing relative amount of polymerizable naphthalimide can be clearly observed. Both the absorption and emission spectra of LSC with the same dye concentration are put together in Figure 4.10 to compare their shapes. Absorption and emission wavelengths of all the LSCs together with their Stoke's shift are listed in Table 4.4.

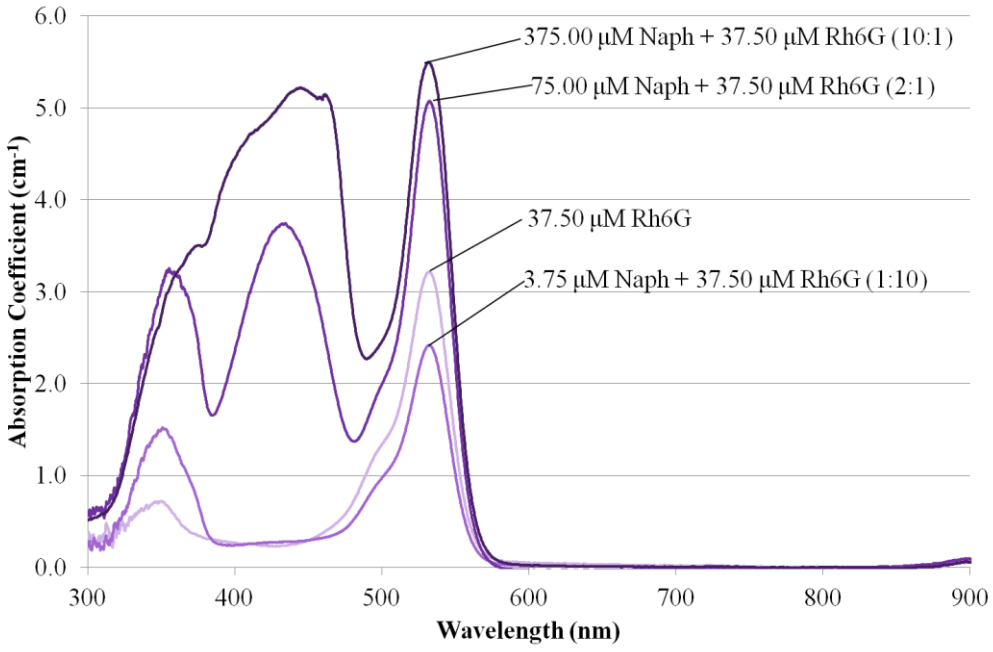

Figure 4.8 Absorption spectrum of multiple-dye PMMA LSC with Rhodamine 6G and naphthalimide dye in different molar ratios

As shown in Figure 4.8, the multiple dye PMMA LSCs has two absorption peaks. They are the absorption peak from polymerizable naphthalimide dye and Rhodamne 6G. The polymerizable naphthalimide dye absorbs at a shorter wavelength (around 420 nm-460 nm) than the Rhodamine 6G (around 520 nm-560 nm). Mixing a relatively small amount of polymerizable naphthalimide dye with Rhodamine 6G reduce the absorption peak from Rhodamine 6G. When the relative amount of polymerizable naphthalimide dye is increased, both the absorption peaks from polymerizable naphthalimide dye and Rhodamine 6G increase. The graph shows that the LSC with 1:10 Naph to Rh6G ratio has the lowest absorption from Rhodamine 6G while that with 10:1 Naph to Rh6G ratio has the highest absorption. Therefore, it is shown that higher relative amount of naphthalimide aids to increase the absorption from naphthalimide and Rhodamine 6G. Formation of polymerizable naphthalimide aggregates, similar to that described in Section 4.3.1, is observed with very high relative amount of polymerizable naphthalimide. It is indicated by broadening of absorption peak from polymerizable naphthalimide at 10:1 Naph to Rh6G ratio.

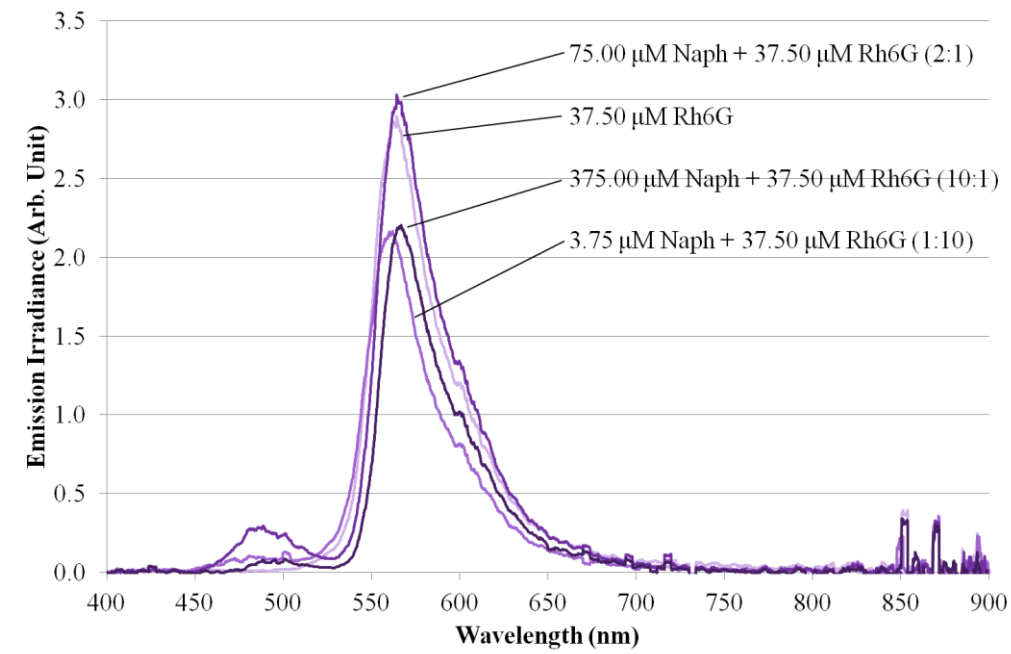

Figure 4.9 Emission spectrum of multiple-dye PMMA LSC with Rhodamine 6G and naphthalimide dye in different molar ratios

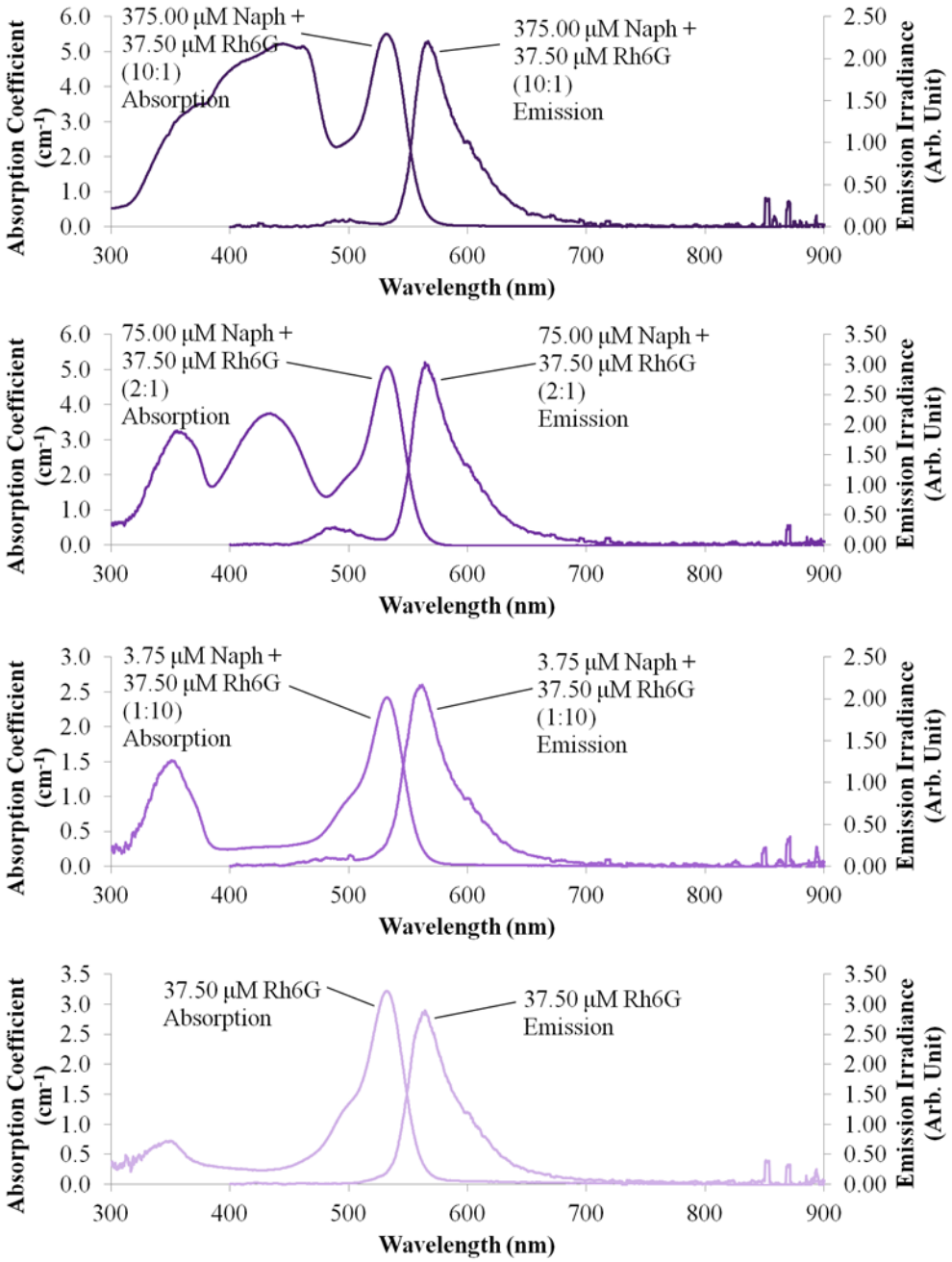

Figure 4.10 Absorption and emission spectrum of multiple-dye PMMA LSC with Rhodamine 6G and naphthalimide dye

From Figure 4.9 and Figure 4.10, two emission peaks are observed for the multiple-dye PMMA LSC. Similarly, they are the emission peaks from polymerizable naphthalimide dye and rhodamine 6G. Naphthalimide dye emits at a shorter wavelength (around 480 nm-520 nm) than the Rhodamine 6G

(around 540 nm-580 nm). However, the emission peak of Rhodamine 6G is much higher than that of the polymerizable naphthalimide dye. The LSC with 2:1 Naph to Rh6G ratio gives the highest emission peak at 564.33 nm. Its emission peak is higher than that from single-dye Rhodamine 6G LSC. Therefore, mixing polymerizable naphthalimide dye with Rhodamine 6G improves the emission from Rhodamine 6G.

The result shows that higher absorption coefficient does not guarantee for higher emission irradiance. For example, 10:1 Naph to Rh6G LSC has the highest absorption coefficient but low emission. This is due to the formation of polymerizable naphthalimide aggregates and re-absorption loss of emission from polymerizable naphthalimide.

Table 4.4 Absorption and emission wavelength for PMMA LSC with multiple dyes in different concentrations

Ratio of Naph:Rh6G	Absorption peak wavelength (nm)	Emission peak wavelength (nm)	Stoke's shift (nm)
1:10	532.05	561.95	29.90
1:5	532.25	561.95	29.70
1:3	531.85	561.95	30.10
1:2	531.85	561.95	30.10
1:1	532.25	564.33	32.08
2:1	532.25	564.33	32.08
3:1	532.65	564.73	32.08
5:1	532.05	564.73	32.68
10:1	531.85	566.71	34.86

The absorption peak wavelength for the multiple-dye PMMA LSCs with different molar ratios are in the range of 531.85nm and 532.65nm. They are almost constant and not affected by the molar ratios. However, the emission peak wavelength shifts to a longer wavelength when the relative amount of polymerizable naphthalimide dye is increased.

4.4.2 Emission Irradiance and Optimum Concentration

Multiple-dye PMMA LSCs were casted using a mixture of polymerizable naphthalimide dye and Rhodamine 6G in different molar ratios. The emission spectra of all the LSCs were measured using a spectrometer. The

emission irradiances of all the LSCs were determined by integrating the area under the emission spectra. Comparing the emission irradiances, as shown in Figure 4.11, the molar ratio that provides the highest emission irradiance can be determined. The optimum molar ratio for multiple-dye PMMA LSC with the polymerizable naphthalimide dye and Rhodamine 6G is found to be 75 μM naphthalimide dye to 37.5 μM Rhodamine 6G (2:1).

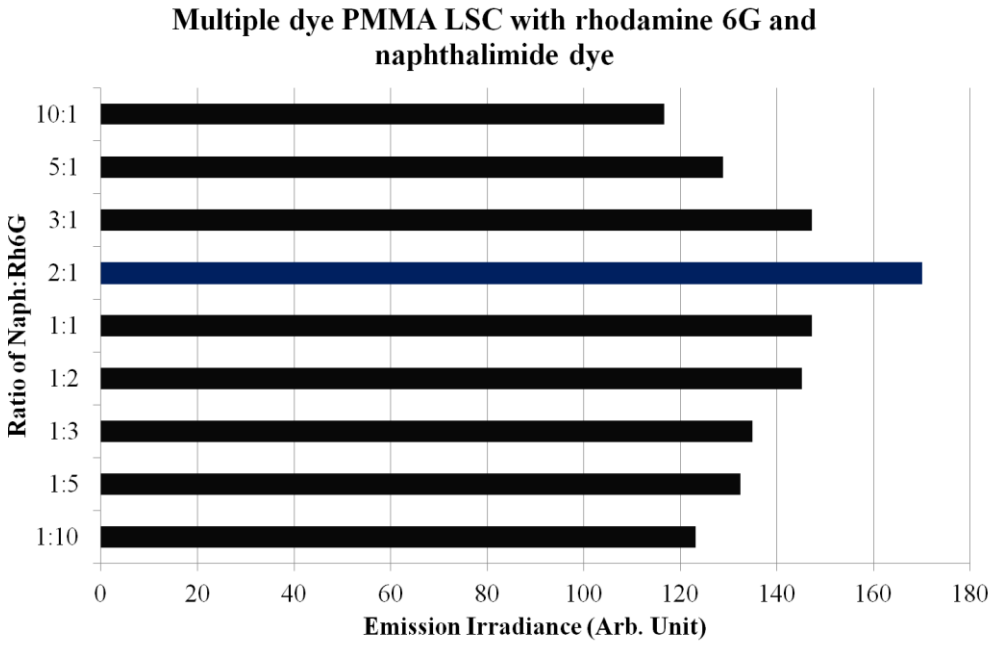

Figure 4.11 Emission irradiance of multiple-dye PMMA LSC with Rhodamine 6G and naphthalimide in different molar ratio

It is shown in Figure 4.11 that the emission irradiance of LSCs increase when the molar ratio of polymerizable naphthalimide dye to Rhodamine 6G is higher. However, the emission irradiance increases until a maximum and then starts to drop. Therefore, the optimum molar ratio of the mixture of polymerizable naphthalimide dye and Rhodamine 6G is 2:1.

4.5 PMMA LSC with PFV Dye

LSCs were also constructed by doping PFV dye - Poly(9,9-di-(2-ethylhexyl)-9H-fluorene-2,7-vinylene) in PMMA matrix as shown in Figure 4.12. They were casted in different concentrations to find out the optimum concentration that provides the highest emission irradiance. Their absorption and emission spectra are reported in the following subsections.

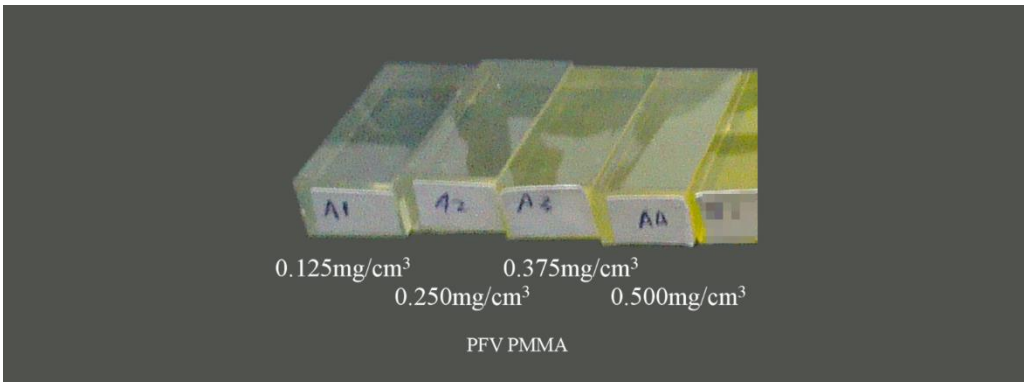

Figure 4.12 PMMA LSC with PFV dye

4.5.1 Absorption, Emission and Stoke's shift

The absorption and emission spectra of the LSCs that were measured in the laboratory using the spectrometer are shown in Figure 4.13 and Figure 4.14 respectively. LSCs with all the 4 concentrations are shown in the figures: 0.125 mg/cm^3, 0.250 mg/cm^3, 0.375 mg/cm^3, and 0.500 mg/cm^3. Concentration in the unit of mg/cm^3 is used here instead of μM because the PFV dye molecules are in polymer form with varying molecular weights. The average molecular weight, that is used to convert mg/cm^3 into μM, is not available in the

datasheet. Both the absorption and emission spectra of LSC with the same dye concentration are put together in Figure 4.15 to compare their shapes. Absorption and emission wavelengths of all the LSCs together with their Stoke's shift are listed in Table 4.5.

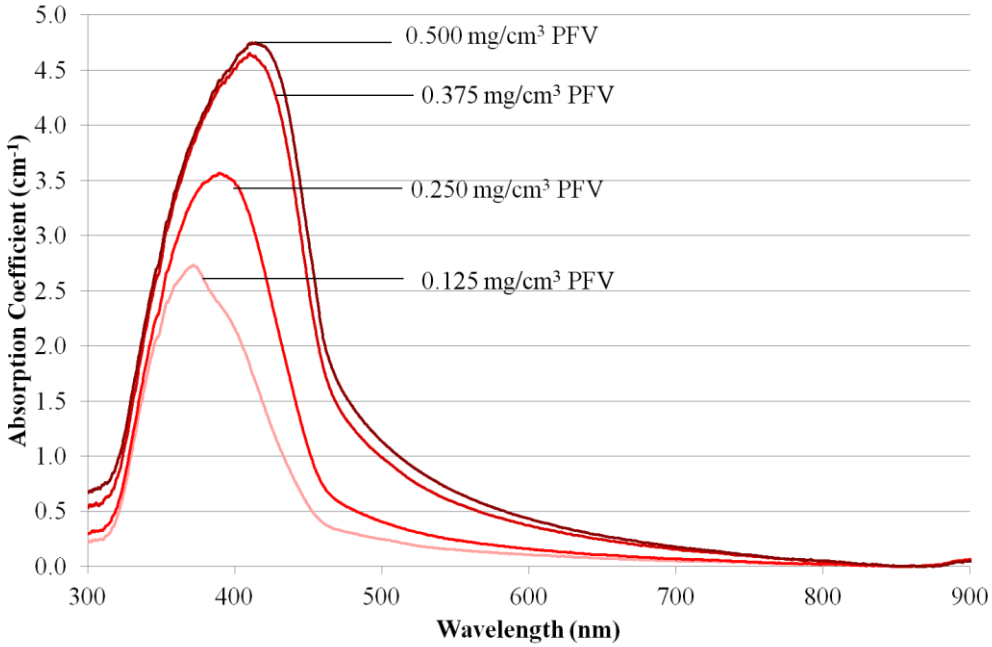

Figure 4.13 Absorption spectrum of PMMA LSC with PFV dye in different concentrations

From Figure 4.13, the peak absorption coefficient increases with the increase in dye concentration. The absorption peak wavelength shifts to longer wavelength when the dye concentration is higher. It indicates the formation of high-luminescent PFV dye J-aggregates in the LSC when the concentration was higher. This is because the J-aggregates have longer absorption peak wavelength as compared to that of the dye monomers (Würthner et al. 2011). However, formation of low-luminescent H-aggregates that have shorter absorption peak wavelength is not observed.

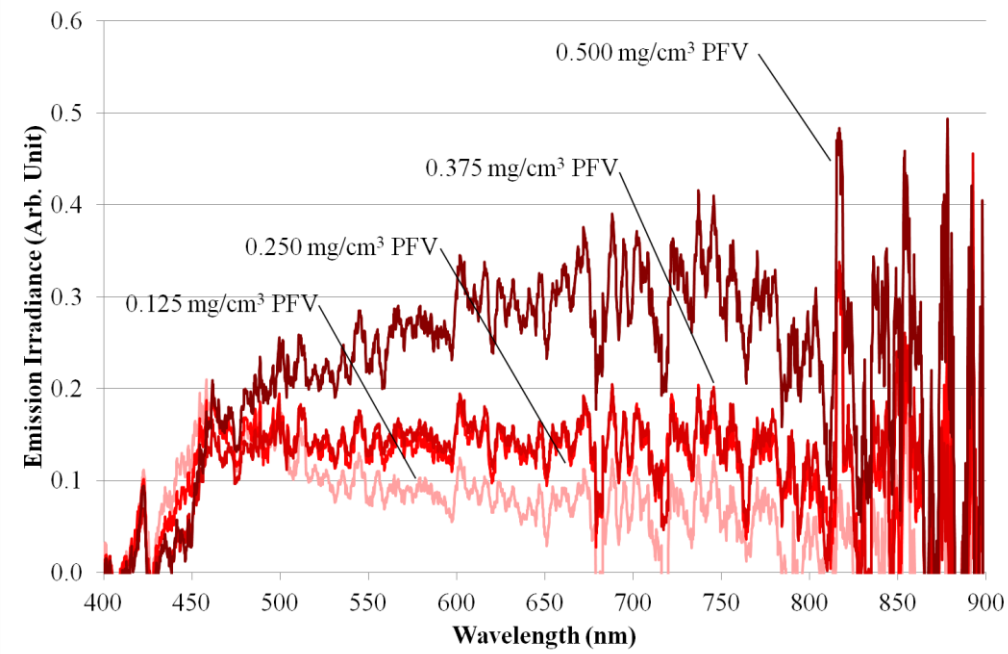

Figure 4.14 Emission spectrum of PMMA LSC with PFV dye in different concentrations

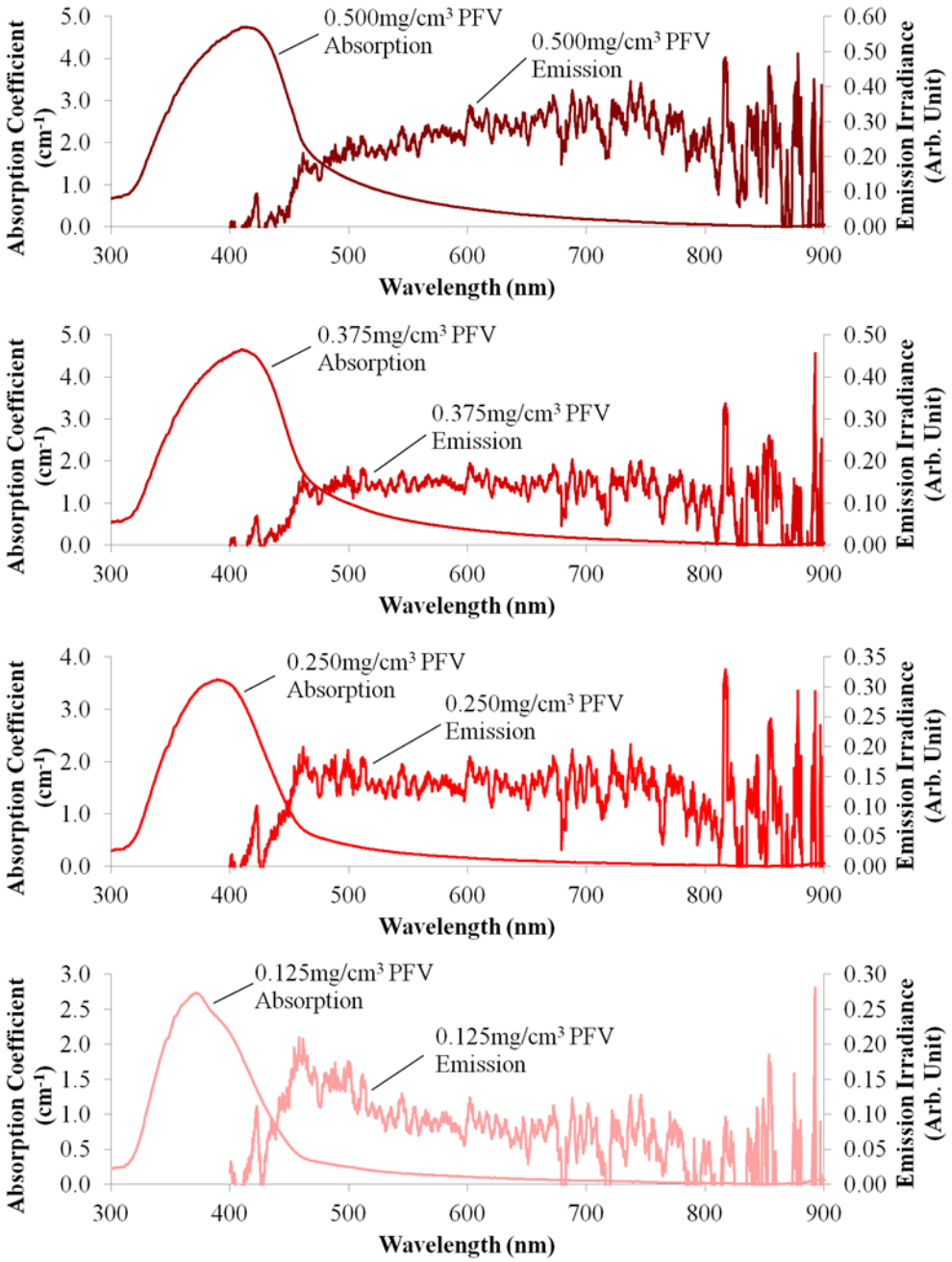

Figure 4.15 Absorption and emission spectrum of PMMA LSC with PFV dye

From Figure 4.14, LSC with dye concentration of 0.500 mg/cm^3 gives the highest emission where that with dye concentration of 0.125 mg/cm^3 gives the lowest emission. The emission peak wavelength shifts to a longer wavelength when the dye concentration is increased. The emission peak wavelength from the LSC cannot be determined accurately because its intensity

is too low, where the emission peak is hidden by electrical noises from the spectrometer.

As shown in Figure 4.15, both the absorption peak and emission peak wavelengths shifts to longer wavelengths with higher dye concentration. This is caused by the formation of J-aggregates. The J-aggregates has longer absorption peak wavelength and high luminescent quantum efficiency (Würthner et al. 2011). The former property shifts both absorption peak and emission peak wavelengths to longer wavelengths; the latter enhances the emission intensity from the LSC.

Table 4.5 Absorption wavelength and emission wavelength for PMMA LSC with PFV dye in different concentration

Dye Concentration (mg/cm^3)	Absorption peak wavelength (nm)	Emission peak wavelength (nm)	Stoke's shift (nm)
0.125	371.12	458.17	87.05
0.250	389.21	461.46	72.25
0.375	409.93	499.40	89.47
0.500	413.89	544.45	130.56

From Table 4.5, the absorption peak wavelengths for the lowest dye concentration (0.125 mg/cm^3) and the highest dye concentration (0.500 mg/cm^3) are 371.12 nm and 413.89 nm, respectively. While their emission peak wavelengths are 458.17 nm and 544.45 nm respectively. Therefore, both

their absorption and emission peak wavelength shift to a longer wavelength when the dye concentration is increased. The red-shift of both spectra can be observed in Figure 4.15 as well.

Larger Stoke's shift of the dye when the concentration is higher contributes to lower re-absorption loss. Lower re-absorption loss at larger Stoke's shift is another factor that contributes to the increase in emission intensity in this case (Rowan et al. 2008).

4.5.2 Emission Irradiance and Optimum Concentration

Emission spectra of PMMA LSCs with PFV dye in different concentrations were measured using a spectrometer. The emission irradiances were determined by integrating the area under emission spectra. Comparing the emission irradiances, as shown in Figure 4.16, the optimum dye concentration that provides the highest emission irradiance can be determined. The optimum dye concentration for PMMA LSC with PFV dye is found to be 0.500mg/cm^3.

The emission irradiance of LSC increased with the increase of dye concentration until the maximum concentration. LSC with further increase in dye concentration was not casted and measured due to cost consideration.

.

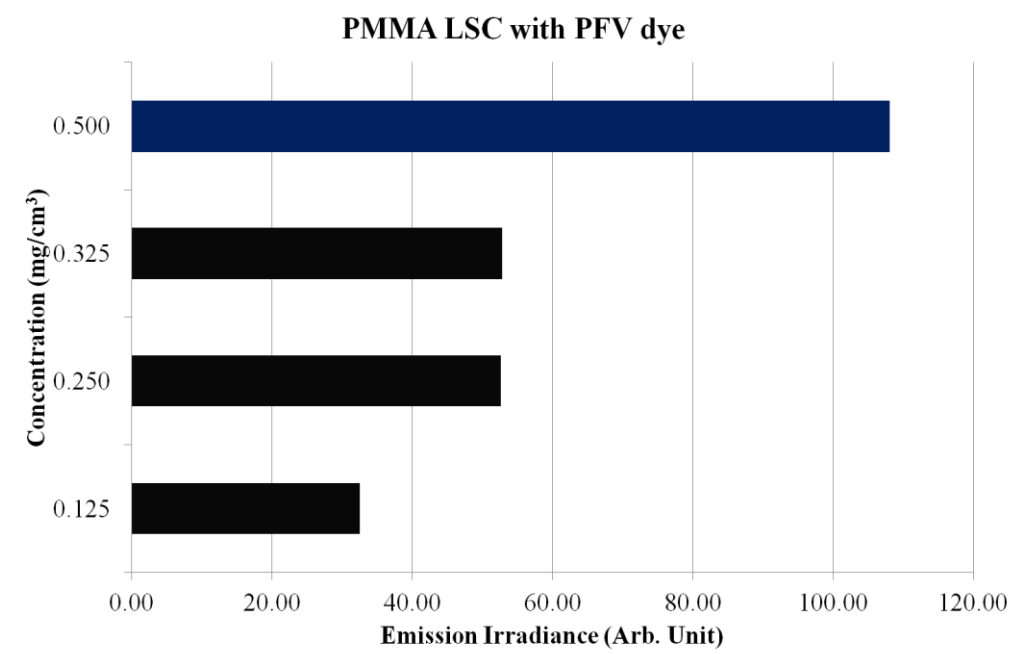

Figure 4.16 Emission irradiance of PMMA LSC with PFV dye in different concentration

4.6 PMMA LSC with PFV Copolymer Dye

For the results reported in this section, LSCs were constructed by doping PFV copolymer dye - Poly((9,9-di-(2-ethylhexyl)-9H-fluorene-2,7-vinylene)-co-(1-methoxy-4-(2-ethylhexyloxy)-2,5-(phenylenevinylene)) with 90:10 molar ratio in PMMA matrix as shown in Figure 4.17. They were casted in different concentrations to find out the optimum concentration that provides the highest emission irradiance. Their absorption and emission spectra are reported in the following subsections.

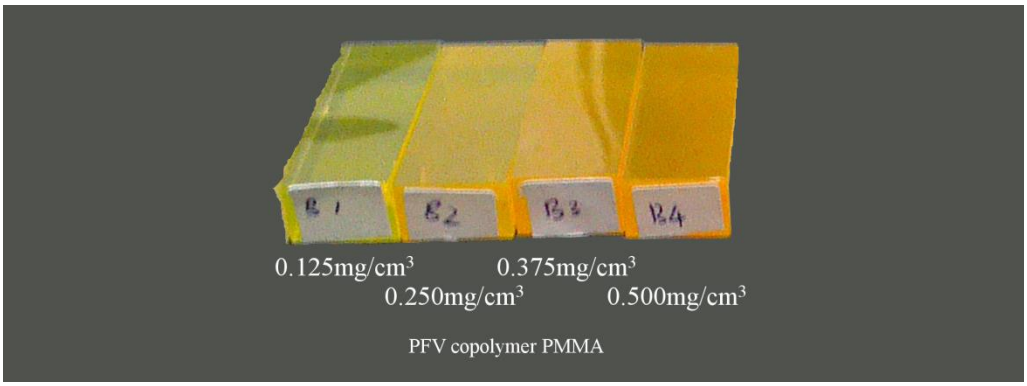

Figure 4.17 PMMA LSC with PFV copolymer dye

4.6.1 Absorption, Emission and Stoke's shift

The absorption and emission spectra of the LSCs that were measured in the laboratory using spectrometer are shown in Figure 4.18 and Figure 4.19 respectively. LSCs with all the 4 concentrations are shown in the figures: 0.125 mg/cm^3, 0.250 mg/cm^3, 0.375 mg/cm^3, and 0.500 mg/cm^3. Concentration in the unit of mg/cm^3 is used here instead of μM because the PFV copolymer dye molecules are in polymer form with varying molecular weights. The average molecular weight, that is used to convert mg/cm^3 into μM, is not available in the datasheet. Both the absorption and emission spectra of LSC with the same dye concentration are put together in Figure 4.20 to compare their shapes. Absorption and emission wavelengths of all the LSCs together with their Stoke's shift are listed in Table 4.6.

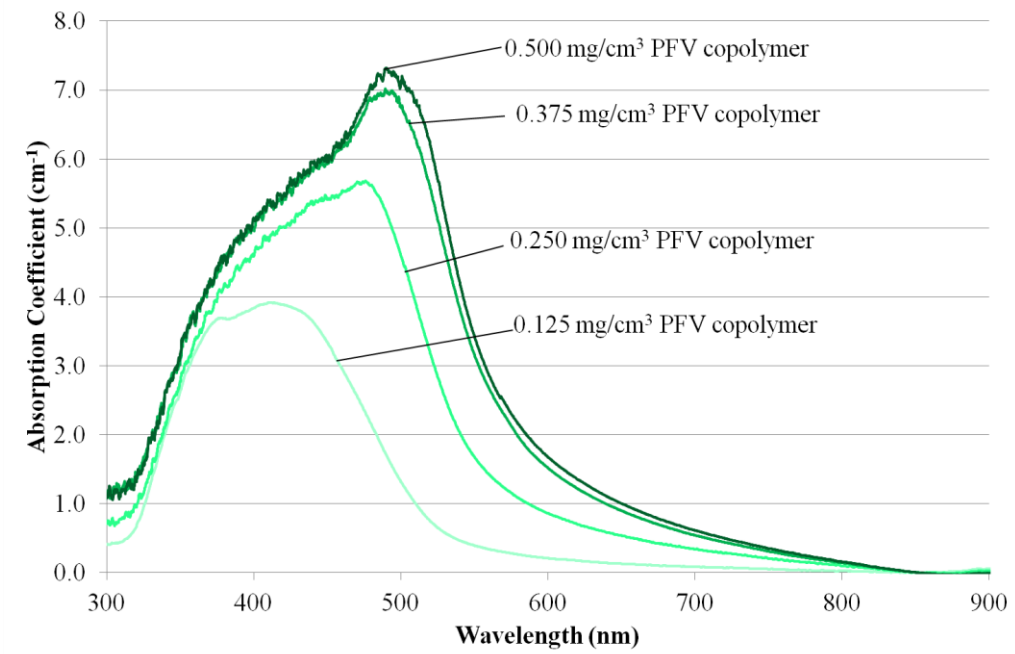

Figure 4.18 Absorption spectrum of PMMA LSC with PFV copolymer dye in different concentrations

From Figure 4.18, the peak absorption coefficient increases with the rise in dye concentration. The absorption peak wavelength shifts to longer wavelength when the dye concentration is higher. It indicates the formation of high-luminescent PFV copolymer dye J-aggregates in the LSC when the concentration is higher. This is because the J-aggregates have longer absorption peak wavelength as compared to that of the dye monomers (Würthner et al. 2011). However, formation of low-luminescent H-aggregates that have shorter absorption peak wavelength is not observed.

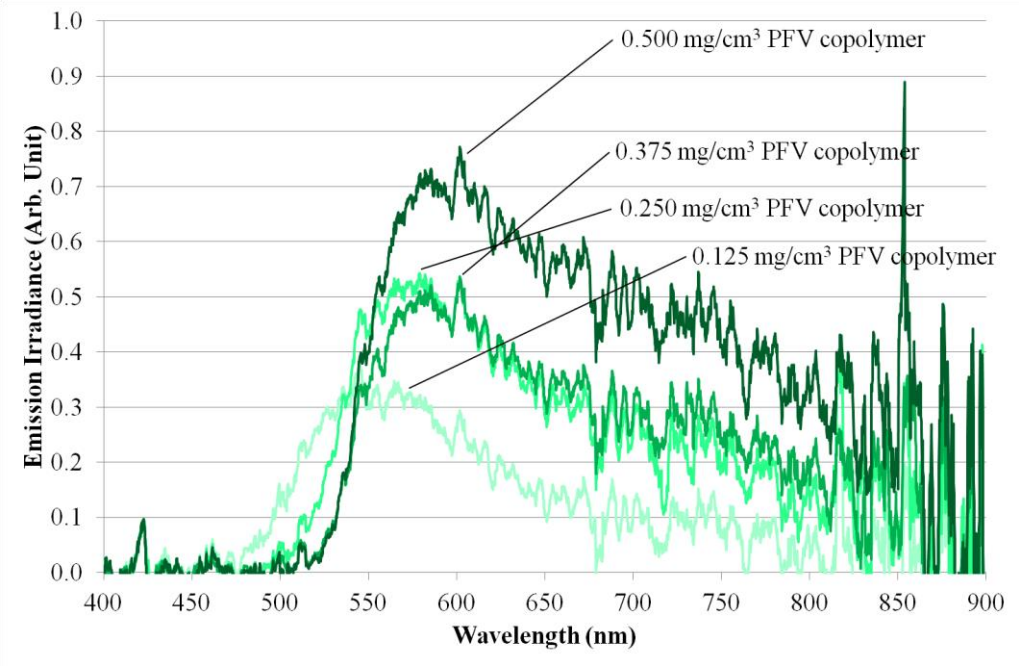

Figure 4.19 Emission spectrum of PMMA LSC with PFV copolymer dye in different concentrations

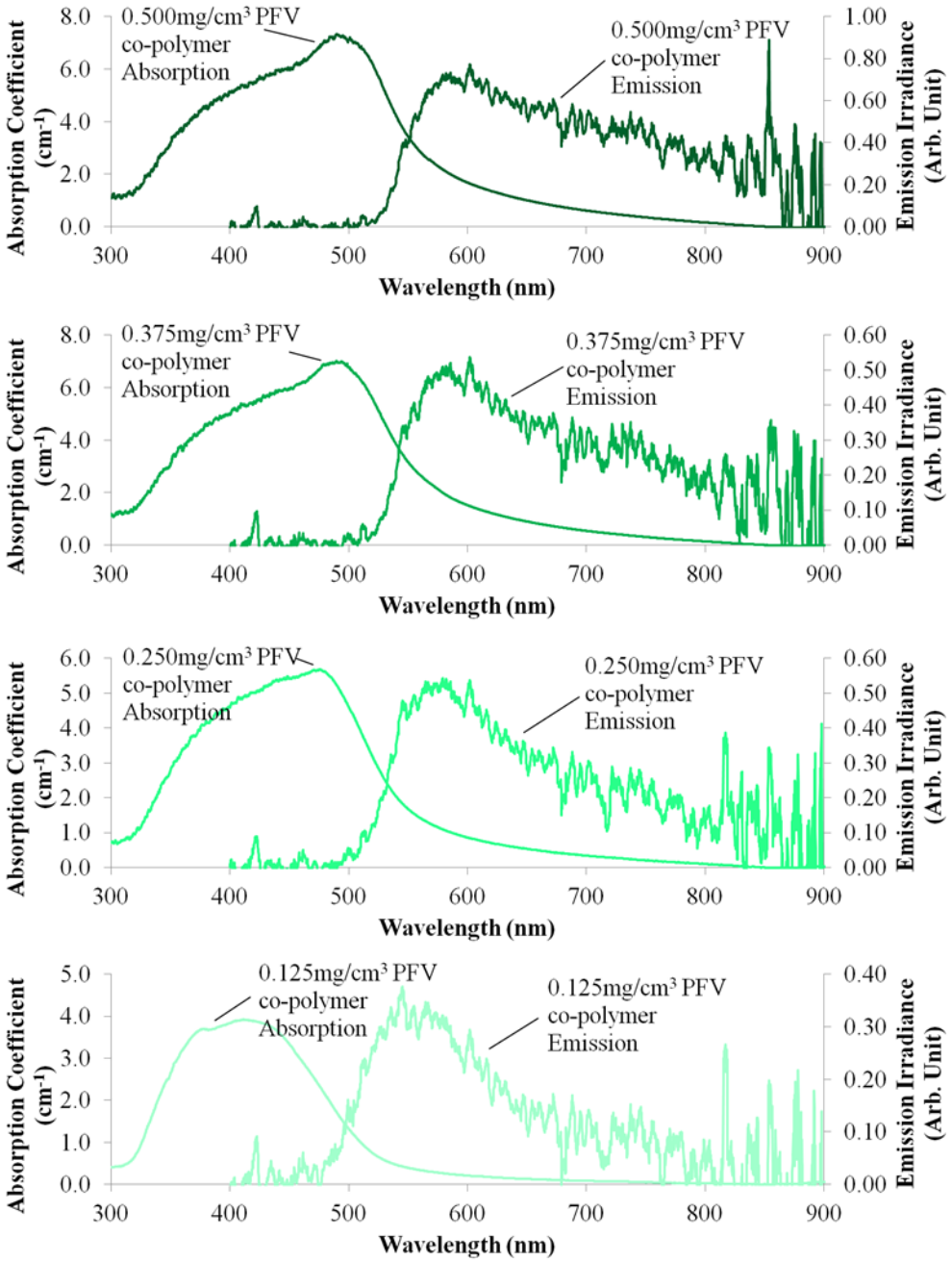

Figure 4.20 Absorption and emission spectrum of PMMA LSC with PFV copolymer dye

From Figure 4.19, LSC with dye concentration of 0.500 mg/cm^3 gives the highest emission and the dye concentration of 0.125 mg/cm^3 gives the lowest emission. The emission peak wavelength shifts to a longer wavelength when the dye concentration is increased. The emission peak wavelength from

the LSC cannot be de determined accurately because its intensity is too low, where the emission peak was hidden by electrical noise from the spectrometer.

As shown in Figure 4.20, both the absorption peak and emission peak wavelengths shift to longer wavelengths with higher dye concentration. This is caused by the formation of J-aggregates. The J-aggregates has longer absorption peak wavelength and high luminescent quantum efficiency (Würthner et al. 2011). The former property shifts both absorption peak and emission peak wavelengths to longer wavelengths; the latter enhances the emission intensity from the LSC.

Table 4.6 Absorption wavelength and emission wavelength for PMMA LSC with PFV copolymer dye in different concentration

Dye Concentration (mg/cm^3)	Absorption peak wavelength (nm)	Emission peak wavelength (nm)	Stoke's shift (nm)
0.125	411.39	545.25	133.86
0.250	476.20	578.95	102.75
0.375	489.45	585.44	95.99
0.500	489.65	585.44	95.79

From Table 4.6, the absorption peak wavelengths for the lowest dye concentration (0.125 mg/cm^3) and the highest dye concentration (0.500 mg/cm^3) are 411.39 nm and 489.65 nm, respectively. While their emission peak wavelengths are 545.25 nm and 585.44nm respectively. Therefore, both

their absorption and emission peak wavelength shift to a longer wavelength when the dye concentration is increased. The red-shift of both spectra can be observed in Figure 4.20 as well.

Larger Stoke's shift of the dye when the concentration is higher contributes to lower re-absorption loss. Lower re-absorption loss at larger Stoke's shift is another factor that contributes to the increase in emission intensity in this case (Rowan et al. 2008).

4.6.2 Emission Irradiance and Optimum Concentration

Emission spectra of PMMA LSCs with PFV copolymer dye in different concentrations were measured using a spectrometer. The emission irradiances were determined by integrating the area under emission spectra. Comparing the emission irradiances, as shown in Figure 4.21, the optimum dye concentration that provides the highest emission irradiance can be determined. The optimum dye concentration for PMMA LSC with PFV copolymer dye is found to be $0.500 mg/cm^3$.

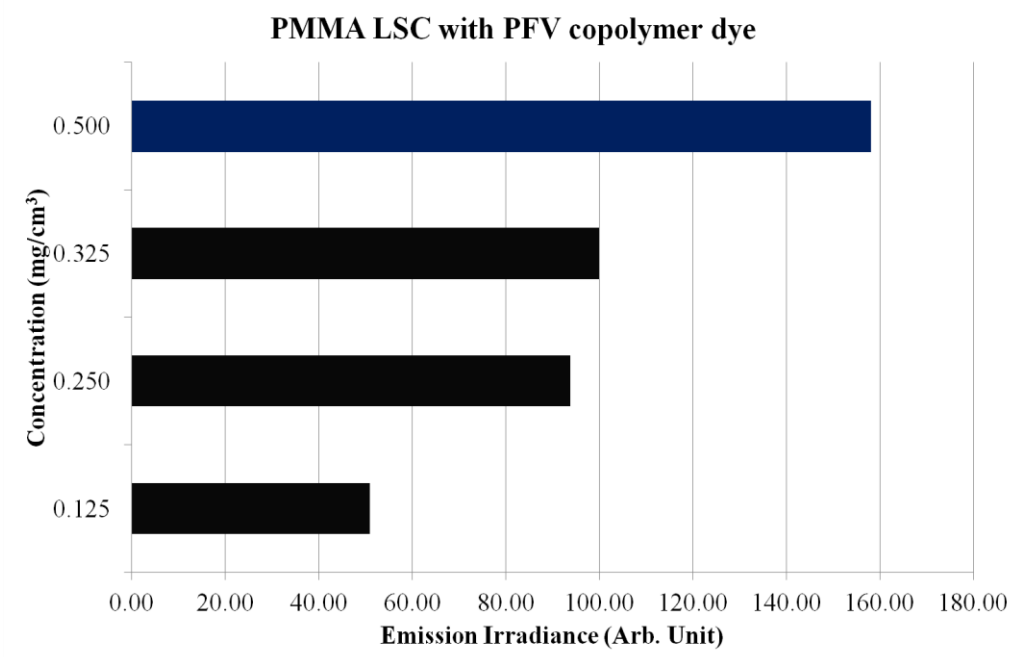

Figure 4.21 Emission irradiance of PMMA LSC with PFV copolymer dye in different concentrations

The emission irradiance of LSC increased with the increase of dye concentration until the maximum concentration. LSC with further increase in dye concentration was not casted and measured due to cost consideration.

4.7 All PMMA LSC with Different Dyes in Their Optimum Concentration

All PMMA LSCs with different dyes in their optimum dye concentration were selected to compare their absorption and emission spectra. They were selected from each category of dyes, including PFV dye, PFV copolymer dye, polymerizable naphthalimide dye, and multiple dyes - mixture of polymerizable naphthalimide dye and Rhodamine 6G.

4.7.1 Absorption and Emission Spectra

In this section, the absorption and emission spectra of all PMMA LSCs with different dyes in their optimum dye concentration were compared with those of a reference LSC that was doped with Rhodamine 6G. Rhodamine 6G was used as a reference dye because it was commonly used in LSC and its luminescent quantum efficiency was 98% (Meredith 1983). The optimum dye concentration of Rhodamine 6G in this study was assumed to be 37.5 μM since it was determined to be the optimum Rh6G concentration for unsaturated polyester LSC in (Lim et al. 2012). The selected PMMA LSCs with their optimum dye concentration were listed as shown in Table 4.7. The absorption and emission spectra of the LSCs that were measured in the laboratory using spectrometer are shown in Figure 4.22 and Figure 4.23 respectively.

Table 4.7 PMMA LSC with optimum dye concentration

Luminescent dye in LSC	Optimum concentration
Polymerizable naphthalimide	75μM
Multiple dye (mixture of polymerizable naphthalimide and Rhodamine 6G)	37.5μM:75μM
PFV	0.5mg/cm^3
PFV copolymer	0.5mg/cm^3
Rh6G	37.5μM

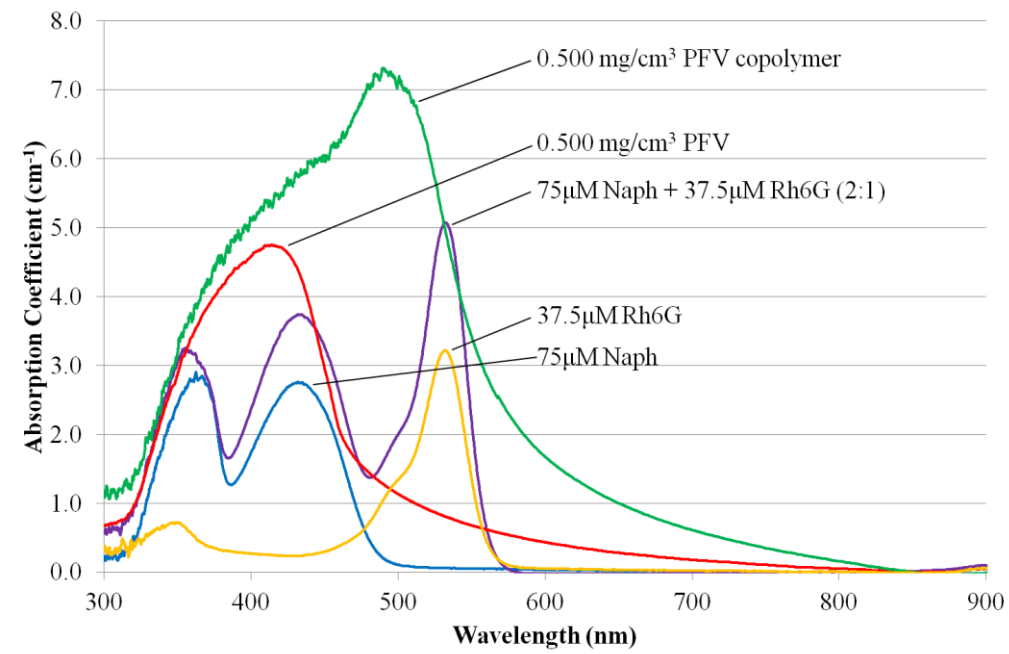

Figure 4.22 Absorption spectrum of all PMMA LSC with different dyes in their optimum dye concentrations

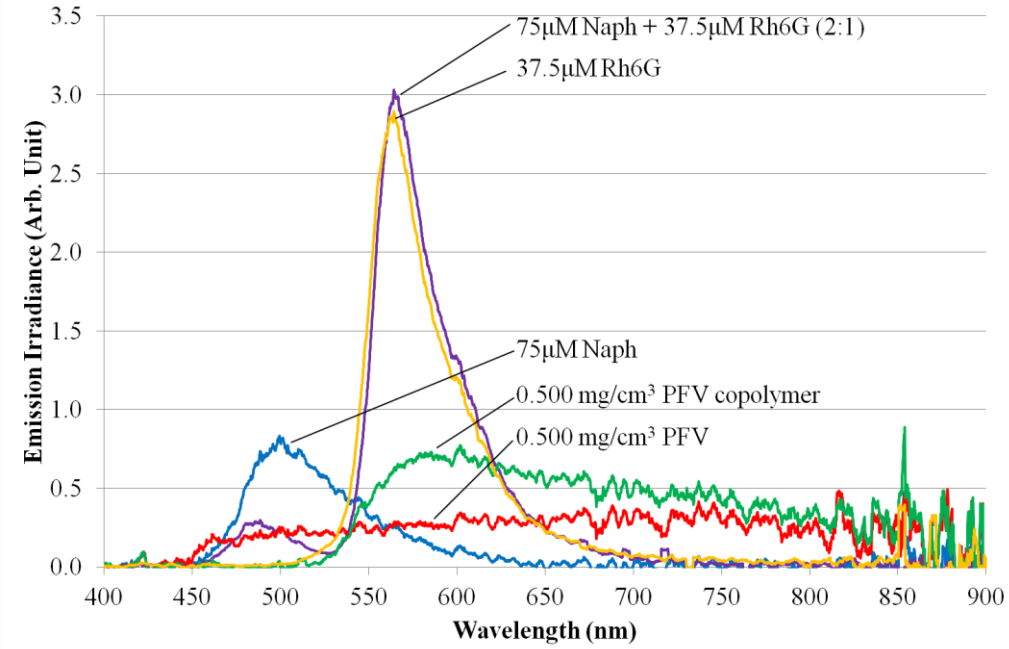

Figure 4.23 Emission spectrum of all PMMA LSC with different dyes in their optimum dye concentrations

Polymerizable naphthalimide dye has the lowest absorption and emission. However, the multiple-dye PMMA LSC (mixture of polymerizable naphthalimide and Rhodamine 6G in the ratio of 2:1) has higher emission peak than its constituent dye: either polymerizable naphthalimide dye or Rhodamine 6G. This result shows that the multiple dyes combination increases the emission irradiance due to its broader and higher absorption. The polymerizable naphthalimide dye absorbs additional incident light at the wavelength shorter than the Rhodamine 6G absorption peak wavelength, as shown in Figure 4.22. Emission of the polymerizable naphthalimide dye is subsequently reabsorbed by Rhodamine 6G that contributes to the emission peak observed in Figure 4.23. Therefore, more incident light power is absorbed and converted to the luminescence, or in other words, the emission is increased. However, the non-unity luminescent quantum efficiency of polymerizable naphthalimide dye limits the increase in emission.

4.7.2 Emission Irradiance

Emission spectra of all PMMA LSCs were measured using a spectrometer. The emission irradiances were also determined by integrating the area under emission spectra. After that, the emission irradiance obtained was normalized as shown in Figure 4.24. The result was used to compare and find out the dye that had potential to be used as luminescent material in LSC.

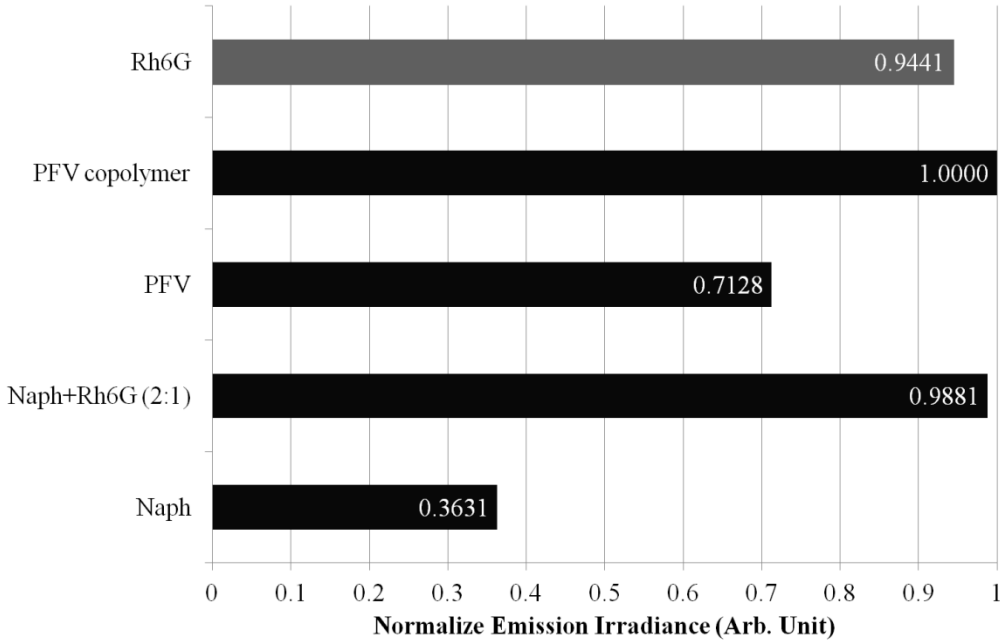

Figure 4.24 Normalized Emission irradiance of all PMMA LSC with optimum dye concentration

The PFV copolymer dye has the highest emission irradiance even though it has lower emission peak intensity. The result shows that the PFV copolymer has the potential to be used in LSC because its emission irradiance was higher than that of the reference dye - Rhodamine 6G.

Another type of dye, PFV has lower emission irradiance than the PFV copolymer. This result is expected because it has been reported that electroluminescent devices constructed from PFV copolymer has significantly higher efficiency and brighter than those constructed from PFV homo-polymer (Hwang et al. 2003).

The multiple-dye LSC (mixture of polymerizable naphthalimide and Rhodamine 6G in the ratio of 2:1) also has 4.45% higher emission irradiance

than Rhodamine 6G dye. However, its emission irradiance is slightly lower than that of PFV dye.

4.8 Summary

The chemical structure of the luminescent dye synthesized in the laboratory - polymerizable naphthalimide dye was characterized using FTIR and MS. The results show that the polymerizable naphthalimide dye is exactly the same as the one described in the publication (Panah et al. 2010). Besides, the absorption and emission measurement result of PMMA LSCs with different dyes – PFV, PFV copolymer, polymerizable naphthalimide, and multiple dyes – are also presented in details. Results of each dye with different concentrations are shown and optimum concentration of each dye that provides the highest emission irradiance is determined.

The LSC with the optimum concentration is selected from each category of dyes to compare their absorption and emission with those of the reference dye, Rhodamine 6G. The results show that the PFV copolymer and the multiple-dye PMMA LSC with polymerizable naphthalimide dye and Rhodamine 6G in the ratio of 2:1 has higher emission irradiance than Rhodamine 6G. Both of them have the potential to be used as new luminescent material in LSC.

CHAPTER 5

RESULTS AND DISCUSSIONS FOR LSC WITH DIFFERENT MATRICES

This chapter begins with the introduction of luminescent materials and polymer matrix materials. The absorption and light irradiance measurement results of unsaturated polyester LSC and epoxy LSC with different dyes and concentrations are presented next. The optimum concentration for each LSC is found from the results. Moreover, the absorption and light irradiance of LSC with different matrix materials at their respective optimum dye concentrations are compared. Lastly, the effect of micro-voids scattering in epoxy matrix is discussed in detail.

5.1 Introduction to Luminescent Material and Polymer Matrix

PFV and PFV copolymer dyes are used and doped into two other types of polymer matrices - unsaturated polyester and epoxy. The PFV copolymer dye is chosen as the luminescent material because it is one of the potential luminescent materials to be used in LSC, as shown in CHAPTER 4. PFV dye is chosen as well for comparison purpose. Rhodamine 6G is used as a reference dye. It is doped in unsaturated polyester and epoxy matrices as well.

It is shown in the following section that Rhodamine 6G in either unsaturated polyester or epoxy matrix has lower emission than Rhodamine 6G

in PMMA. Multiple-dye LSC with polymerizable naphthalimide dye and Rhodamine 6G is not shown in this chapter because emission from the multiple-dye LSC is mostly contributed by the emission from Rhodamine 6G and enhanced by the presence of polymerizable naphthalimide dye, as shown in Chapter 4.4. Therefore, the emission from either unsaturated polyester or epoxy LSC with the multiple dyes is expected to be lower than that with PFV co-polymer dye.

The results of PMMA LSCs that were casted previously were used in this chapter to compare with unsaturated polyester LSC and epoxy LSC. Therefore, the performance of different commercially available polymer host matrix materials are studied and compared.

5.2 Unsaturated Polyester LSC with PFV Dye

LSCs were constructed by doping PFV dye - Poly(9,9-di-(2-ethylhexyl)-9H-fluorene-2,7-vinylene) - in unsaturated polyester matrix as shown in Figure 5.1. They were casted in different concentrations to determine the optimum concentration that provides the highest light irradiance. Their absorption and light irradiance spectra are reported in the following sections.

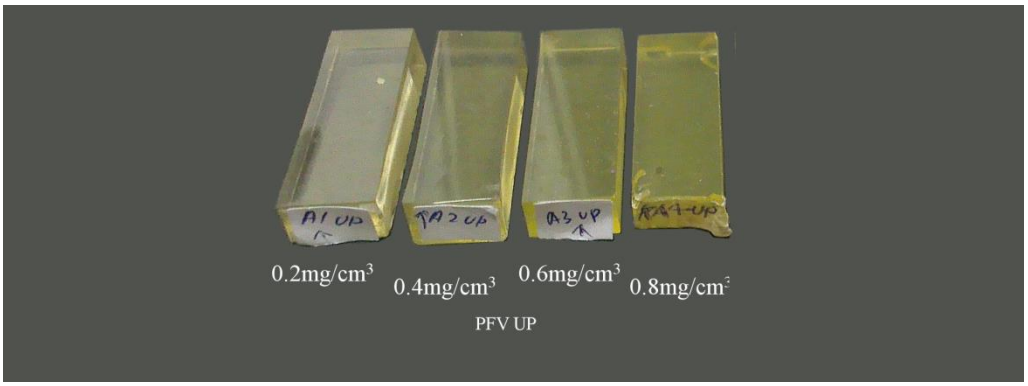

Figure 5.1 UP LSC with PFV dye

5.2.1 Absorption, light irradiance and Stoke's shift

The absorption and light irradiance spectra of the LSCs that were measured in the laboratory using a spectrometer are shown in Figure 5.2 and Figure 5.3 respectively. All dye concentrations are shown in the figures – 0.200 mg/cm^3, 0.400 mg/cm^3, 0.600 mg/cm^3, and 0.800 mg/cm^3. Besides, both the absorption and light irradiance spectra of LSC with the same dye concentration are put together in Figure 5.4 to compare their shapes. Absorption and light irradiance wavelengths of all the LSCs together with their Stoke's shift are listed in Table 5.1.

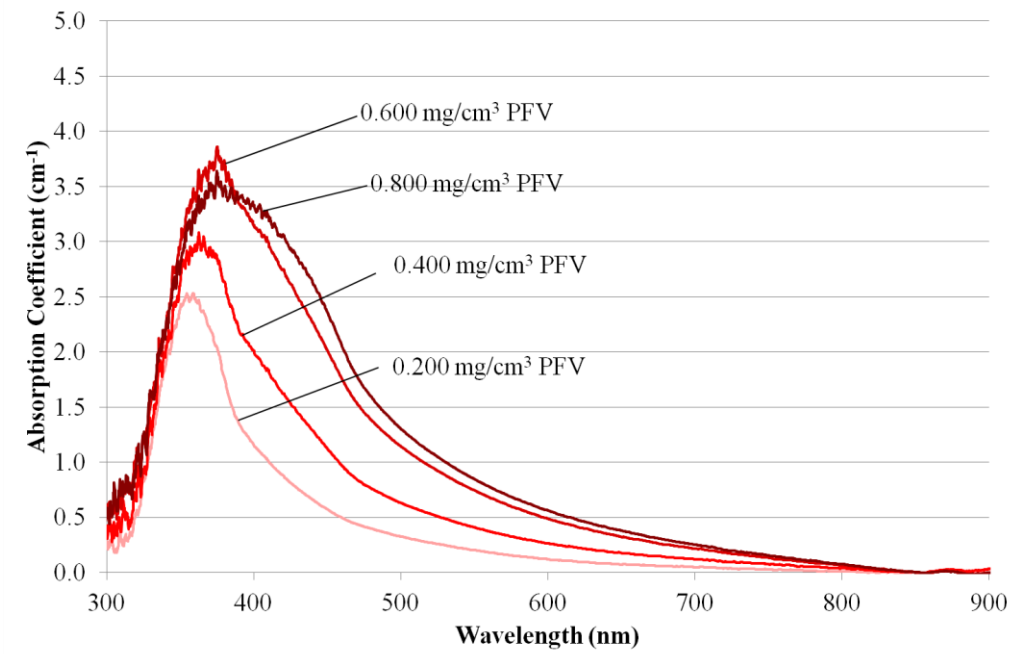

Figure 5.2 Absorption spectrum of UP LSC with PFV dye in different concentration

Figure 5.2 shows that the peak absorption coefficient generally increases with the dye concentration, but the peak absorption coefficient for dye concentration of 0.800 mg/cm^3 is lower than that of 0.600 mg/cm^3. The absorption peak wavelength for the lowest dye concentration (0.200 mg/cm^3) is 358.86 nm while that for the highest dye concentration (0.800 mg/cm^3) is 374.70 nm. It is noticed that the absorption peak wavelength becomes broader and shifts to a longer wavelength when the dye concentration is increased. This phenomenon is related to the formation of dye J-aggregates that have longer absorption peak wavelength as compared to that of the dye monomers (Würthner et al. 2011), as described in section 4.5.1. The absorption peak for dye concentration of 0.800 mg/cm^3 is saturated. Therefore, it appears to be lower than that for the dye concentration of 0.600mg/cm^3.

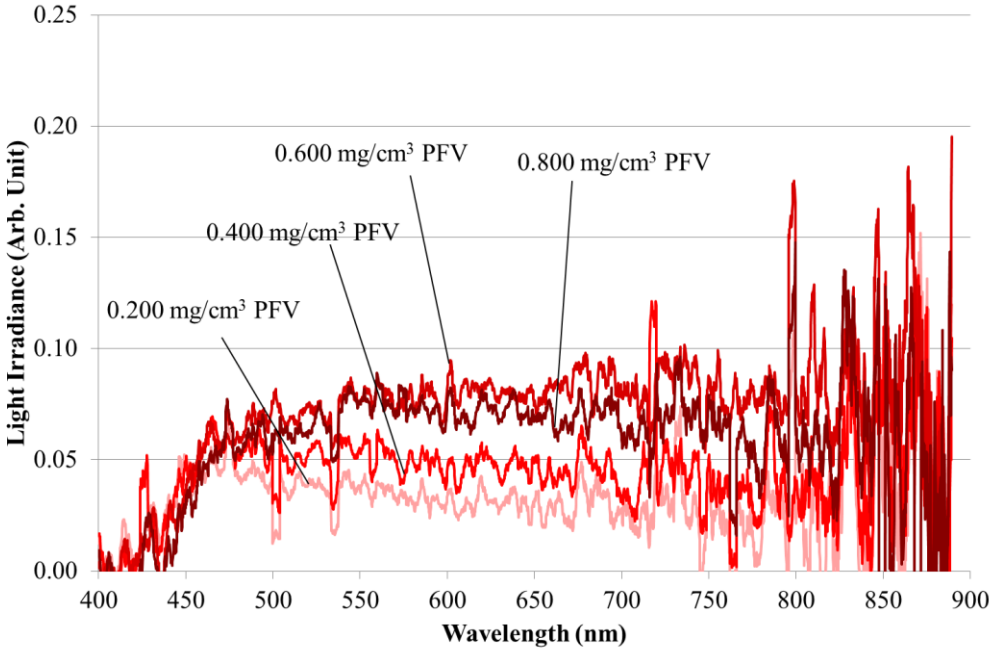

Figure 5.3 Light irradiance spectrum of UP LSC with PFV dye in different concentration

From Figure 5.3, LSC with dye concentration of 0.200 mg/cm^3 has the lowest light irradiance where 0.600 mg/cm^3 has the highest light irradiance. The increase in light irradiance from dye concentration of 0.200mg/cm^3 to 0.600 mg/cm^3 is due to the increase in number of dye molecules available to emit the luminescence. However, the dye emission decreases at higher concentration despite the increase in the number of dye molecules. This is due to the formation of dye aggregates that shifts the dye emission peak to a longer wavelength and hence reduces the emission intensity. Detailed description of the formation of aggregates can be found in section 4.5.1.

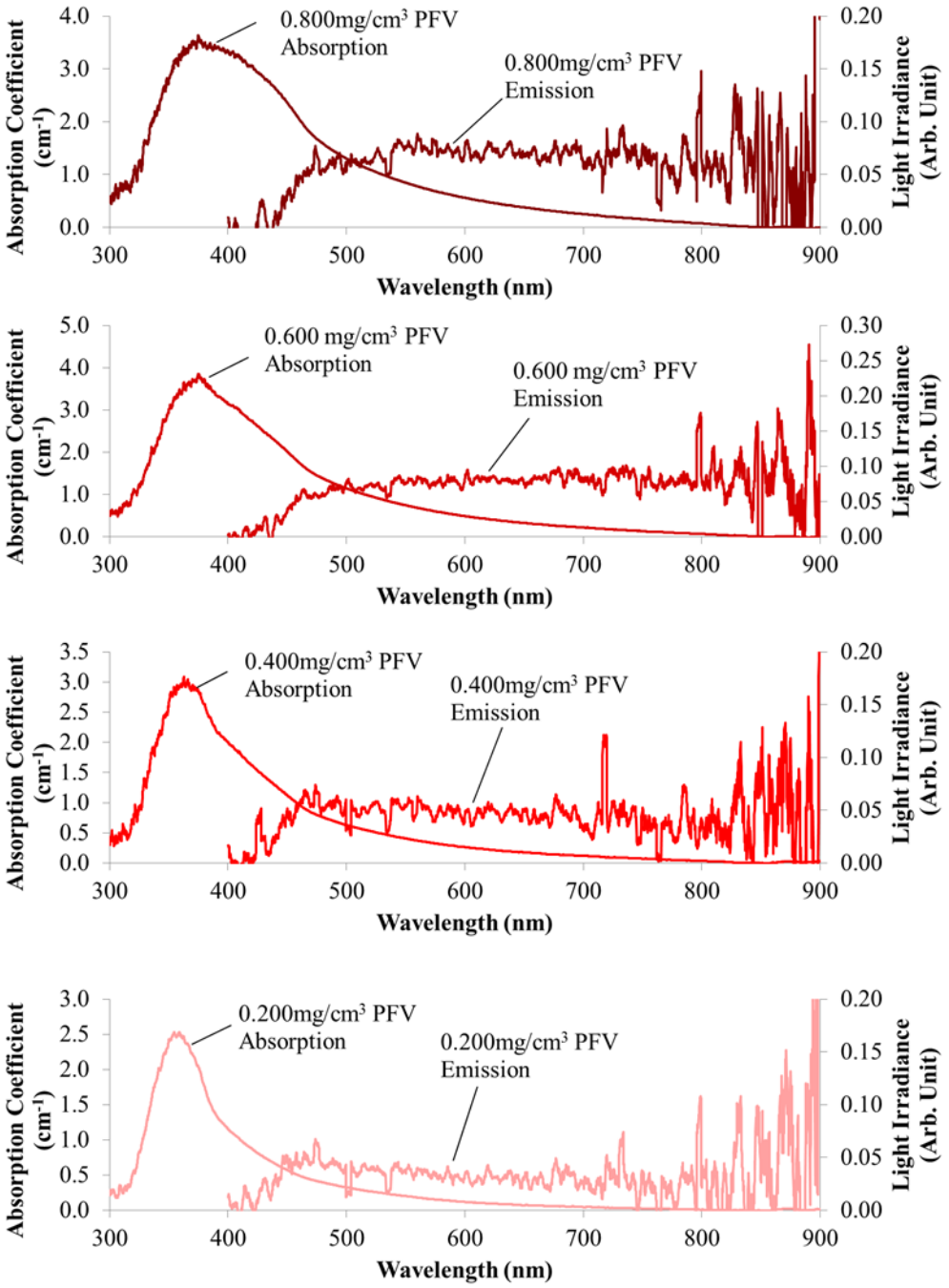

Figure 5.4 Absorption and light irradiance spectrum of UP LSC with PFV dye

Table 5.1 Absorption and light irradiance wavelength for UP LSC with PFV dye in different concentration

Dye Concentration (mg/cm^3)	Absorption peak wavelength (nm)	Light irradiance peak wavelength (nm)	Stoke's shift (nm)
0.200	358.86	473.75	114.89
0.400	362.67	473.75	111.08
0.600	374.70	488.64	113.94
0.800	375.13	488.89	113.76

From Table 5.1, the absorption wavelength for the lowest dye concentration (0.200 mg/cm^3) and the highest dye concentration (0.800 mg/cm^3) are 358.86 nm and 375.13 nm, respectively while their light irradiance wavelengths are 473.75 nm and 488.89 nm respectively. Therefore, both their absorption and light irradiance wavelengths shift to a longer wavelength when the dye concentration is increased. However, the wavelength of the light irradiance peak cannot be determined accurately in this case because its intensity is too low, where the light irradiance peak is hidden by electrical noises from the spectrometer.

5.2.2 Light Irradiance and Optimum Concentration

Light irradiance spectra of UP LSCs with PFV dye in different concentrations were measured using a spectrometer. The light irradiances were then determined by integrating the area under the light irradiance spectra. Comparing the light irradiance, as shown in Figure 5.5, the optimum

concentration that provides the highest light irradiance can be determined. The optimum concentration for UP LSC with PFV dye is found to be 0.600mg/cm^3.

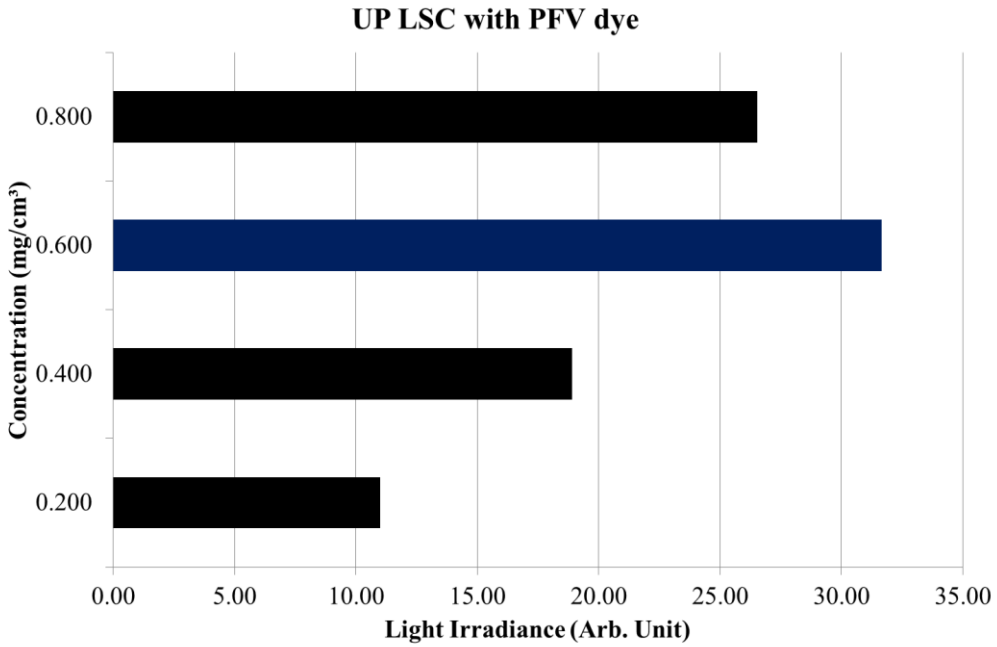

Figure 5.5 Light irradiance of UP LSC with PFV dye in different concentration

The light irradiance of LSC increases with the dye concentration and then reduces with further increase in the dye concentration. The decrease in light irradiance at higher dye concentration beyond the optimum concentration has been explained in section 4.3.1.

5.3 Unsaturated Polyester LSC with PFV Copolymer Dye

LSCs described in this section were constructed by doping PFV copolymer dye - Poly((9,9-di-(2-ethylhexyl)-9H-fluorene-2,7-vinylene)-co-(1-methoxy-4-(2-ethylhexyloxy)-2,5-(phenylenevinylene))--90:10 molar ratio - in unsaturated polyester matrix as shown in Figure 5.6. They were casted in

different PFV copolymer dye concentrations to determine the optimum concentration that provides the highest light irradiance. Their absorption and light irradiance spectra are reported in the following sections.

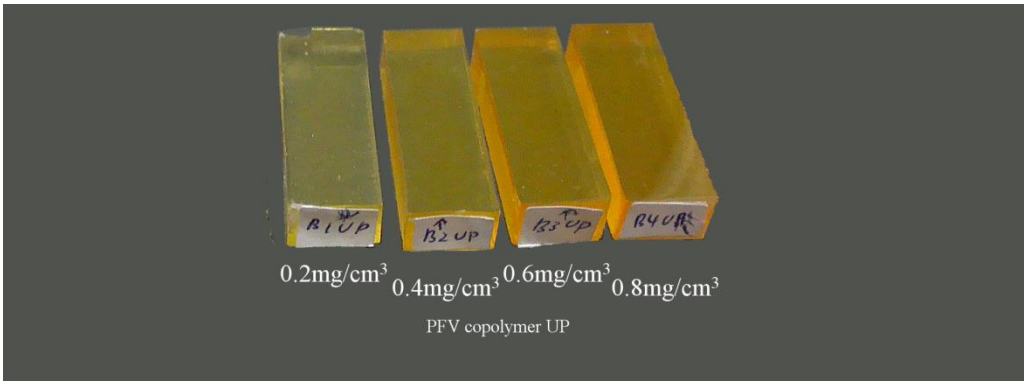

Figure 5.6 UP LSC with PFV copolymer

5.3.1 Absorption, Light irradiance and Stoke's shift

The absorption and light irradiance spectra of the LSCs that were measured in the laboratory using spectrometer are shown in Figure 5.7 and Figure 5.8 respectively. All dye concentrations are shown in the figures – 0.200 mg/cm^3, 0.400 mg/cm^3, 0.600 mg/cm^3, and 0.800 mg/cm^3. Both the absorption and light irradiance spectra of LSC with same dye concentrations are put together in Figure 5.9 to compare their shapes. Absorption and light irradiance wavelength of all the LSCs together with their Stoke's shift are listed in Table 5.2.

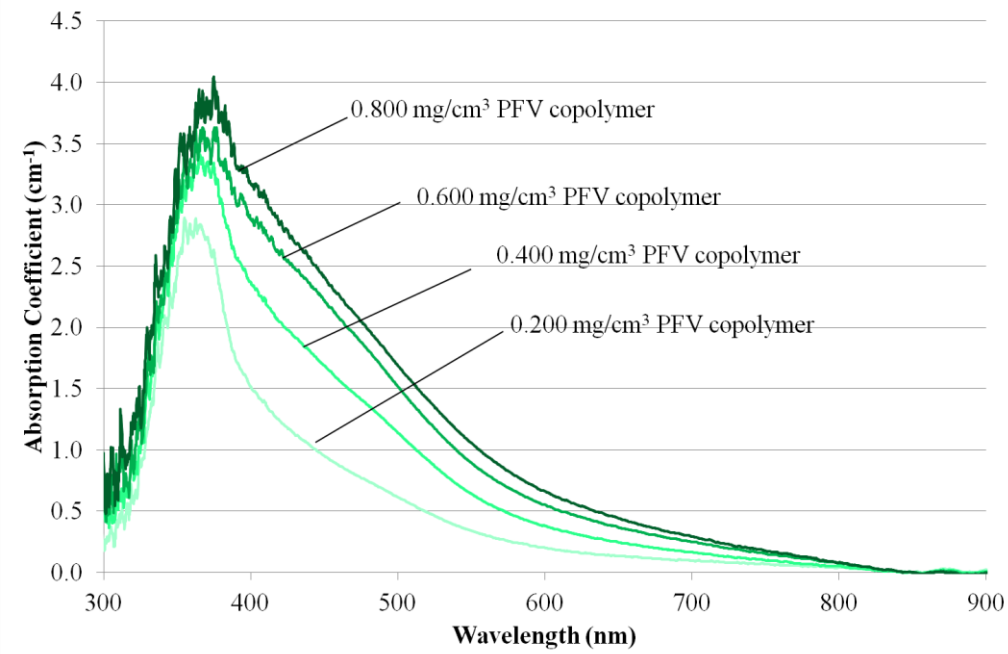

Figure 5.7 Absorption spectrum of UP LSC with PFV copolymer dye in different concentration

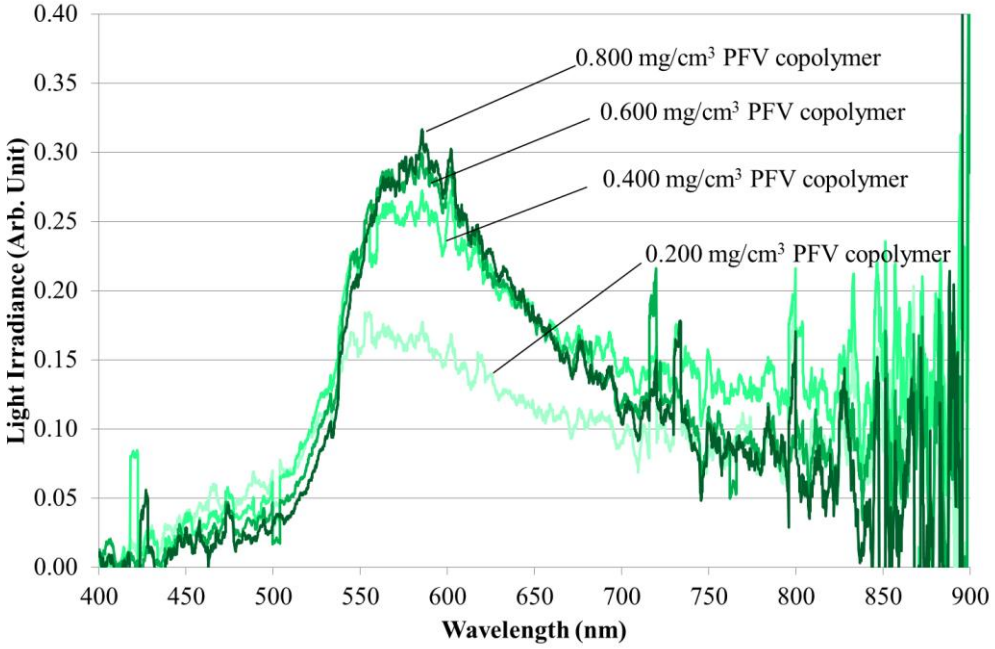

Figure 5.8 Light irradiance spectrum of UP LSC with PFV copolymer dye in different concentration

Figure 5.7 shows that the peak absorption coefficient increases with the increase in dye concentration. The absorption peak happens at 354.84 nm for the lowest dye concentration (0.200 mg/cm^3). It becomes broader and the maximum absorption wavelength is longer a bit when the dye concentration is higher. This is due to the formation of the dye J-aggregates as discussed in section 4.5.1. Similarly, the light irradiance peak increases with the dye concentration. From Figure 5.8, LSC with dye concentration of 0.800 mg/cm^3 has the highest light irradiance peak at 585.44 nm whereas 0.200 mg/cm^3 gives the lowest light irradiance peak at 555.01 nm. The light irradiance peak wavelength shifts to a longer wavelength when the dye concentration is increased. However, the light irradiance peak wavelength cannot be determined accurately because its intensity is too low, where the light irradiance peak is hidden by electrical noises from the spectrometer.

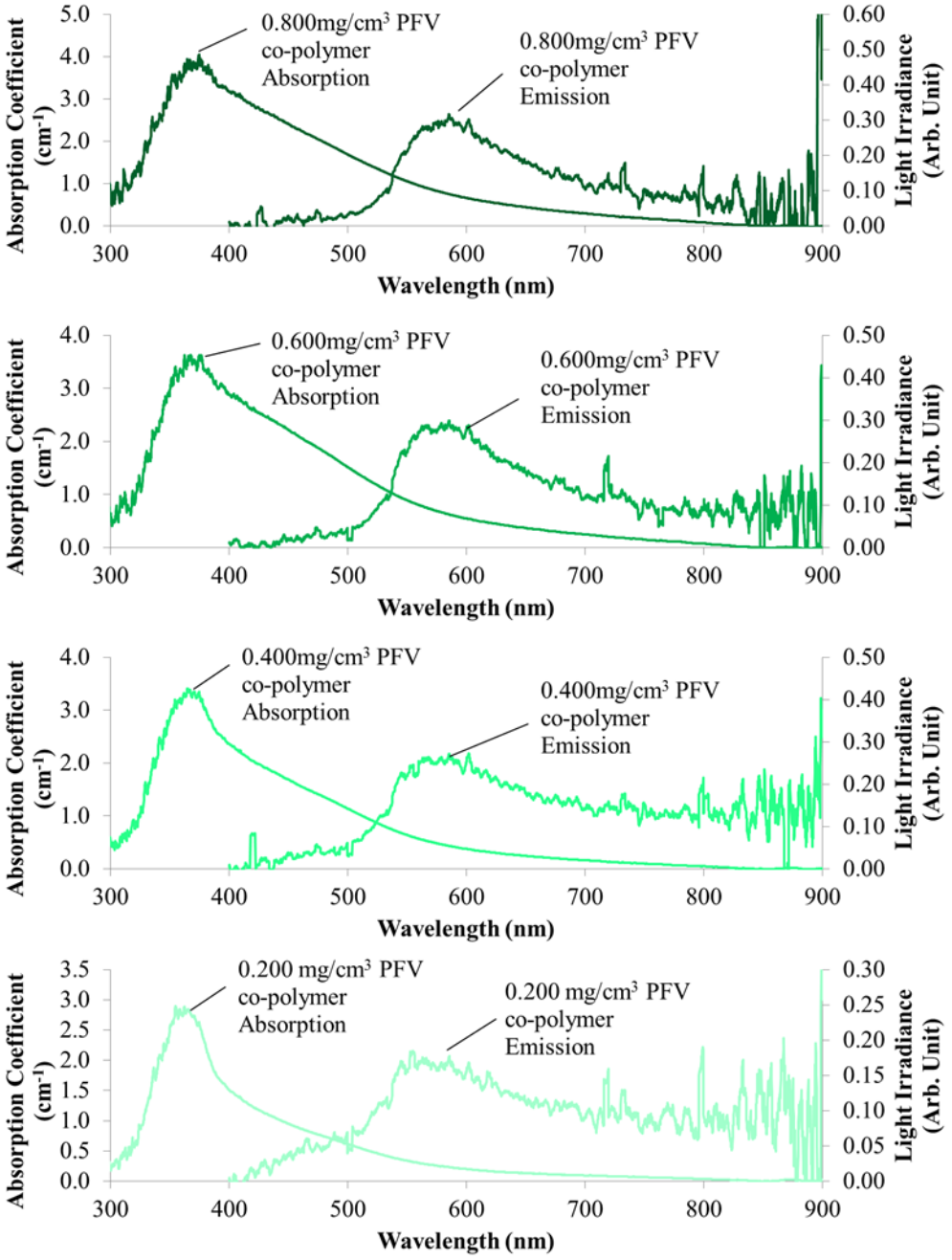

Figure 5.9 Absorption and light irradiance spectrum of UP LSC with PFV copolymer dye

Table 5.2 Absorption and light irradiance wavelength for UP LSC with PFV copolymer dye in different concentration

Dye Concentration (mg/cm^3)	Absorption peak wavelength (nm)	Light irradiance peak wavelength (nm)	Stoke's shift (nm)
0.200	354.84	555.01	200.17
0.400	364.78	601.90	237.12
0.600	375.13	585.05	209.92
0.800	374.70	585.44	210.74

From Table 5.2, the absorption wavelength for the lowest dye concentration (0.200 mg/cm^3) and the highest dye concentration (0.800 mg/cm^3) are 354.84 nm and 374.70 nm, respectively. While their light irradiance wavelengths are 555.01 nm and 585.44 nm respectively. Therefore, both their absorption and light irradiance peaks shift to a longer wavelength when the dye concentration is increased. The red-shift of both the absorption and light irradiance spectra can be observed in Figure 5.9. This is caused by the formation of J-aggregates that have longer absorption peak wavelength (Würthner et al. 2011). The explanation has been presented in section 4.5.1.

5.3.2 Light Irradiance and Optimum Concentration

Light irradiance spectra of UP LSCs with PFV copolymer in different concentrations were measured using a spectrometer. The light irradiance

irradiances were determined by integrating the area under light irradiance spectra. Comparing the light irradiances, as shown in Figure 5.10, the optimum dye concentration that provides the highest light irradiance can be determined. The optimum dye concentration for UP LSC with PFV copolymer dye is found to be 0.400mg/cm^3.

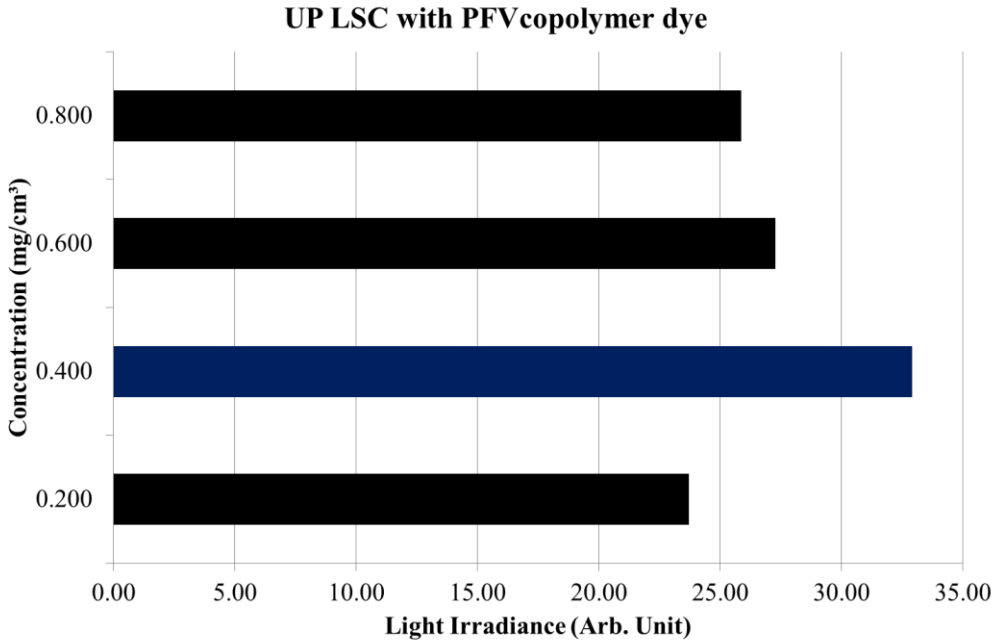

Figure 5.10 Light irradiance of UP LSC with PFVcopolymer dye in different concentration

5.4 Epoxy LSC with PFV Dye

LSCs presented in this section were constructed by doping PFV dye - Poly(9,9-di-(2-ethylhexyl)-9H-fluorene-2,7-vinylene) - in epoxy matrix as shown in Figure 5.11. They were casted in different dye concentrations to find out the optimum concentration that provides the highest light irradiance. Furthermore, a large amount of micro-voids was also formed in epoxy LSC

because the epoxy resin has high viscosity that facilitates the entrapment of micro-voids during casting process. Their absorption and light irradiance spectra are reported in the following section.

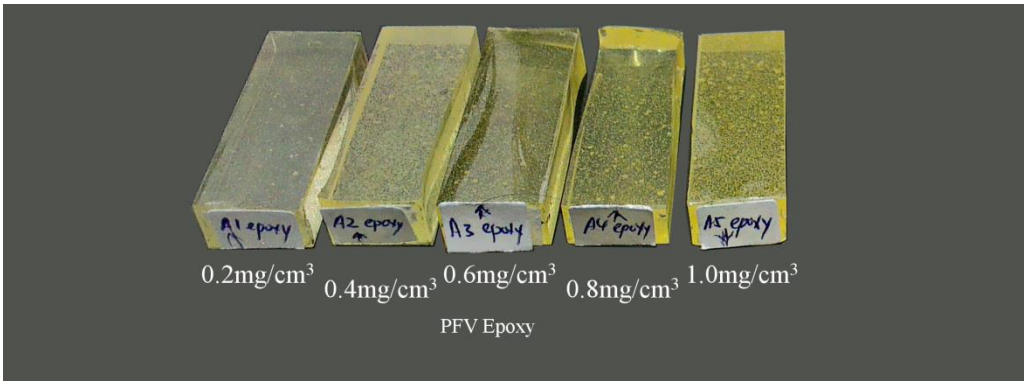

Figure 5.11 Epoxy LSC with PFV dye

5.4.1 Absorption and Light irradiance

The absorption and light irradiance spectra of the LSCs that were measured in the laboratory using spectrometer are shown in Figure 5.12 and Figure 5.13 respectively. Only 4 dye concentrations are shown in the figures - 0.400 mg/cm^3, 0.600 mg/cm^3, 0.800 mg/cm^3, and 1.000mg/cm^3 - so that changes in the spectra shapes between LSCs with increasing dye concentrations can be clearly observed. Absorption and light irradiance wavelengths of all the LSCs are listed in Table 5.3.

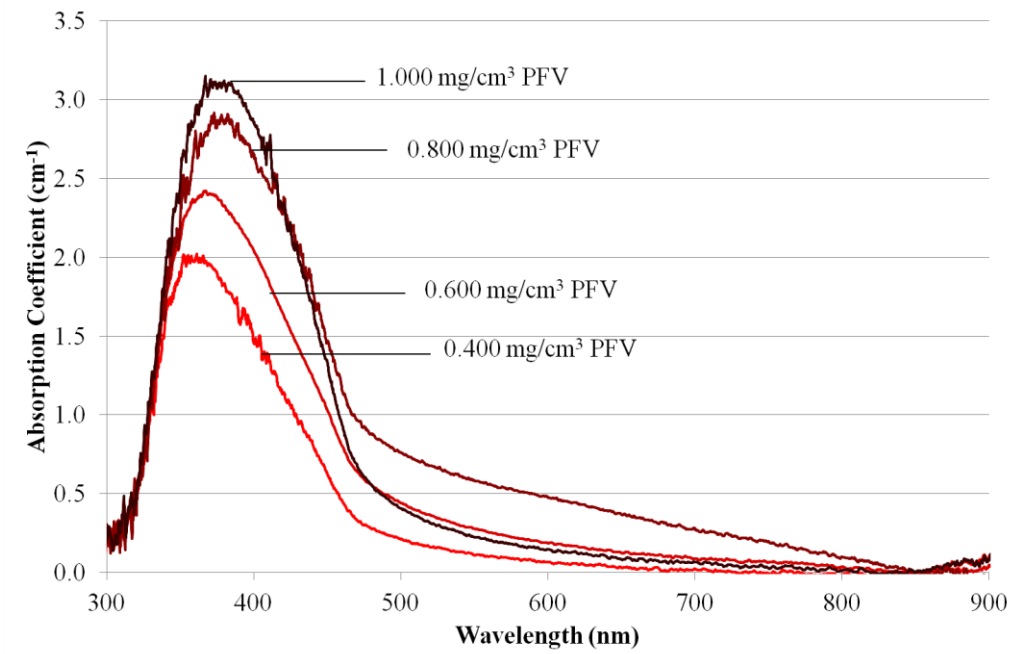

Figure 5.12 Absorption coefficient spectrum of epoxy LSC with PFV dye in different concentrations

Figure 5.12 shows that the peak absorption coefficient increases with the dye concentration. The absorption peak at 352.29 nm is observed for LSC with the lowest dye concentration. It is the absorption peak of dye monomers. When the dye concentration is higher, broader absorption peak with longer maximum absorption wavelength is observed. The absorption peak in this case is contributed by both the dye monomers and its aggregates. Further explanation on the formation of aggregates has been discussed in section 4.5.1.

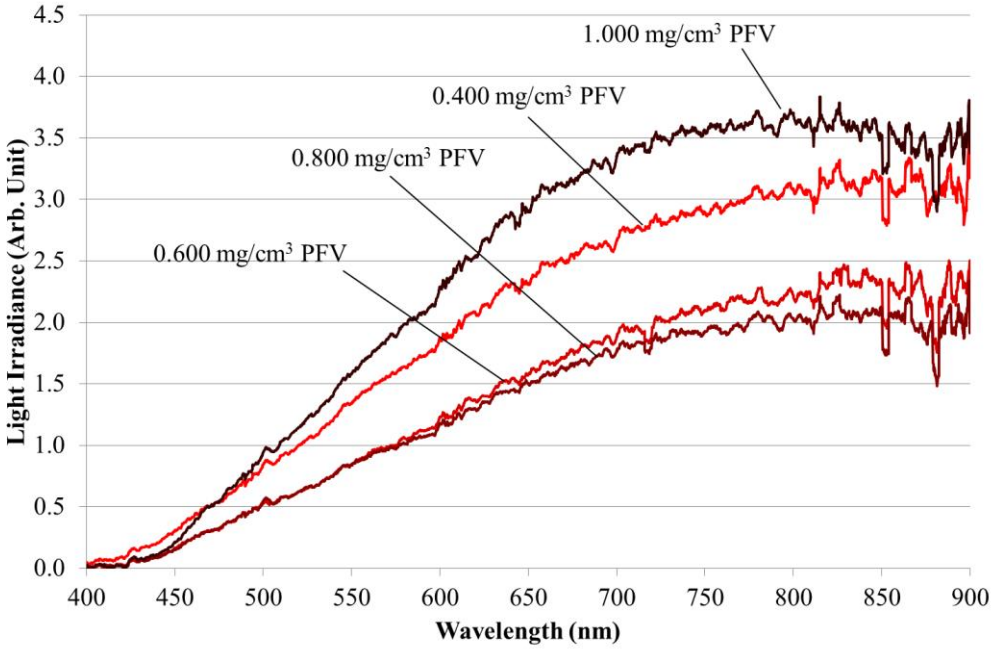

Figure 5.13 Light irradiance spectrum of epoxy LSC with PFV dye in different concentrations

From Figure 5.13, LSC with dye concentration of 1.000 mg/cm^3 has the highest light irradiance, but the light irradiance intensity does not increase with the dye concentration. The epoxy LSC has a broadband light irradiance spectrum that is similar to the incident light spectrum in shape, but different from the typical narrow band dye emission spectrum. This is because its light irradiance is not only contributed by the dye emission but also micro-voids scattering in LSC, which will be discussed in detail in section 5.7. In fact, the light irradiance is mainly contributed by the micro-void scattering. Dye emission doesn't contribute much to the total irradiance.

In Table 5.3, the absorption wavelengths for the lowest dye concentration (0.200 mg/cm^3) and the highest dye concentration (1.000 mg/cm^3) are 352.29 nm and 367.11 nm, respectively. The peak absorption wavelength is

predominantly affected by the dye absorption. The red-shift of absorption spectra can be observed, which is contributed by the dye aggregation. However, the actual dye light irradiance peak wavelength cannot be determined because micro-voids scatter light over a wide range of wavelengths. Therefore, the light irradiance peak wavelength in Table 5.3 is actually the micro-voids scattering peak wavelength. Variation in the light irradiance peak wavelength at different dye concentration is caused by electrical noise from the spectrometer at long wavelength and thus is random.

Table 5.3 Absorption wavelength and emission wavelength for epoxy LSC with PFV dye in different concentration

Dye Concentration (mg/cm^3)	Absorption peak wavelength (nm)	Light irradiance peak wavelength (nm)
0.200	352.29	736.42
0.400	361.19	747.25
0.600	366.69	744.31
0.800	373.02	736.60
1.000	367.11	736.60

5.4.2 Light Irradiance and Optimum Concentration

Light irradiance spectra of epoxy LSCs with PFV dye in different concentrations were measured using a spectrometer. The light irradiances were determined by integrating the area under light irradiance spectrum. Comparing the light irradiances, as shown in Figure 5.14, the LSC that provides the highest light irradiance is found to be 1.000 mg/cm^3. Unlike the LSC made of other

matrix materials, light irradiance of epoxy LSC is independent on the dye concentration. This is because its light irradiance is not entirely contributed by dye emission, but also micro-voids scattering. Since micro-voids scattering is much higher than that from the dye emission, its dye concentration that provides emissions has little influence on the light irradiance in this case. Detailed scattering mechanism of the micro-voids will be discussed in Section 5.7.

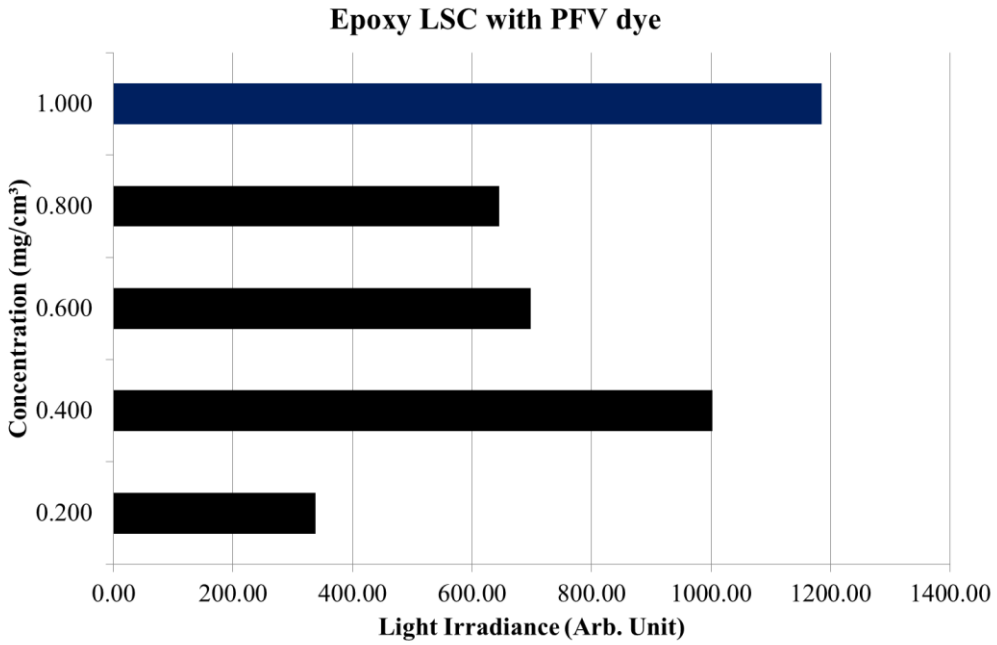

Figure 5.14 Light irradiance of epoxy LSC with PFV dye in different concentration

5.5 Epoxy LSC with PFV Copolymer

LSCs in this section were constructed by doping the PFV copolymer dye - Poly((9,9-di-(2-ethylhexyl)-9H-fluorene-2,7-vinylene)-co-(1-methoxy-4-(2-ethylhexyloxy)-2,5-(phenylenevinylene))--90:10 molar ratio - in epoxy

matrix as shown in Figure 5.15. They were casted in different dye concentrations to find out the optimum concentration that provides the highest light irradiance. Furthermore, numerous micro-voids were also formed in epoxy LSC due to the high viscosity of epoxy resin which promotes micro-voids entrapment during casting process. Their absorption and light irradiance spectra are reported in the following section.

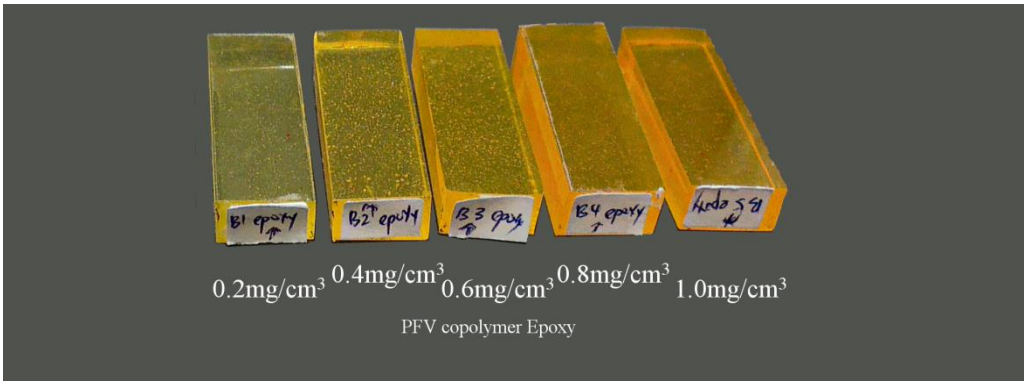

Figure 5.15 Epoxy LSC with PFV copolymer

5.5.1 Absorption and Light irradiance

The absorption and light irradiance spectra of the LSCs that were measured in the laboratory using spectrometer are shown in Figure 5.16 and Figure 5.17 respectively. Only 4 dye concentrations are shown in the figures - 0.400 mg/cm^3, 0.600 mg/cm^3, 0.800 mg/cm^3, and 1.000 mg/cm^3 - so that changes in the spectra shapes between LSCs with increasing dye concentrations can be clearly observed. Absorption and light irradiance wavelengths of all the LSCs are listed in Table 5.4.

Figure 5.16 shows that the peak absorption coefficient increases with the increase in dye concentration. The absorption peak at around 358.23 nm is observed for LSC with low dye concentration while broader absorption peak with longer absorption peak wavelength up to 385.02 nm is found for that with higher dye concentration. The former is the dye monomers absorption peak; the latter is contributed by both dye monomers and its aggregates. Further description of dye aggregates is presented in 4.3.1.

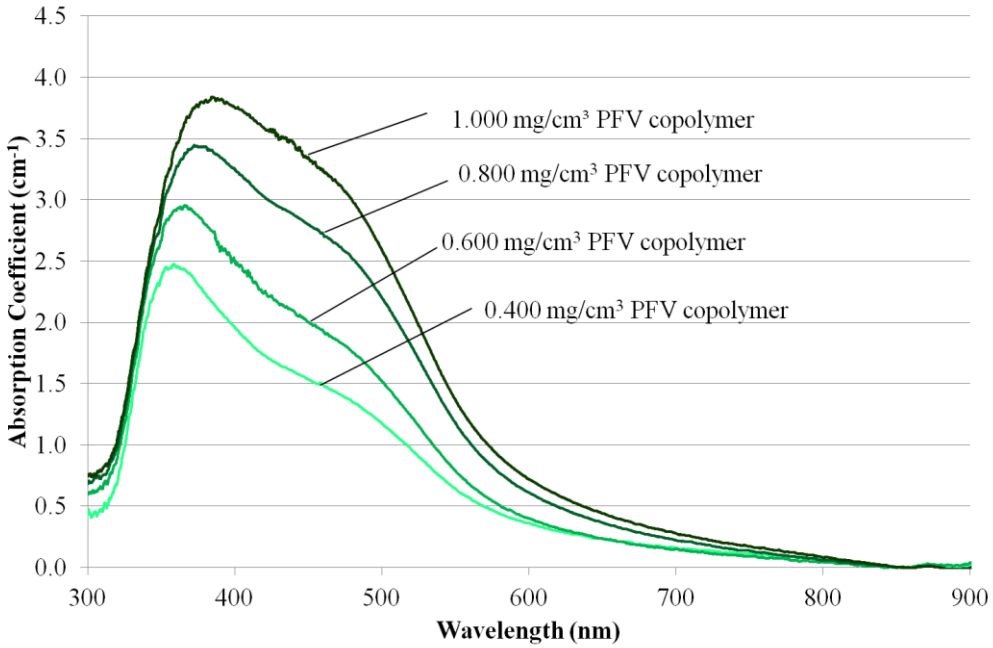

Figure 5.16 Absorption coefficient spectrum of epoxy LSC with PFV copolymer dye in different concentration

From Figure 5.17, LSC with dye concentration of 0.800 mg/cm^3 has the lowest light irradiance while 0.600 mg/cm^3 has the highest light irradiance, and the light irradiance intensity does not increase with the increase of dye concentration. Similar to the result in Section 5.4.1, the light irradiance is not only contributed by the dye emission but also, predominantly contributed by

the micro-voids scattering. Further explanation on the micro-voids scattering will be presented in Section 5.7.

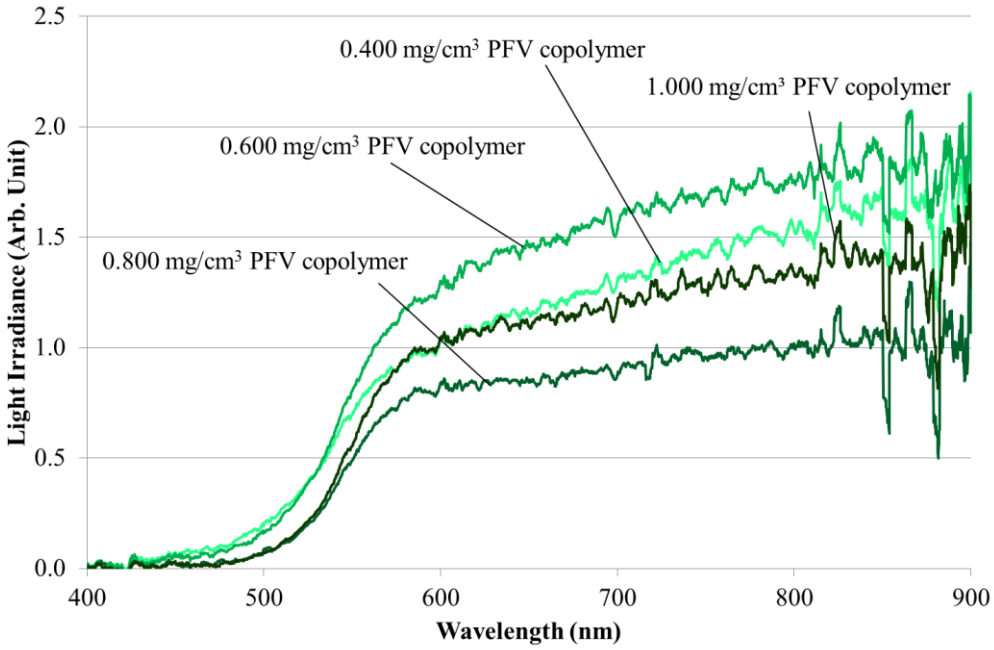

Figure 5.17 Light irradiance spectrum of epoxy LSC with PFV copolymer dye in different concentration

From Table 5.4, the absorption wavelengths for the lowest dye concentration (0.200 mg/cm^3) and the highest dye concentration (1.000 mg/cm^3) are 353.14 nm and 385.02 nm, respectively. The peak absorption wavelength is predominantly affected by the dye absorption. It shifts to a longer wavelength when the concentration is higher due to dye aggregation. However, the actual light irradiance peak wavelength cannot be determined because it is hidden by micro-voids scattering that has much higher intensity. Therefore, the light irradiance peak wavelength in Table 5.4 is actually the micro-voids scattering peak wavelength. Variation in the light irradiance peak wavelength at different

dye concentration is random because it is only affected by electrical noises from the spectrometer at long wavelength.

Table 5.4 Absorption wavelength and light irradiance wavelength for epoxy LSC with PFV copolymer dye in different concentration

Dye Concentration (mg/cm^3)	Absorption wavelength (nm)	Light irradiance wavelength (nm)
0.200	353.14	711.98
0.400	358.23	743.21
0.600	365.63	736.42
0.800	372.17	722.20
1.000	385.02	736.42

5.5.2 Light irradiance and Optimum Concentration

Light irradiance spectra of epoxy LSCs with PFV copolymer dye in different concentrations were measured using a spectrometer. The light irradiances were determined by integrating the area under light irradiance spectrum. Comparing the light irradiances, as shown in Figure 5.18, the LSC that provides the highest light irradiance can be determined. It is found to be $0.600mg/cm^3$.

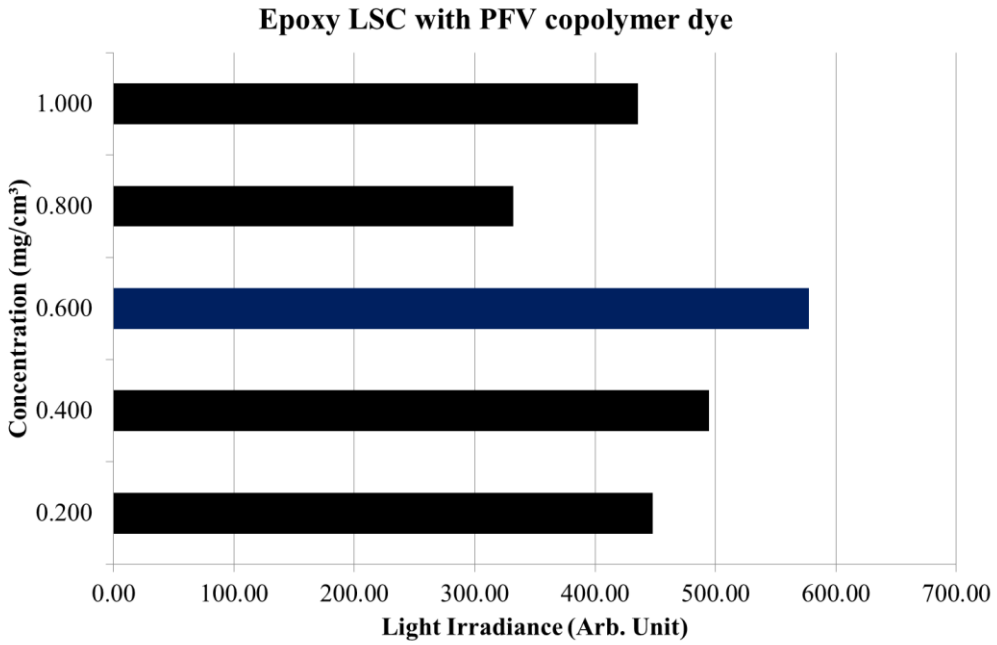

Figure 5.18 Light irradiance of epoxy LSC with PFV copolymer dye in different concentration

5.6 Comparison of LSCs with Different Matrices at Their Optimum Dye Concentrations

PFV dye, PFV copolymer dye and Rhodamine 6G LSCs with different matrices (PMMA, unsaturated polyester and epoxy) at their respective optimum dye concentrations were selected to compare their absorption and light irradiance. The selected LSCs with their optimum dye concentrations are listed in Table 5.5. Their absorption and light irradiance spectra are plotted in Figure 5.19.

Table 5.5 LSCs with different matrices at their optimum dye concentrations

LSC	Matrices	Optimum concentration
PFV dye	PMMA	0.5 mg/cm^3
	Unsaturated Polyester	0.6 mg/cm^3
	Epoxy	1.0 mg/cm^3
PFV copolymer dye	PMMA	0.5 mg/cm^3
	Unsaturated Polyester	0.4 mg/cm^3
	Epoxy	0.6 mg/cm^3
Rhodamine 6G	PMMA	0.0375 mM
	Unsaturated Polyester	0.0375 mM
	Epoxy	0.0375 mM

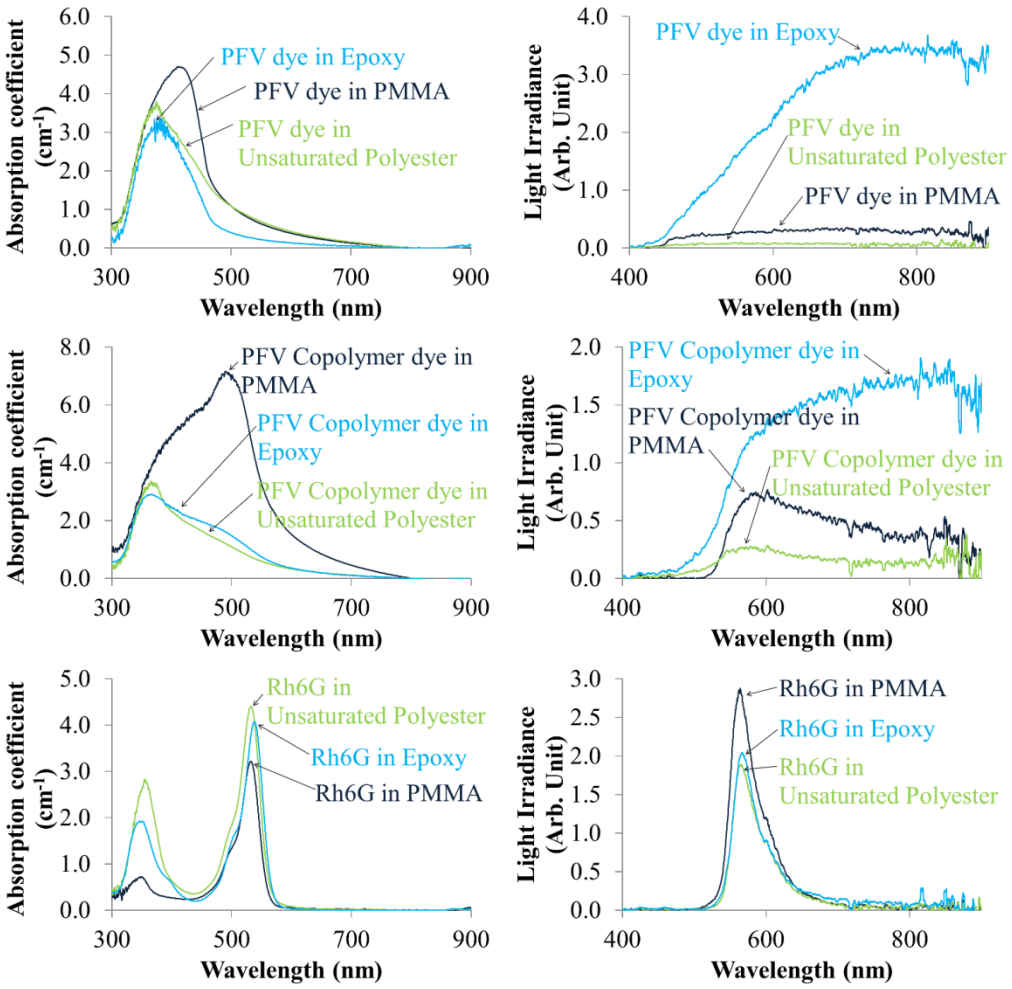

Figure 5.19 Absorption and Light irradiance of LSCs with different matrices at their optimum dye concentrations

The light irradiances of all the LSCs are determined by integrating the area under the light irradiance spectrum. They are shown in Figure 5.20. The graph was also labeled with the number of micro-voids found in epoxy LSC. It is used to compare and find out which polymer matrix has the potential to be used in LSC.

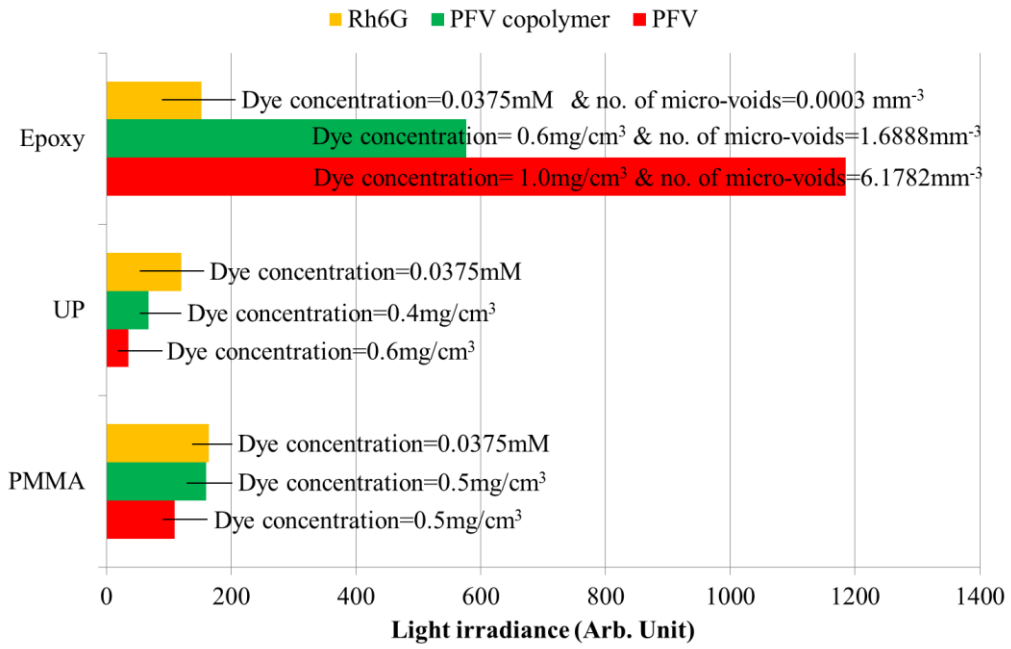

Figure 5.20 Light irradiance of LSCs with different matrices at their optimum dye concentrations

In PMMA and UP matrices, it is noticed that Rh6G dye gives the highest light irradiance, followed by PFV copolymer dye and PFV dye. However, epoxy LSCs give the highest light irradiance among all the LSCs. This is because of the existent of numerous micro-voids embedded in the epoxy LSC that scatter and trap additional incoming sunlight in LSCs. This results in higher light irradiance at the edges of the LSC which will be further discussed in section 5.7.

5.7 Micro-voids Scattering in Epoxy LSC

From the results in Section 5.4 and 5.5, it was shown that light irradiance of LSC is not entirely contributed by the dye emission. In fact it is contributed by micro-voids scattering as well. In other words, the micro-voids help increase the light irradiance of LSC. Therefore, in this section, four epoxy LSCs: LSCs with PFV dye at optimum concentration, second optimum concentration and the worst concentration, as well as one LSC with Rh6G have been selected to study the effect of micro-voids concentration on scattering intensity. The scattering mechanism of microvoids will be presented in this section as well.

5.7.1 Measurement of Micro-voids Sizes and Concentration

The sizes and concentration of micro-voids in epoxy LSCs were measured using an optical microscope – Meiji Techno MT4300L biological microscope – with a digital camera attached on it as shown in Figure 5.21. As illustrated in Figure 5.22, the micro-voids images were captured from the top surface to the bottom surface of LSC by adjusting vertical position of the LSC sample and the micro-voids sizes were measured and labeled using ViS digital imaging and measurement software. Micro-void concentration was calculated as the division of number of distinct micro-voids observed in all microscope images from top surface to bottom surface by the volume being measured. The measurement was repeated for at least 3 locations chosen randomly in the LSC and the average micro-void concentration was taken as the final result. Sizes of

all distinct micro-voids in the repeated measurements were used to study the distribution of micro-void size in each LSC.

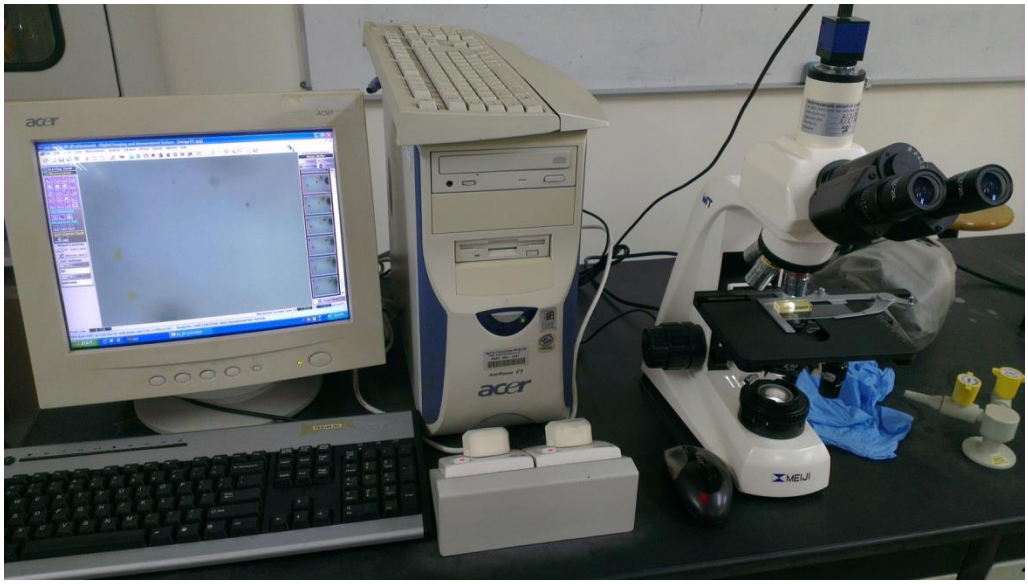

Figure 5.21 Optical microscope attached with digital camera and the digital imaging and measurement software.

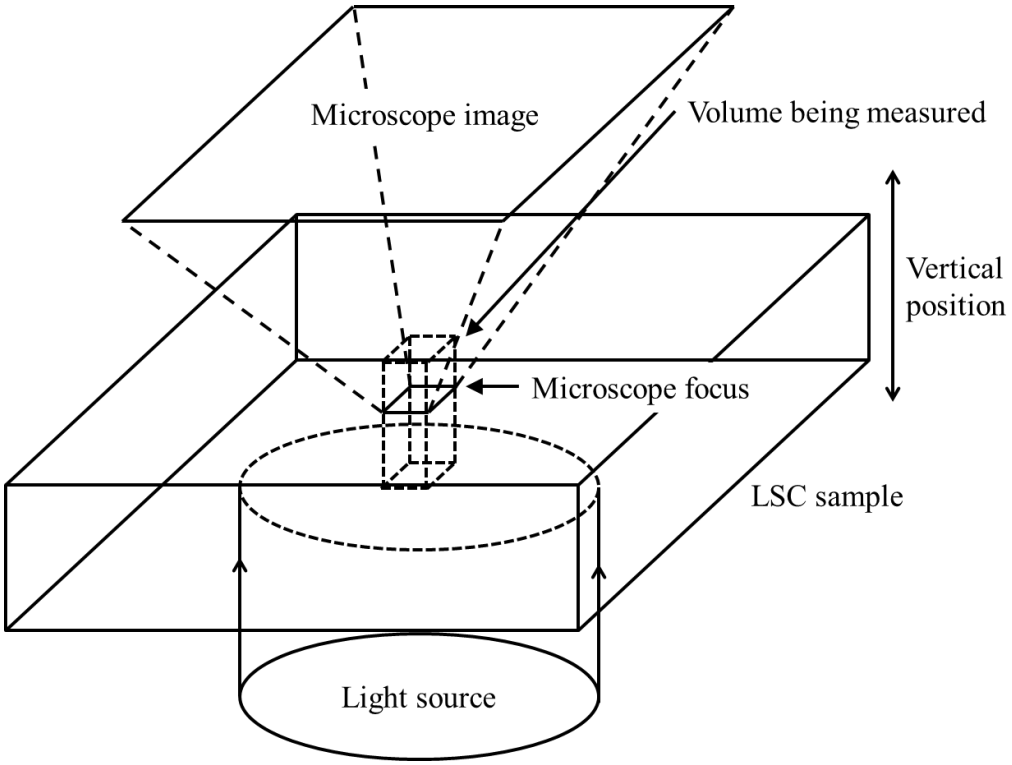

Figure 5.22 Illustration of micro-voids sizes and concentration measurement method.

5.7.2 Distribution of Micro-voids Sizes

Figure 5.23 and Figure 5.24 are the optical microscope images of PFV and Rh6G epoxy LSCs respectively, showing only a small portion of the full image in each figure. The figures show the actual appearance of micro-voids in epoxy LSC under optical microscope when they were viewed from the opposite surface where the incident light was illuminating. The incident light passed through the middle part of the micro-void and the rest was scattered away from the micro-void. Detailed explanation of this observation will be given in Section 5.7.4.

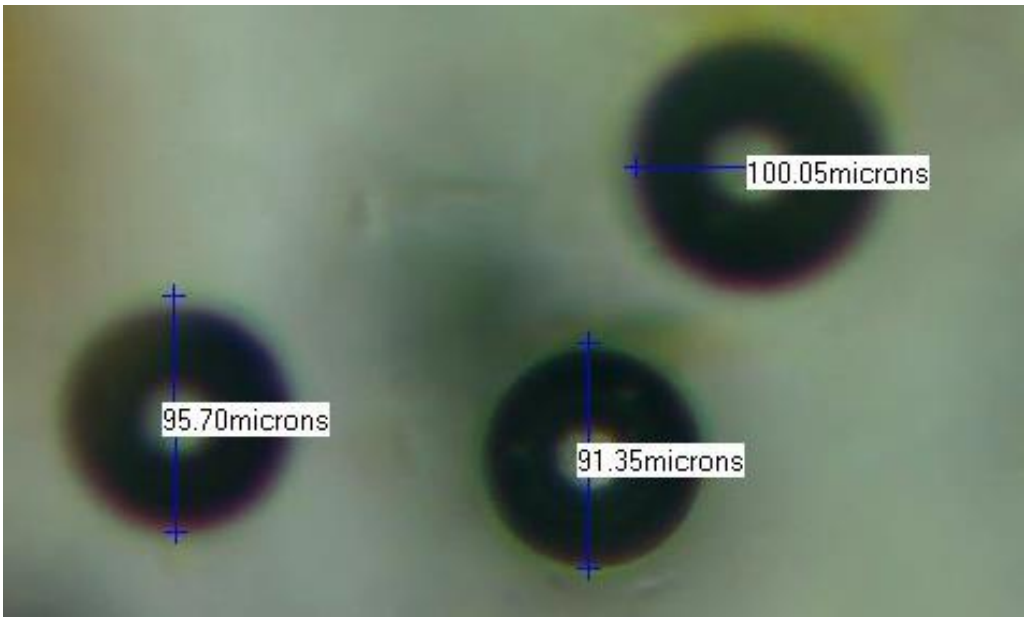

Figure 5.23 Micro-void sizes for epoxy LSC with PFV dye

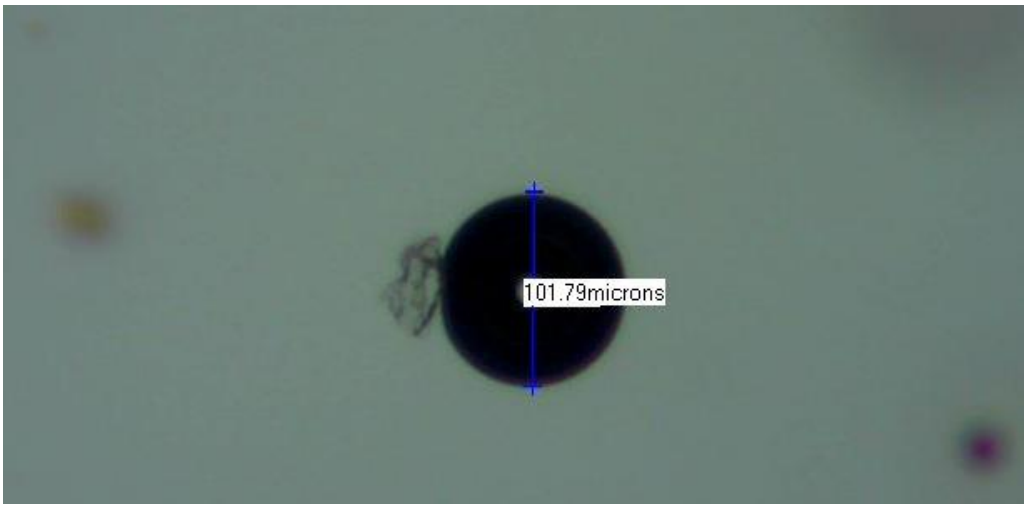

Figure 5.24 Micro-void sizes for epoxy LSC with Rh6G dye

Histograms showing the distribution of bubble size for the three PFV epoxy LSC at 1.0 mg/cm^3, 0.4 mg/cm^3 and 0.2 mg/cm^3 are shown in Figure 5.25, Figure 5.26 and Figure 5.27, for the LSC with highest light irradiance, second highest light irradiance and the lowest light irradiance respectively. The results show that micro-void sizes are normally distributed.

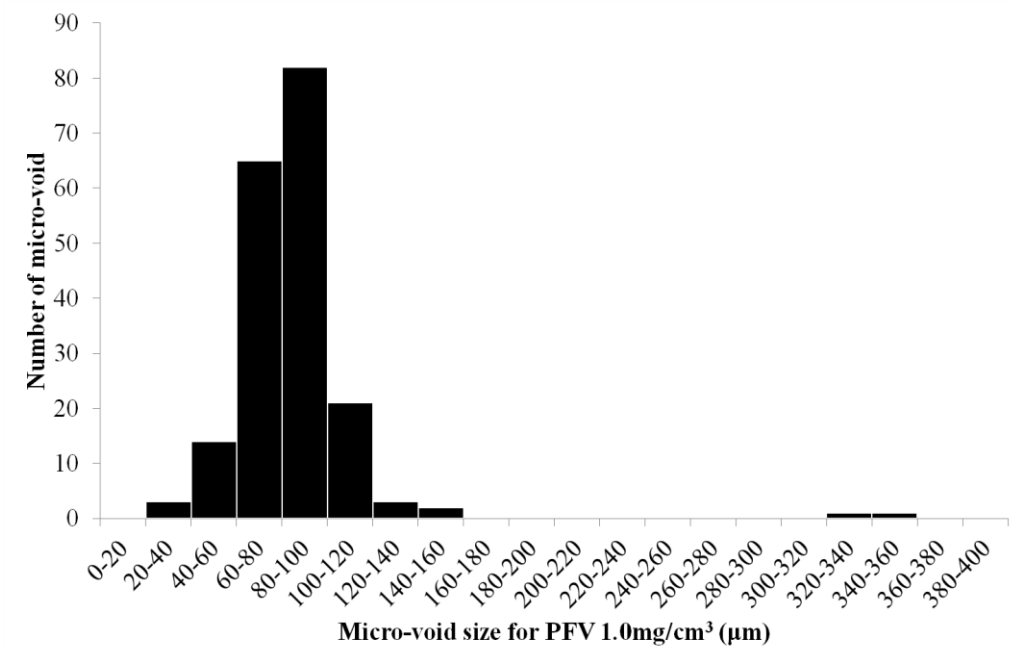

Figure 5.25 Histogram showing the distribution of micro-void size for Epoxy LSC with PFV dye at 1.0 mg/cm^3 (optimum concentration)

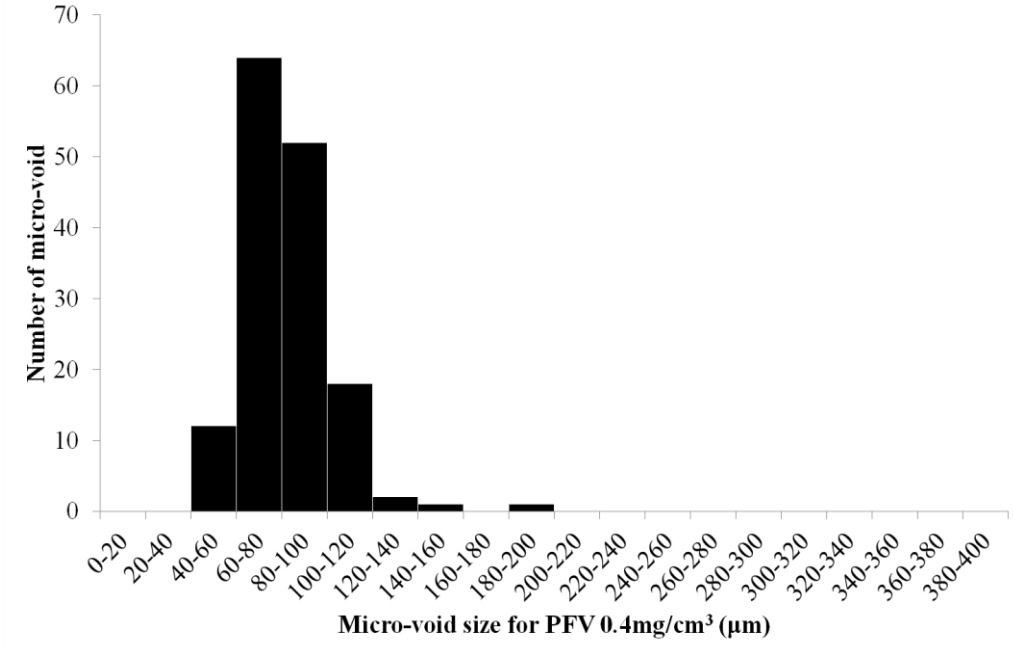

Figure 5.26 Histogram showing the distribution of micro-void size for Epoxy LSC with PFV dye at 0.4 mg/cm^3 (second optimum concentration)

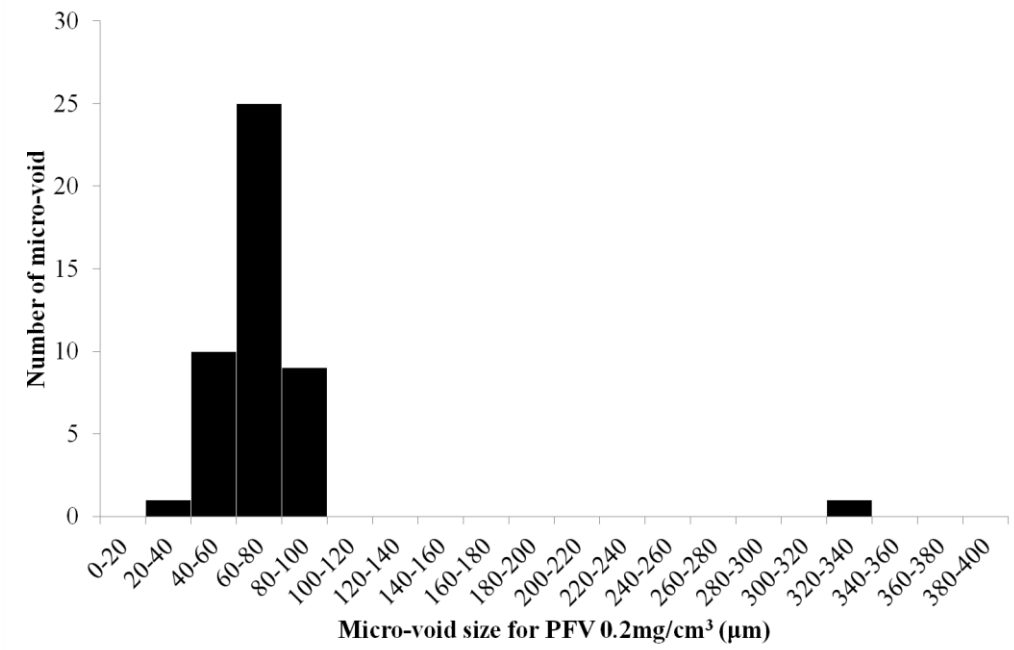

Figure 5.27 Histogram showing the distribution of micro-void size for Epoxy LSC with PFV dye at 0.2 mg/cm^3 (worst concentration)

5.7.3 Effect of Micro-voids Concentration to Scattering Intensity

The relationship between the light irradiance, average micro-void diameter and the micro-void concentration are tabulated as shown in Table 5.6. It is noticed that the micro-void scattering is affected by micro-void concentration as shown in Figure 5.28. The epoxy LSC with PFV dye has higher light irradiance because it has higher micro-void concentration (6.1782 mm^{-3}) compared to epoxy LSC with Rh6G dye that has a very low micro-void concentration (0.0003 mm^{-3}). Therefore, it can be concluded that high micro-void concentration favor the bubble scattering and increase the light irradiance of LSC.

The average micro-void size for the three PFV epoxy LSC is in the range of 101.96 - 104.90 μm. The micro-voids concentration for the LSC with the highest light irradiance (1.0 mg/cm^3) is 6.1782 per mm^3 and that for the lowest light irradiance (0.2 mg/cm^3) is 1.4718 per mm^3.

Table 5.6 Light irradiance, average micro-void diameter and micro-void concentration for three optimum dye concentration of epoxy LSC

Luminescent dye in epoxy LSC	Dye concentration	Light irradiance (Arb. unit)	Average micro-void diameter (μm)	Micro-void concentration[1] (mm^{-3})
PFV dye	1.0 mg/cm^3	1145.40	104.90	6.1782
	0.4 mg/cm^3	964.52	102.18	3.2247
	0.2 mg/cm^3	338.54	101.96	1.4718
Rh6G	0.0375 mM	142.73	101.79	0.0003

[1] Number of micro-void per mm^3.

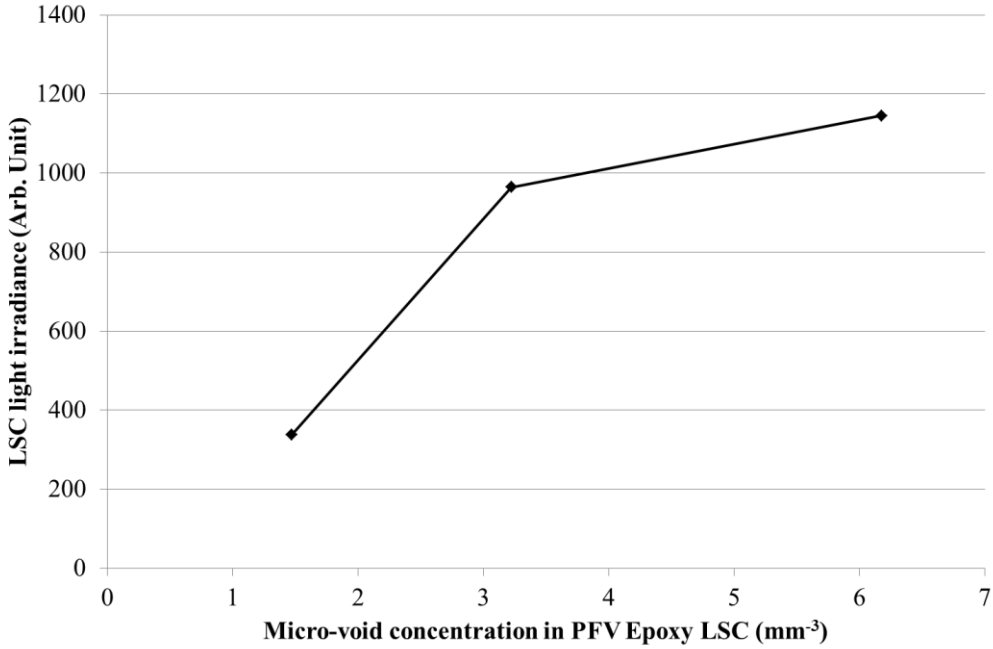

Figure 5.28 Effect of micro-void concentration on PFV epoxy LSC light irradiance

5.7.4 Mechanism of Micro-voids Scattering in Epoxy LSC

There are three modes of light scatterings, namely Rayleigh, Mie and Geometric scatterings (Bohren & Huffman 2008). The parameter $\alpha=\pi D_p/\lambda$ can be used to identify the types of light scattering that predominantly happen in a medium containing scatterers, where πD_p is the circumference of a scatterer and λ is the wavelength of the incident radiation.

The modes of light scatterings depending on the value of α are given below:

1. Rayleigh scattering happens if α is less than 1.

2. Mie scattering happens if α is about 1
3. Geometric scattering happens if α is larger than 1.

The average diameters of the micro-voids in epoxy LSC are within the range of 101.96 to 104.90 μm which are much larger than the wavelengths of sunlight ranging from 0.25 to 3.0 μm. Therefore, the value of α is always greater than 10. It is concluded that Geometric scattering is the major scattering mechanism during the interaction of incident light with the micro-voids in epoxy LSC. The incident light is scattered to different directions as it propagates across a micro-void as illustrated in Figure 5.29. The majority of the scattered light is therefore trapped within the LSC, hence improving the output of the LSC.

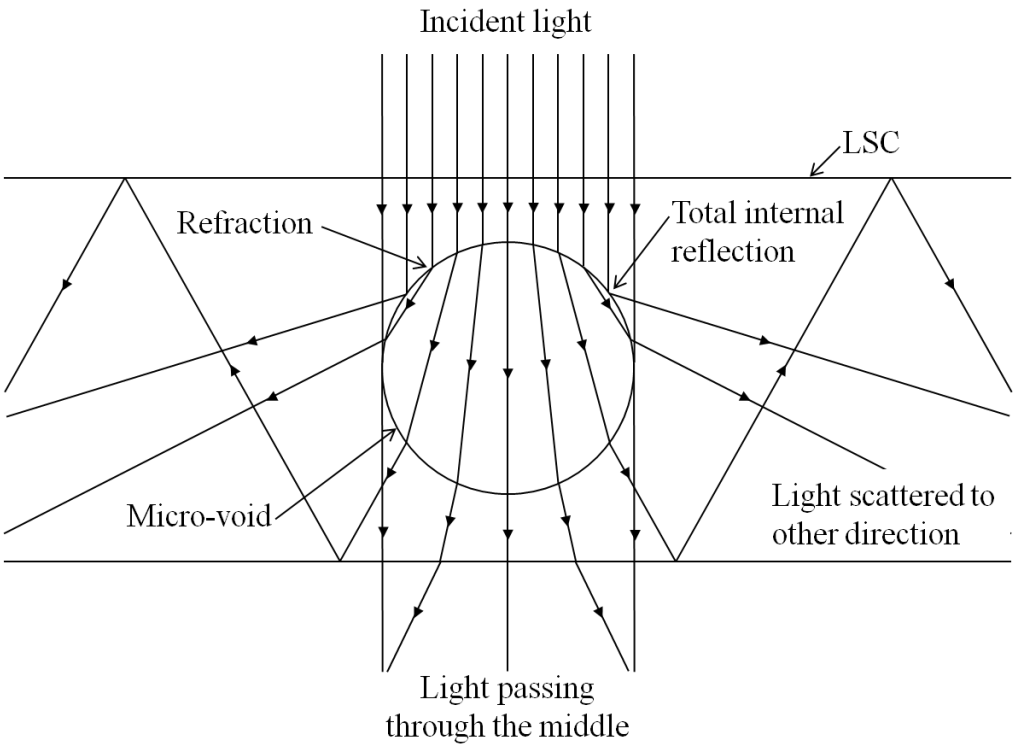

Figure 5.29 Scattering of sunlight when it crosses a micro-void in epoxy LSC

5.8 Summary

The absorption and light irradiance measurement results of unsaturated polyester LSC and epoxy LSC with different dyes – PFV and PFV copolymer – have been presented in details in this chapter. Results of each dye with different concentrations have been shown and optimum concentration of each dye that provides the highest light irradiance has been determined.

After that, the LSCs with optimum PFV and PFV copolymer concentration from each polymer matrix have been selected to compare their absorption and light irradiance with that of a reference dye, Rhodamine 6G.

Besides, the light irradiances of LSCs with different polymer matrices are compared. The results show that the LSC with epoxy matrix gives much higher light irradiance than that with PMMA or unsaturated polyester matrix.

The formation of micro-voids embedded in the epoxy matrix scatters some amount of the incident light and increased the LSC light irradiance. Furthermore, the micro-void size distribution, effect of micro-voids concentration to scattering intensity, and mechanism of micro-voids scattering in epoxy LSC have been described as well in this chapter.

CHAPTER 6

THE PERFORMANCE OF LUMINESCENT SOLAR CONCENTRATORS

This chapter presents the performance evaluation of luminescent solar concentrators by comparing the short circuit current densities output from different solar cells attached to their edges, determining the power conversion efficiencies of solar cells attached to the LSCs with micro-voids and evaluating the photo-degradation rates of LSCs. The current densities and power conversion efficiencies are calculated from the spectral response of different commercially available solar cells. The photo-degradation rates of LSCs are determined by monitoring their peak absorption coefficient and light irradiance over a period of 30 days under the sun.

6.1 Short Circuit Current Density of Different Solar Cells for LSCs

The short circuit current density (J_{sc}) of a solar cell is defined as its electrical current output per unit solar cell area. Short circuit current density of the solar cells attached to a LSC was calculated by integrating the multiplication of the light irradiance of the LSC measured in cuvette holder with the spectral response of the respective solar cells, as shown in Equation 6.1. The light irradiances of LSCs are shown in Figure 4.4, Figure 4.9, Figure 4.14, Figure 4.19, Figure 5.3, Figure 5.8, Figure 5.13, and Figure 5.17. The spectral responses of a number of solar cells were obtained from other

publication (Field 1997). The types of solar cells and their spectral responses are shown in Figure 6.1.

In this section, the spectral response has a unit of current per unit power (AW^{-1}). However, the calculated short circuit current density generated by the solar cells attached to the LSC has arbitrary unit. This is because radiometric calibration on the spectrometer connected to the cuvette holder was only carried out using a light source with known normalized spectral irradiance and therefore the light irradiance it measured has arbitrary units instead of absolute spectral irradiance unit of $Wm^{-2}nm^{-1}$.

$$J_{sc} = \int I_{em}(\lambda)\, SR(\lambda)\, d\lambda \qquad 6.1$$

Where,

J_{sc} = Short circuit current density of solar cell (Arbitrary unit);

$I_{em}(\lambda)$ = Light irradiance of LSC measured in cuvette holder (Arbitrary unit);

$SR(\lambda)$ = Spectral response of solar cell (AW^{-1}).

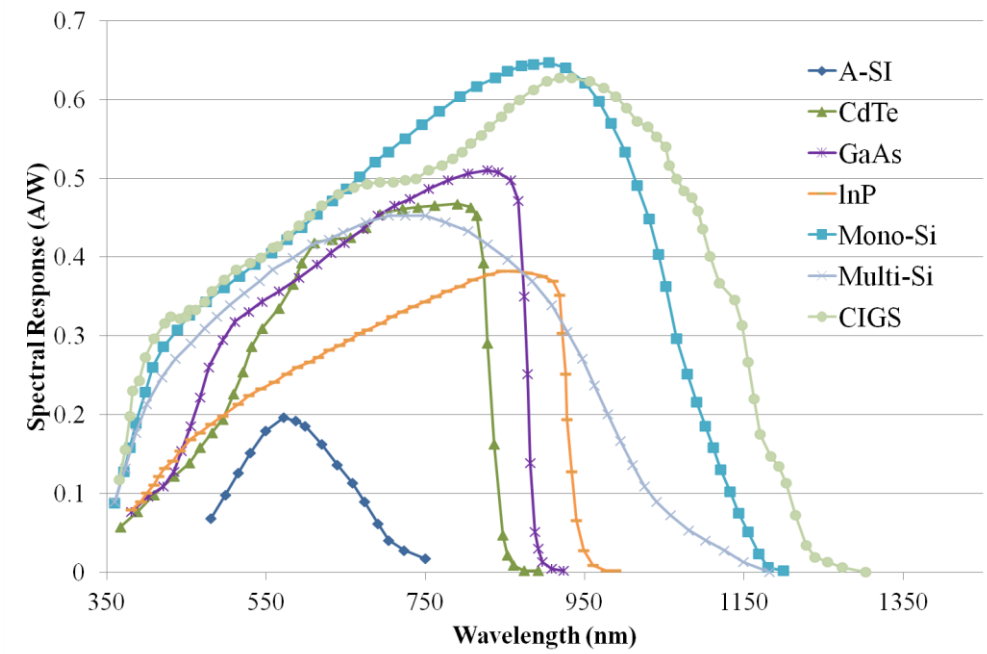

Figure 6.1 Spectral response of solar cells

6.1.1 Short Circuit Current Density for PMMA LSC with Polymerizable Naphthalimide Dye

The short circuit current density of solar cells attached to PMMA LSCs with different concentrations of polymerizable naphtahlimide dye (4-butylamino-N-allyl-1,8-naphthalimide dye) are shown in Figure 6.2. The mono-crystalline silicon solar cell (Mono-Si) and copper indium gallium selenide solar cell (CIGS) give the highest short circuit current density for all LSCs. For all types of solar cells, the solar cell attached to LSC with the optimum dye concentration - 75 μM as determined in Chapter 4.3.2 - generated the highest short circuit current density, as compared with those attached to LSCs with other dye concentration.

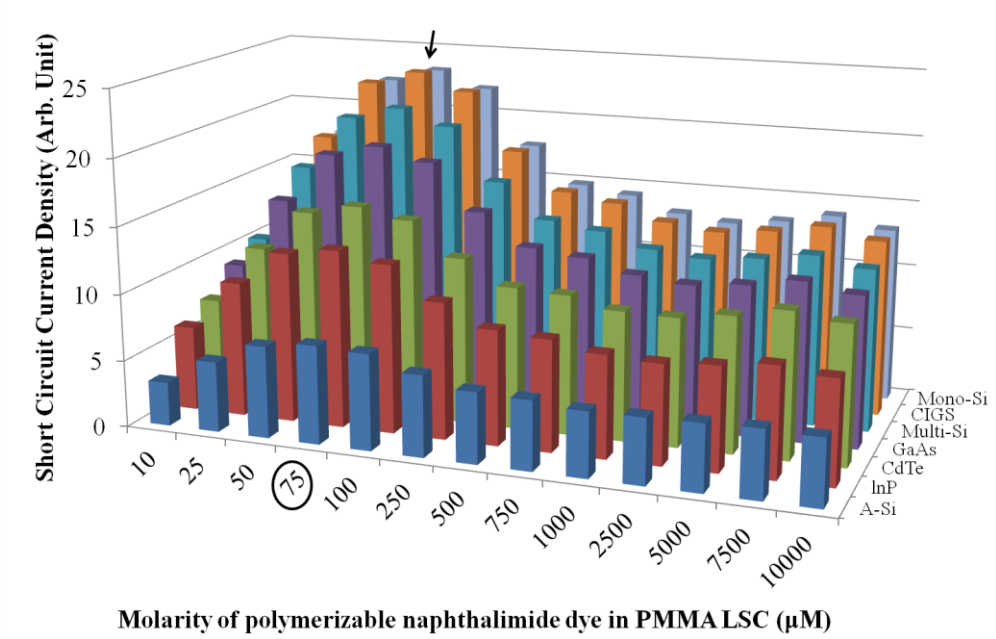

Figure 6.2 Short circuit current density for PMMA LSC with polymerizable naphthalimide dye in different concentration

6.1.2 Short Circuit Current Density for Multiple-dye PMMA LSC with Polymerizable Naphthalimide Dye and Rhodamine 6G

The short circuit current density of solar cells attached to PMMA LSC with the mixture of polymerizable naphtahlimide dye (4-butylamino-N-allyl-1,8-naphthalimide dye) and Rhodamine 6G in different ratio are plotted as shown in Figure 6.3. Similar to the result in section 6.1.1, the mono-crystalline silicon solar cell (Mono-Si) and the copper indium gallium selenide solar cell (CIGS) are still the solar cells that give the highest short circuit current density for all LSC. For all types of solar cells, the solar cells attached to LSC with the optimum polymerizable naphthalimide dye to Rhodamine 6G mixing ratio of 2:1 (75 µM Naph + 37.5 µM Rh6G), as obtained in Chapter 4.4.1 generates the highest short circuit current density, as compared with those attached to LSCs

with other dye mixing ratio. Moreover, solar cells with the optimum multiple-dye PMMA LSC also give slightly higher short circuit current density than that with Rhodamine 6G LSC.

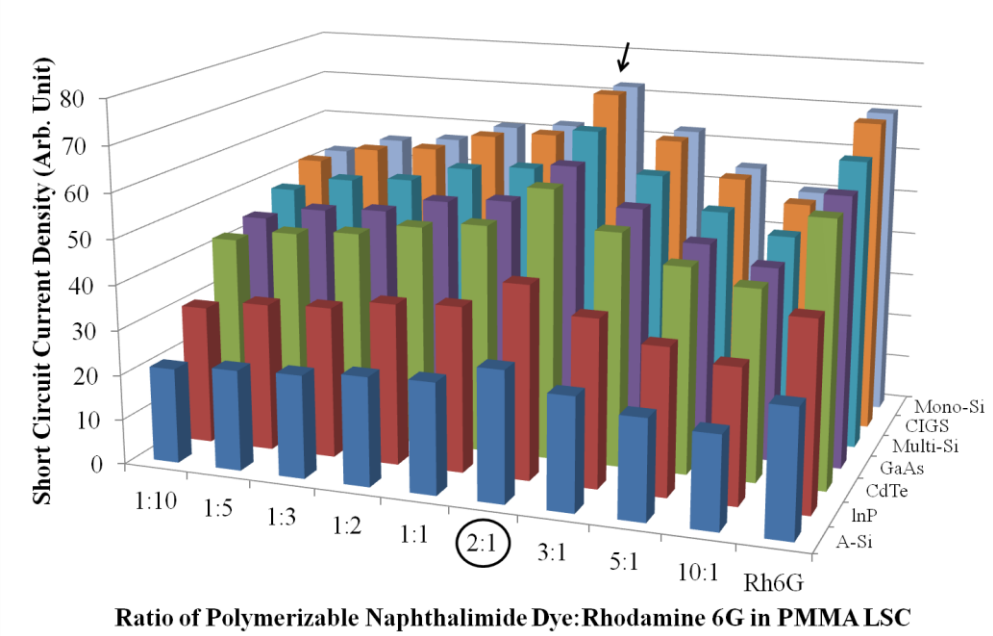

Figure 6.3 Short circuit current density for multiple dye PMMA LSC with polymerizable naphthalimide dye and rhodamine 6G

6.1.3 Short Circuit Current Density for PMMA LSC with PFV dye and PFV copolymer dye

The short circuit current density of solar cells attached to PMMA LSC with PFV dye and PFV copolymer dye are plotted as shown in Figure 6.4 and Figure 6.5 respectively. Similarly, the mono-crystalline silicon solar cell (Mono-Si) and the copper indium gallium selenide solar cell (CIGS) give the highest short circuit current density for all LSCs. Besides, for all types of solar cells, the solar cell attached to LSC with the highest concentration (0.500

mg/cm^3) of either PFV dye or PFV copolymer dye generate the highest short circuit current density, as compared with those attached to LSCs with other dye concentration. From both figures, PMMA LSC with PFV copolymer dye has higher short circuit current density than that with PFV dye.

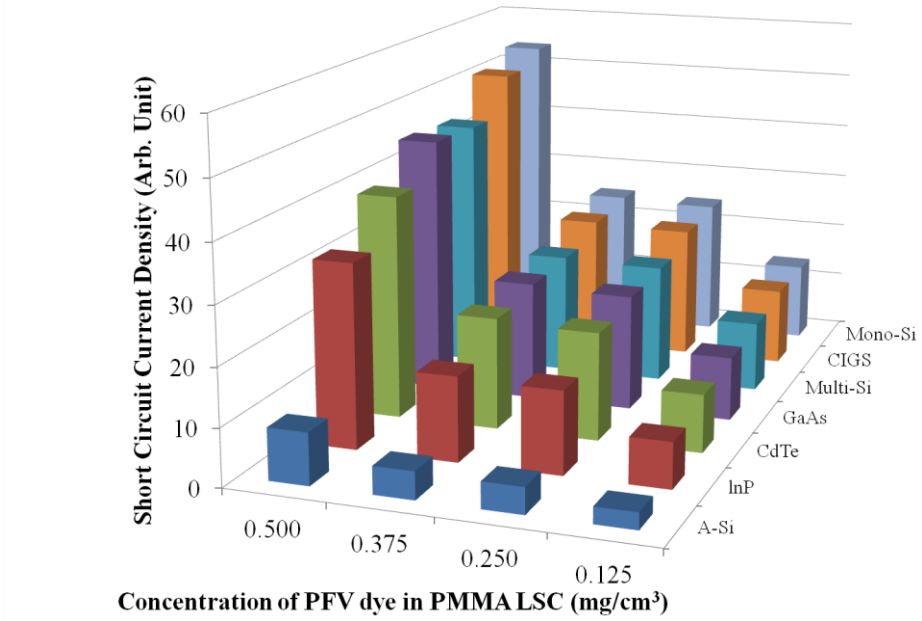

Figure 6.4 Short circuit current density for PMMA LSC with PFV dye

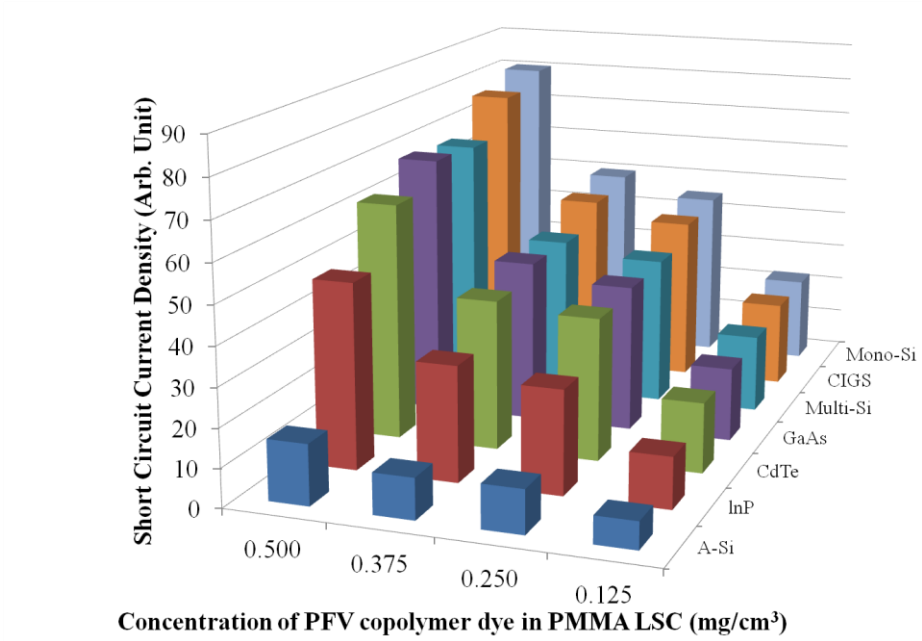

Figure 6.5 Short circuit current density for PMMA LSC with PFV copolymer dye

6.1.4 Short Circuit Current Density for UP LSC with PFV dye and PFV copolymer dye

The short circuit current density of solar cells attached to UP LSC with PFV dye and PFV copolymer dye are plotted as shown in Figure 6.6 and Figure 6.7 respectively. Mono-crystalline silicon solar cell (Mono-Si) and copper indium gallium selenide solar cell (CIGS) give the highest short circuit current density for all LSCs regardless to dye type. Solar cells attached to the LSCs with dye concentration of 0.600 mg/cm^3 for PFV dye or 0.400 mg/cm^3 for PFV copolymer dye provide the highest short circuit current density, as compared with those attached to LSCs with other dye concentration.

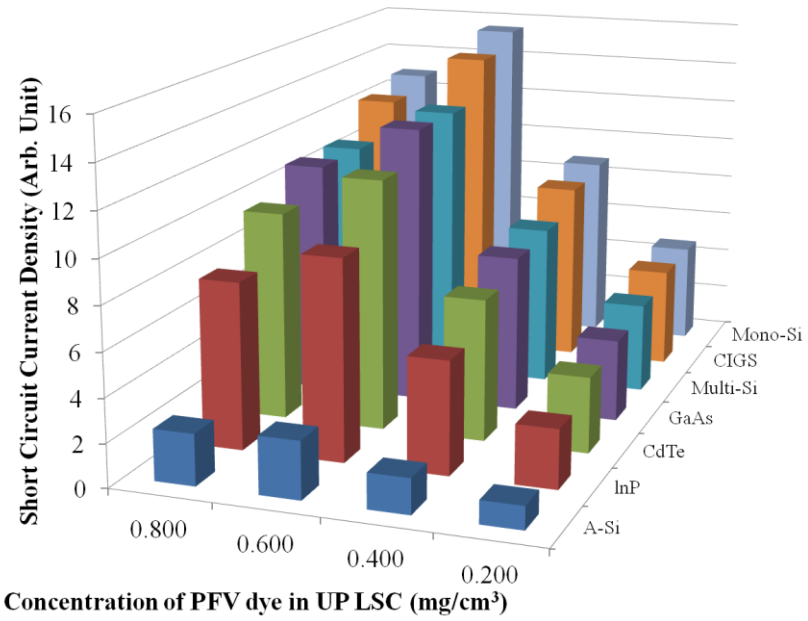

Figure 6.6 Short circuit current density for UP LSC with PFV dye

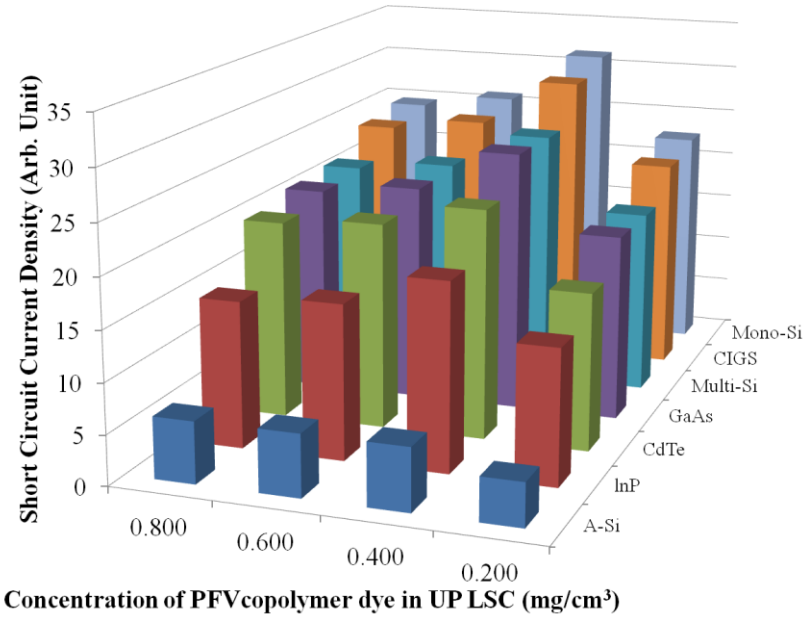

Figure 6.7 Short circuit current density for UP LSC with PFV copolymer dye

6.1.5 Short circuit Current Density for epoxy LSC with PFV dye and PFV copolymer dye

The short circuit current density of solar cells attached to epoxy LSC of PFV and PFV copolymer dye are plotted as shown in Figure 6.8 and Figure 6.9 respectively. Mono-crystalline silicon solar cell (Mono-Si) and copper indium gallium selenide solar cell (CIGS) give the highest short circuit current density while amorphous silicon solar cell (A-Si) gives the lowest short circuit current density for all LSC. In this case, short circuit current density of epoxy LSC is dependent on the micro-void concentration instead of the type of dye and its concentration. This is because the micro-void scattering contributes much more than the dye emission in the overall LSC light irradiance. The short circuit current density is closely related to the light irradiance of LSC as shown in Chapter 5.4.2 and Chapter 5.5.2, which was shown to be dependent on the micro-void concentration in Chapter 5.7.3.

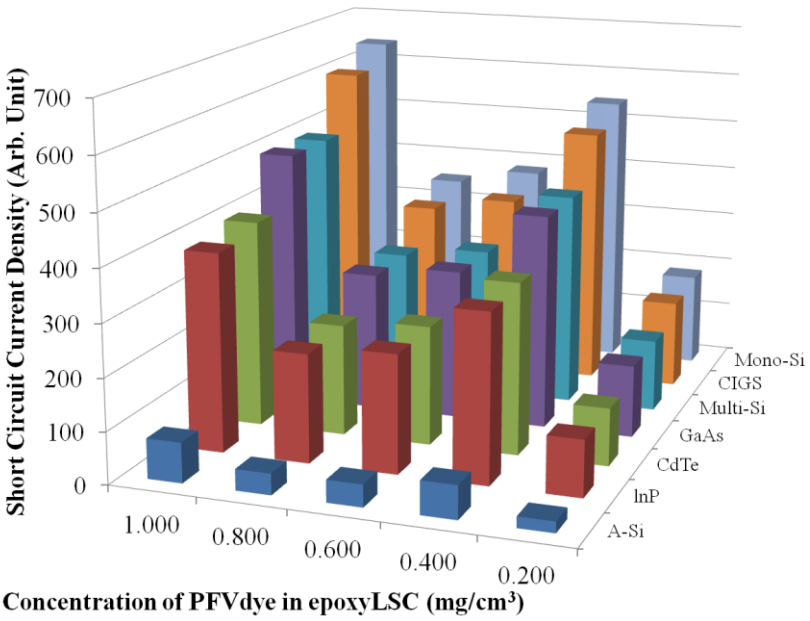

Figure 6.8 Short circuit current density for epoxy LSC with PFV dye

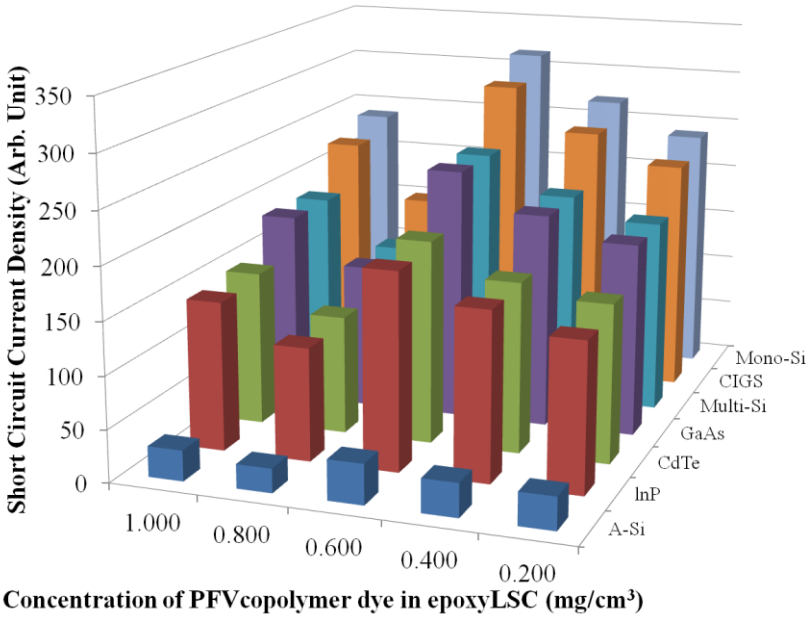

Figure 6.9 Short circuit current density for epoxy LSC with PFV copolymer dye

6.1.6 Comparison of LSC with different matrices at their optimum dye concentration

In this section, the LSC with the highest short circuit current density from each type of dye and matrix is selected and compared as shown in Figure 6.10. Their short circuit current density is compared to the reference dye - Rhodamine 6G. All the LSC used in this section are summarized and listed in Table 6.1.

Table 6.1 All LSCs with optimum dye concentration

Matrices	LSC	Optimum concentration	Label
PMMA	Polymerizable naphthalimide dye	75μm	Naph in PMMA
	Mixture of polymerizable naphthalimide dye and Rhodamine 6G	75 μm Naph + 37.5 μm Rh6G (2:1)	Naph + Rh6G in PMMA
	PFV	0.5 mg/cm^3	PFV in PMMA
	PFV copolymer	0.5 mg/cm^3	PFV copolymer in PMMA
	Rhodamine 6G	37.5 μm	Rh6G in PMMA
Unsaturated polyester	PFV	0.6 mg/cm^3	PFV in UP
	PFV copolymer	0.4 mg/cm^3	PFV copolymer in UP
	Rhodamine 6G	37.5 μm	Rh6G in UP
Epoxy	PFV	1.0 mg/cm^3	PFV in epoxy
	PFV copolymer	0.6 mg/cm^3	PFV copolymer in epoxy
	Rhodamine 6G	37.5 μm	Rh6G in epoxy

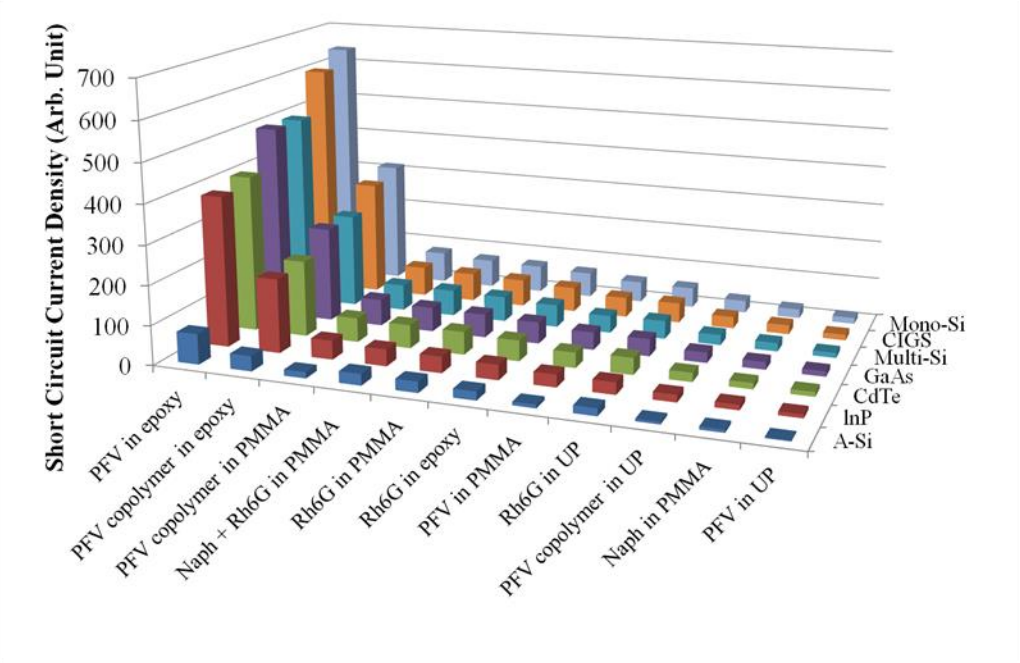

Figure 6.10 Comparison of short circuit current density for LSC in different matrices and dyes

The graph shows that the solar cells attached to epoxy LSC generate much higher short circuit current density than those attached to LSC with other matrices. The result in Figure 6.10 is closely related to the result of light irradiance in Chapter 5.6. As discussed in the previous chapter, the light irradiance for epoxy LSC is contributed by both the dye emission and the micro-voids scattering while that for PMMA and UP LSCs is contributed by dye emission only. Therefore, solar cells attached at epoxy LSC produce the highest short circuit current density due to the highest light irradiance. A large amount of micro-voids in the epoxy LSC diverted the incident light at long wavelength that cannot be emitted by any of the dyes used in this study. The scattered light with the long wavelength part matched very well with the spectral response of most solar cells, hence making the solar cells to produce very high short circuit current density.

Moreover, contribution from the micro-voids scattering is much higher than that from the dye emission. So the micro-voids concentration in epoxy LSC determines the short circuit current density from the solar cells attached to it. For example, epoxy LSC with PFV dye that has the highest micro-voids concentration also gives the highest short circuit current density from all types of solar cells attached to it.

However, for LSCs without micro-voids such as PMMA LSC and UP LSC, the short circuit current density from solar cells attached to them is contributed entirely by the dye emission. Figure 6.10 shows that the PMMA LSC with multiple dye (Naph + Rh6G) gives higher short circuit current density than Rhodamine 6G dye (Rh6G) or naphthalimide dye (Naph) alone. Among the commercially available dyes, LSC with PFV copolymer dye gives the higher short circuit current density, followed by LSC with PFV dye.

In this section, mono-crystalline silicon solar cell (Mono-Si) and copper indium gallium selenide solar cell (CIGS) are identified as the best solar cells that have excellent spectral matching with light irradiance spectrum from all types of LSC to produce very high short circuit current density.

6.2 Short Circuit Current Concentration Factor and Power Conversion Efficiency of Epoxy LSC

In this section, two epoxy LSCs with PFV dye and PFV copolymer dye are selected to calculate their power conversion efficiencies after exposing to

sunlight. They are selected because they have the highest light irradiance due to the micro-voids scattering as discussed in Chapter 5.6 and outstanding photo-stability which will be discussed in Chapter 6.3.3. The solar cells used in this section are the same as those listed in Chapter 6.1.

6.2.1 Definition of Geometric Gain, Short Circuit Current Concentration Factor and Power Conversion Efficiency

Geometric gain (G_{geom}) of the LSC is calculated as the ratio of A_{top} to A_{cell} where A_{top} is the top surface area of LSC and A_{cell} is the total surface area of solar cells attached to the LSC sides as shown in Equation 6.2.

$$G_{geom} = \frac{A_{top}}{A_{cell}} \qquad 6.2$$

Where,

G_{geom} = Geometric gain of LSC;

A_{top} = Top surface area of LSC (m^2);

A_{cell} = Total surface area of solar cells attached to the LSC sides (m^2).

Short circuit current concentration factor (CF_{Jsc}) is calculated by the ratio of solar cell short circuit current density to reference short circuit current density, as shown in Equation 6.3. CF_{Jsc} is used to evaluate the ability of LSC to concentrate the short circuit current density. The solar cell short circuit current density (J_{sc}) output is calculated by taking the integration with respect

to wavelength of the multiplication of light irradiance of LSC (I_{em}) and spectral response of solar cell (SR), as shown in Equation 6.4. The light irradiance of LSC in this section is measured under a solar simulator using a spectrometer with radiometric calibration via a fiber optic connected to a cosine corrector, as shown in Chapter 3.4.3. The spectral response of solar cell (A/W) is obtained from the published journal (Field 1997). The reference short circuit current density, $J_{sc(ref)}$ is short circuit current density of the same solar cell illuminated under the light source directly, calculated using the incident light spectral irradiance from solar simulator (AM1.5G spectrum) as shown in Equation 6.5.

$$CF_{Jsc} = \frac{J_{sc}}{J_{sc(ref)}} \tag{6.3}$$

Where,

CF_{Jsc} = Short circuit current concentration factor;

J_{sc} = Short circuit current density of solar cell (Am^{-2});

$J_{sc(ref)}$ = Reference short circuit current density (Am^{-2}).

$$J_{sc} = \int I_{em}(\lambda)\, SR(\lambda)\, d\lambda \tag{6.4}$$

Where,

J_{sc} = Short circuit current density of solar cell (Am^{-2});

$I_{em}(\lambda)$ = Light irradiance of LSC ($Wm^{-2}nm^{-1}$);

$SR(\lambda)$ = Spectral response of solar cell ($AW^{-1}nm^{-1}$).

$$J_{sc(ref)} = \int I_{AM1.5G}(\lambda)\, SR(\lambda)\, d\lambda \qquad 6.5$$

Where,

$J_{sc(ref)}$ = Reference short circuit current density (Am^{-2});

$I_{AM1.5G}(\lambda)$ = Spectral irradiance of solar simulator ($Wm^{-2}nm^{-1}$);

$SR(\lambda)$ = Spectral response of solar cell ($AW^{-1}nm^{-1}$).

Power conversion efficiency is calculated by Equation 6.6. It is calculated by assuming that the I-V response of the device can be approximated by the substraction of the dark current from the short circuit current. In other words, it is assumed that both the open circuit voltage and fill factor are not affected by the light source intensity. The short circuit current (I_{sc}) in Equation 6.6 is calculated by multiplying the short circuit current density (J_{sc}) to the total surface area of solar cells attached to the LSC sides (A_{cell}), as shown in Equation 6.7.

$$PCE = \frac{P_{out}}{P_{in}} = \frac{I_{sc} V_{oc} FF}{P_{lamp} A_{top}} \times 100\% \qquad 6.6$$

Where,

PCE = Power conversion efficiency (%);

P_{out} = Electrical power output of solar cell (W);

P_{in} = Light power input to solar cell (W);

I_{sc} = Short circuit current of solar cell (A);

V_{oc} = Open circuit voltage of solar cell (V);

FF = Fill factor of solar cell;

P_{lamp} = Light source irradiance (Wm^{-2});

A_{top} = Top surface area of LSC (m^2).

$$I_{sc} = J_{sc} A_{cell} \quad 6.7$$

Where,

I_{sc} = Short circuit current of solar cell (A);

J_{sc} = Short circuit current density of solar cell (Am^{-2});

A_{cell} = Total surface area of solar cells attached to the LSC sides (m^2).

Power conversion efficiency is important because it is used to evaluate the percentage of solar energy converted into electrical energy by LSC that is coupled with solar cells.

6.2.2 Arrangement of Solar Cells Attached to LSC

Each LSC sample has a dimension of 35 mm × 12 mm × 7.5 mm where the dimension of the top surface that receives incident light is 35 mm × 12 mm. Solar cells can be attached to any of the four sides of the LSC. Four different arrangements were studied in this section: 1) Solar cell attached to 1 side with dimension of 12 mm × 7.5 mm; 2) Solar cell attached to 1 side with dimension of 35 mm × 7.5 mm; 3) Solar cells attached to 2 sides with dimension of 12 mm × 7.5 mm on each side; 4) Solar cells attached to 2 sides with dimension of

35 mm × 7.5 mm on each side. All the four solar cell arrangements are illustrated in Figure 6.11. Geometric gains of the LSC with the four different arrangements are 4.67, 1.60, 2.33, and 0.80 respectively. The solar cells that are attached to 2 sides of the LSC are connected in parallel, so their short circuit currents are added up.

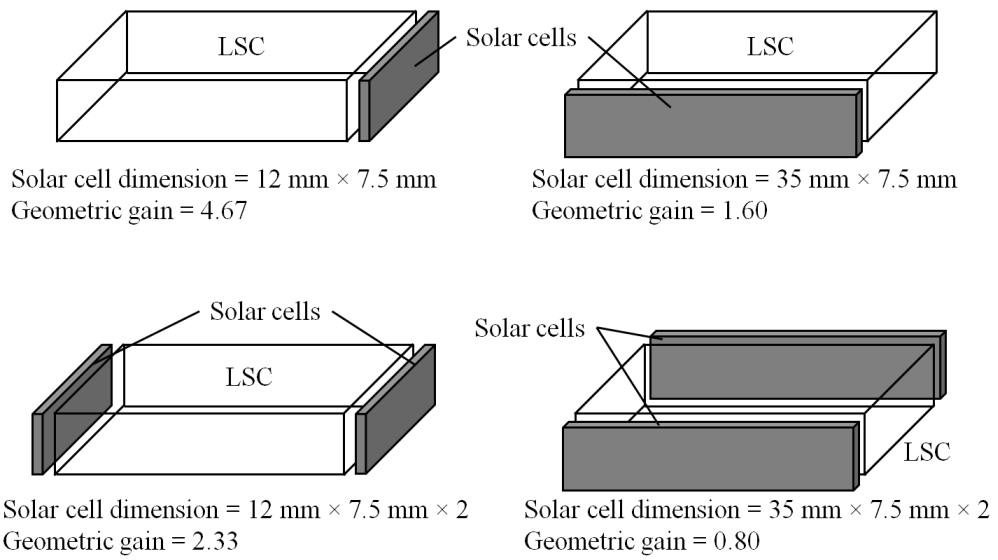

Figure 6.11 Arrangement of solar cells attached to the sides of LSC

6.2.3 Short Circuit Current Concentration Factor of Epoxy LSC

The short circuit current concentration factor of epoxy LSC with solar cells arrangement that gives two different geometric gains: 4.67 and 1.60 are plotted as shown in Figure 6.12 and Figure 6.13 respectively. The short circuit current concentration factors for LSC with geometric gains of 2.33 and 0.80 are the same as those for geometric gains of 4.67 and 1.60 respectively. The results show that the type of solar cells does not affect much on the short circuit current concentration factor. However, the type of dyes affects the short circuit

current concentration factor. For example, LSC with PFV dye has higher short circuit current concentration factor than that with PFV copolymer dye. Moreover, higher geometry gain gives higher short circuit current concentration factor for LSC with PFV dye but negligible increase for LSC with PFV copolymer dye.

Besides, the short circuit current concentration factor of epoxy LSC with micro-voids has a value of 0.3 – 0.5 only. It gives 30% - 50% of the short circuit current that is generated from solar cells without any LSC. In other words, the LSC sample design in this study does not give any concentration effect on any type of solar cells. Simulation study on the micro-voids scattering and design optimization of LSC are required to increase the short circuit current concentration factor of the actual LSC to be more than 1. Besides, it can also be further improved by reducing the top surface reflection loss of LSC by anti-reflection coating.

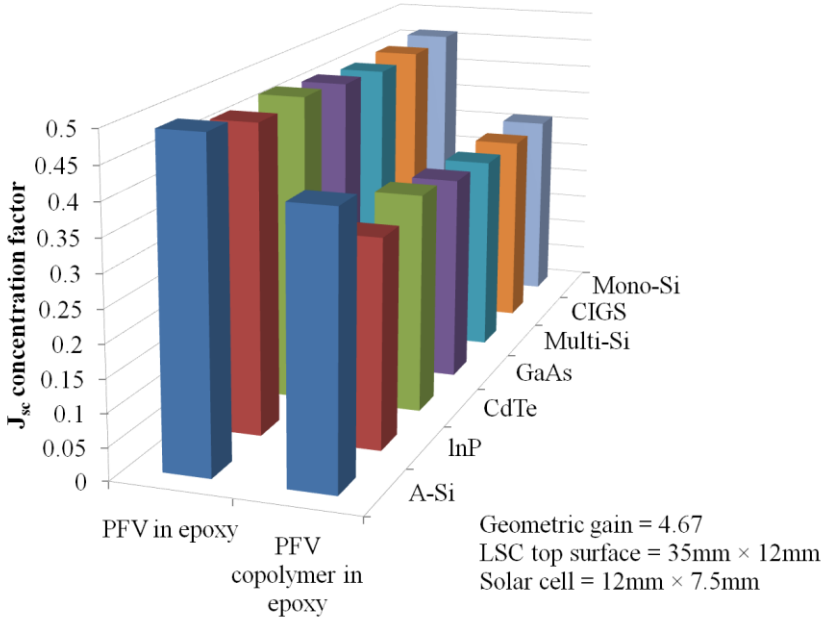

Figure 6.12 Short circuit current concentration factor of epoxy LSC with geometric gain of 4.67

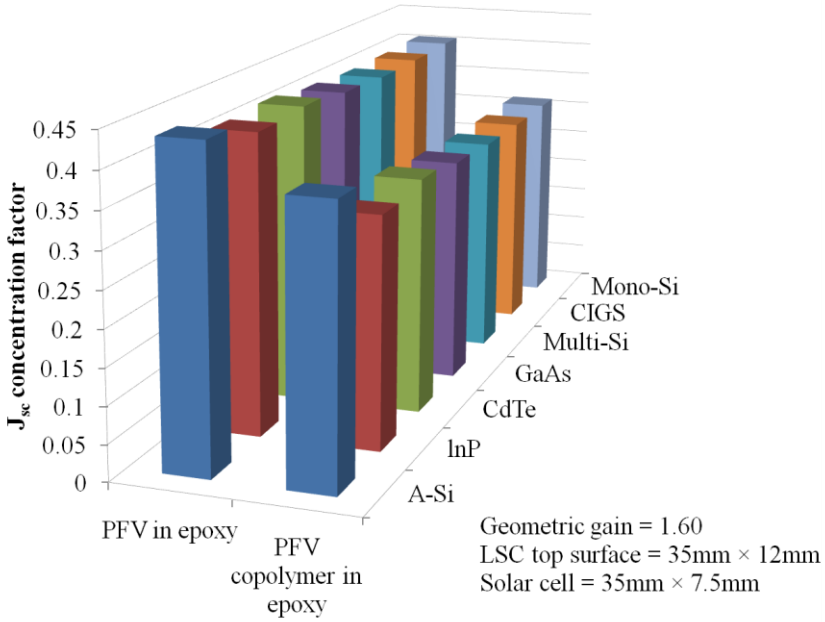

Figure 6.13 Short circuit current concentration factor of epoxy LSC with geometric gain of 1.60

6.2.4 Power Conversion Efficiency of Epoxy LSC

Power conversion efficiency of epoxy LSC with four different geometric gains: 4.67, 1.60, 2.33, and 0.80 are plotted as shown in Figure 6.14, Figure 6.15, Figure 6.16, and Figure 6.17 respectively. LSC with PFV dye has higher power conversion efficiency than LSC with PFV copolymer dye regardless of the geometric gain or the type of solar cells. Comparing different types of solar cells, Gallium Arsenide solar cell (GaAs) gives the highest power conversion efficiency. Therefore, it is very suitable to be coupled with epoxy LSC with micro-voids.

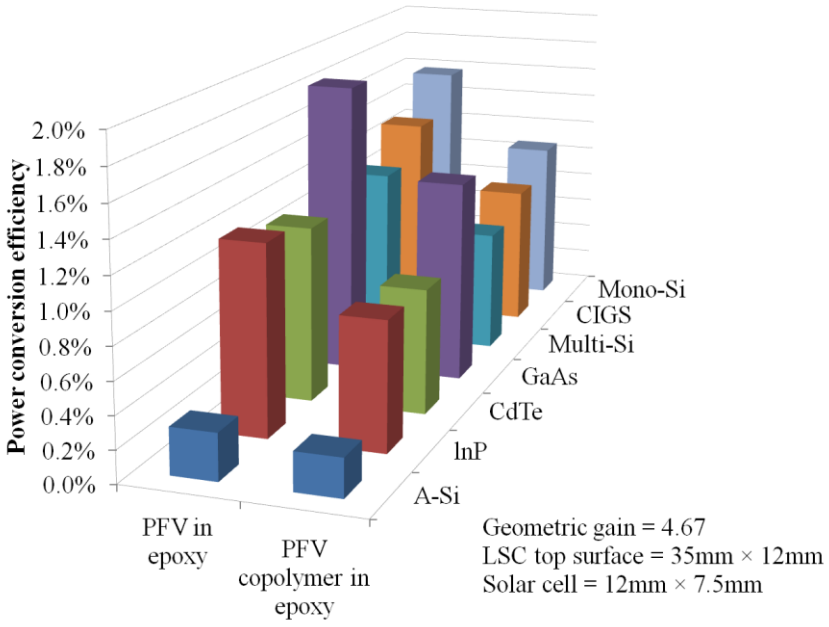

Figure 6.14 Power conversion efficiency of epoxy LSC with geometry gain of 4.67

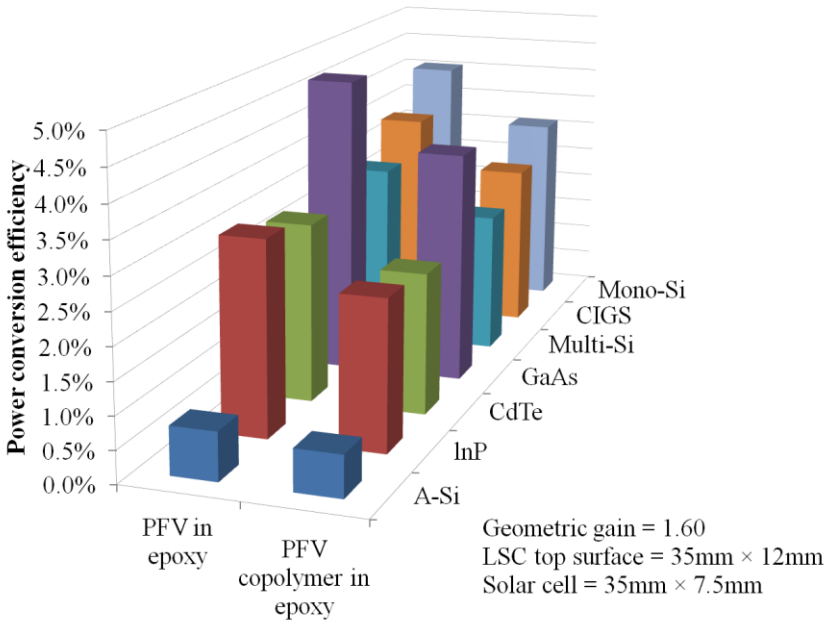

Figure 6.15 Power conversion efficiency of epoxy LSC with geometry gain of 1.60

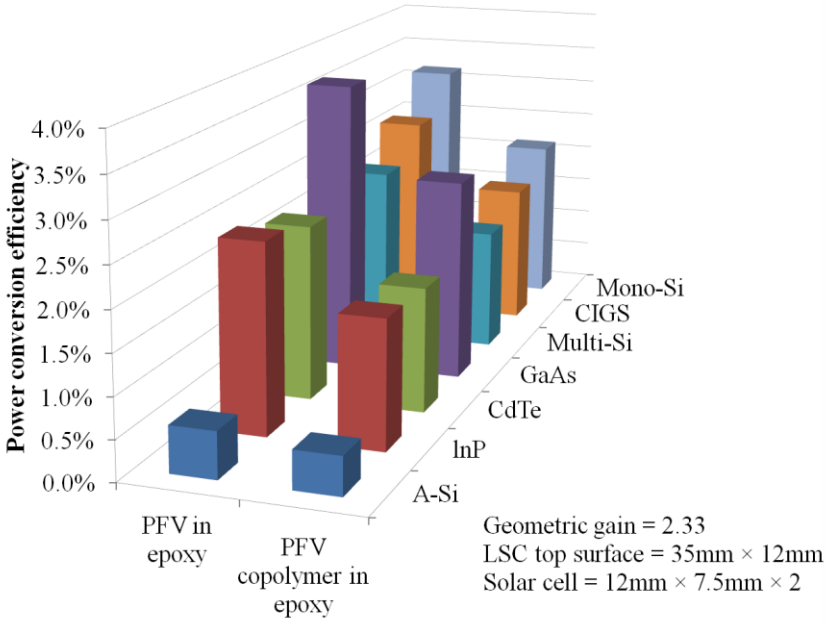

Figure 6.16 Power conversion efficiency of epoxy LSC with geometry gain of 2.33

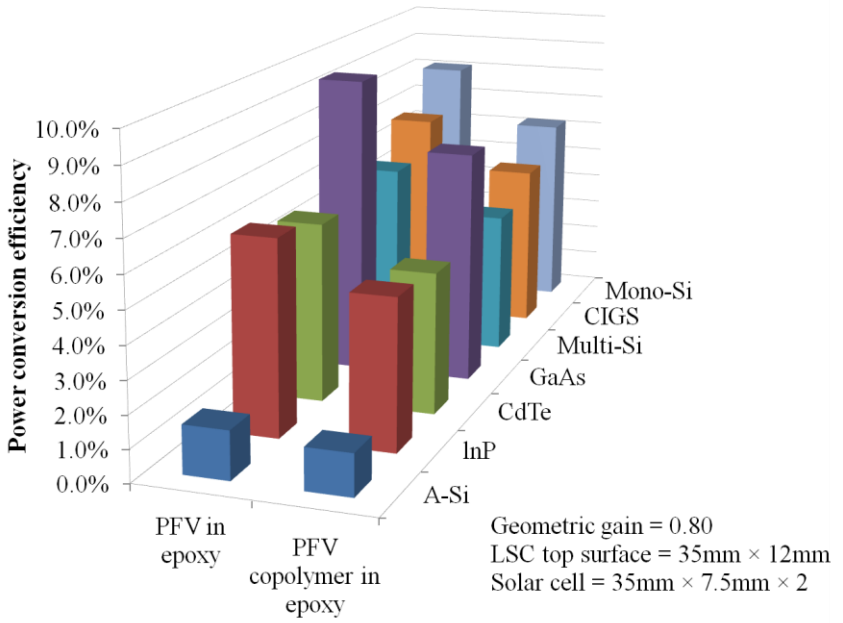

Figure 6.17 Power conversion efficiency of epoxy LSC with geometry gain of 0.80

The short circuit current concentration factor and power conversion efficiency of epoxy LSC with micro-voids are also compared with the results obtained from other publications as shown in Table 6.2. Only the results of mono-crystalline Silicon solar cell and Gallium Arsenide solar cell that give the highest power conversion efficiency are used in the comparison. Epoxy LSCs coupled with Gallium Arsenide solar cells that have different geometry gains are shown in the table. The result shows that the PFV dye in epoxy LSC coupled with Gallium Arsenide (GaAs) solar cell has higher power conversion efficiency (4.72%) than that coupled with silicon monocrystalline (Si) solar cell (4.05%).

Generally, comparing LSCs coupled with the same type of solar cell, the LSC with higher geometric gain has higher short circuit current

concentration factor but lower power conversion efficiency. The LSC with micro-voids (PFV dye in epoxy) has very little increase in short circuit current concentration factor but huge drop in power conversion efficiency when it has higher geometric gain. This is because of its large reabsorption loss: the scattered light is absorbed by other micro-voids and re-scattered to other directions. Most of the collected light irradiance is contributed by the micro-voids near the side where solar cell is coupled to. In other words, the LSC with microvoids does not benefit from having a design with large geometric gain, to the contrary of ordinary dye-doped LSC that is usually designed to have very large geometric gain.

Table 6.2 Power conversion efficiency of LSC with micro-voids (PFV dye in epoxy)

LSC material	Top surface area (mm^2)	Solar cell material	Solar cell area (mm^2)	G_{geom} [1]	CF_{Jsc} [2]	PCE [3] (%)
PFV dye in Epoxy	35 × 12	Si	35 × 7.5	1.60	0.40	4.05
	35 × 12	GaAs	12 × 7.5	4.67	0.46	1.85
	35 × 12	GaAs	35 × 7.5	1.60	0.40	4.72
	35 × 12	2 GaAs	35 × 7.5	0.80	0.40	9.45
PFV copolymer in Epoxy	35 × 12	Si	35 × 7.5	1.60	0.31	3.11
	35 × 12	GaAs	12 × 7.5	4.67	0.32	1.28
	35 × 12	GaAs	35 × 7.5	1.60	0.32	4.72
	35 × 12	2 GaAs	35 × 7.5	0.80	0.32	7.34
Perylene + Coumarine dyes in PMMA (Slooff et al. 2008)	50 × 50	Si	50 × 5	10.00	N/A [4]	2.69
	50 × 50	GaAs	50 × 5	10.00	N/A [4]	4.62
	50 × 50	4 GaAs	50 × 5	2.50	N/A [4]	7.05
Quantum dot in P(LMA-co-EGDM) (Bomm et al. 2011)	50 × 31	Si	31 × 4	12.50	1.92	2.82

[1] G_{geom} = Geometric Gain.

[2] CF_{Jsc} = Short Circuit Current Concentration Factor.

[3] PCE = Power Conversion Efficiency.

[4] Values are not available in the reference publication.

In fact, the LSC coupled with 2 GaAs solar cell with near unity (≈1) geometric gain has 9.45% power conversion efficiency. This is higher than the LSC with perylene and coumarine dye in PMMA (Slooff et al. 2008) and quantum dot in P(LMA-co-EGDM) (Bomm et al. 2011). Unlike organic dyes or quantum dots, the micro-voids inside the matrix do not degrade under sunlight, which will be shown in Chapter 6.3.3. Besides, its short circuit

current concentration factor can be further improved by reducing its top surface reflection loss by anti-reflection coating.

The use of LSC with microvoids is not only limited to standalone LSC, it can also be coupled to ordinary dye-doped LSC at the edge next to the mirror or in the middle, and serves as a light coupling element to the planar waveguide (LSC). A long rectangular LSC with microvoids coupled to the ordinary dye-doped LSC before the mirror acts like a slanted mirror, re-directing the sunlight at the edge into the LSC. However, the slanted mirror reflection is dependent on the sunlight direction but microvoids scattering is not, therefore making it suitable to couple both direct and diffuse sunlight into the LSC.

6.3 Degradation Rate of LSC

All LSC with the optimum dye concentrations giving the highest light irradiance were selected to examine their degradation rate under the sun for 30 days. The solar irradiance was recorded at one second intervals using pyranometer. After the exposure of sunlight for a day, the absorption and light irradiance intensities of the LSCs were determined using the spectrometer. Finally, the peak absorption coefficient and light irradiance of the LSC were plotted against the cumulative solar energy received by the LSC to study the degradation rate. The peak absorption coefficient represents the ability of the dyes in absorbing the incoming sunlight while the light irradiance is used to determine the photo-stability of the LSC. In other words, the LSC with high

photo-stability has little drop in its light irradiance. The cumulative solar energy received by the LSC on a day was calculated by summing up all the solar energy prior to and including that day, where the solar energy on a day was calculated by integrating the solar irradiance over the period of sunlight exposure on that day, as shown in Equation 6.8.

$$CSE_N = \sum_{n=1}^{N} \int_{t_{1(n)}}^{t_{2(n)}} I_{solar(n)} dt = \int_{t_{1(1)}}^{t_{2(1)}} I_{solar(1)} dt + \int_{t_{1(2)}}^{t_{2(2)}} I_{solar(2)} dt + \ldots + \int_{t_{1(N)}}^{t_{2(N)}} I_{solar(N)} dt \quad 6.8$$

Where,

CSE_N = Cumulative solar energy on day N (Jm^{-2});

$I_{solar(n)}$ = Solar irradiance on day n (Wm^{-2});

$t_{1(n)}$ = The time when the sunlight exposure begins on day n (s);

$t_{2(n)}$ = The time when the sunlight exposure ends on day n (s).

To avoid any measurement error due to different measurement spot and orientation of the LSC in every measurement, the cuvette-shape LSC was fitted tightly inside the cuvette holder so that exactly the same spot on the LSC was being measured every time. However, measurement error due to intensity variation of the light source used for all absorption and light irradiance measurements was unavoidable. The average measurement error due to the light source was less than 5%. It was determined by measuring and comparing absorption and light irradiance of a reference LSC sample that was never exposed to sunlight during the measurement period. However, some of the

LSCs had larger measurement errors because their absorption or light irradiance intensity was too low and the measurement result was affected too much by electrical noise from the spectrometer.

6.3.1 Degradation of Absorption Coefficient and Light Irradiance for PMMA LSC

PMMA LSCs with PFV dye, PFV copolymer dye, Rhodamine 6G, naphthalimide dye, and multiple dye (naphthalimide dye + Rhodamine 6G) at their respective optimum dye concentration were selected to study their degradation rate. The degradation of peak absorption coefficient and light irradiance for LSC were monitored and plotted against the cumulative solar energy received by the LSC as shown in Figure 6.18 and Figure 6.19.

It is shown that all the dyes have a drastic reduction in their peak absorption coefficients after the first cycle of sunlight exposure. However, the peak absorption coefficients become relatively stable after that. This result indicates that the ability of the dyes in absorbing the incoming sunlight reduced significantly after the first exposure and then becomes stable.

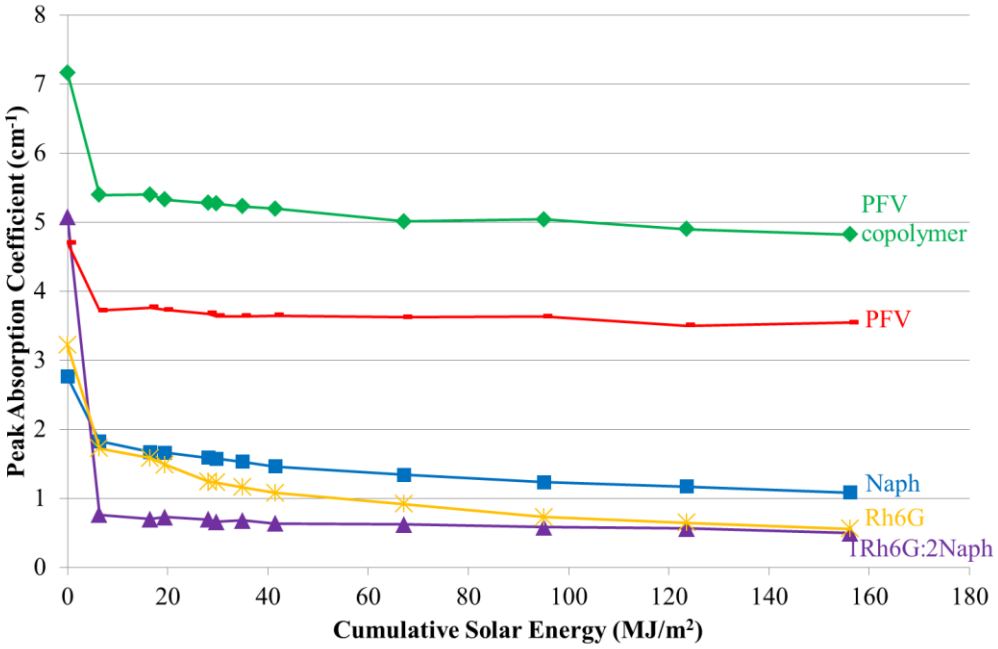

Figure 6.18 Degradation of peak absorption coefficient for PMMA LSC with optimum dye concentration

Similarly, all the dyes have a drastic reduction in their light irradiance after the first cycle of sunlight exposure. After that, the dye degradation becomes smaller in subsequent days. The graph showed that the reference dye - Rhodamine 6G degrade much more rapidly than the other four dyes and eventually its light irradiance becomes the lowest in the end of the experiment. Among all these dyes, PFV copolymer dye degrades with the slowest rate and therefore it has the highest light irradiance towards the end of the experiment. Therefore, it has the potential to be used as a new luminescent material in LSC.

Besides, polymerizable naphthalimide dye also has better photo-stability than other dyes. Figure 6.19 shows that its light irradiance is almost constant throughout the sunlight exposing period. The small variation in its light irradiance was due to the light source intensity variation. The

polymerizable naphthalimide dye has high photo-stability because it iscopolymerized with the methyl methacrylate monomer – the LSC matrix material. The chromogenic of dye is included along the polymer chain in the copolymer, causing it to have better photo-stability (Panah et al. 2010).

The mixture of polymerizable naphthalimide dye and Rhodamine 6G (1Rh6G:2Naph) has a better photo-stability than Rhodamine 6G alone. It degrades quickly only in the first cycle of sunlight exposure and becomes stable after that. Therefore, it has higher light irradiance than Rhodamine 6G toward the end of the experiment. The result shows that this combination of dyes aids to improve the emission and prolong their lifetime.

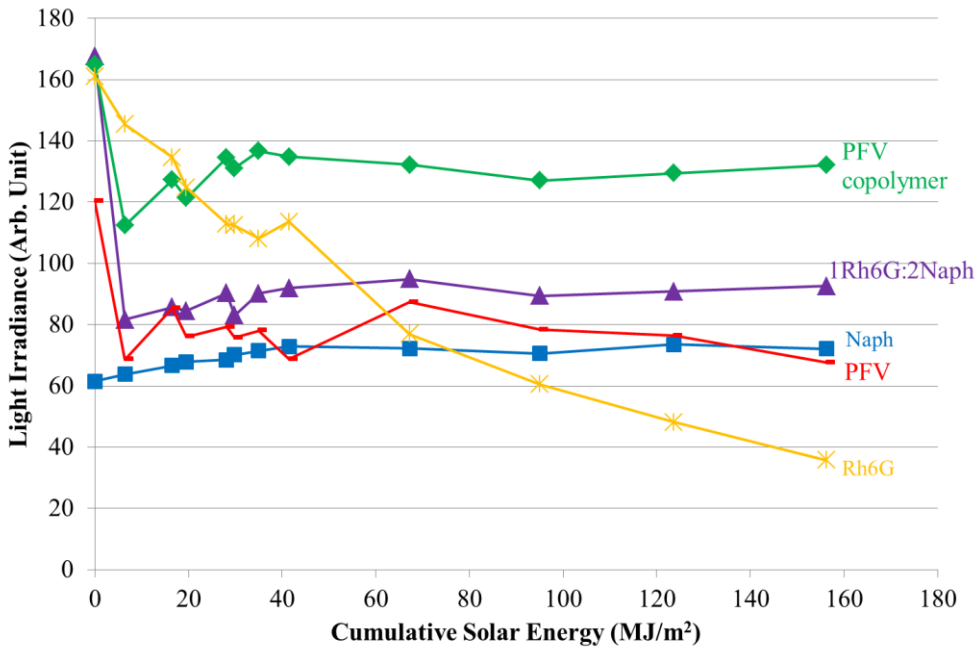

Figure 6.19 Degradation of light irradiance for PMMA LSC with optimum dye concentration

6.3.2 Degradation of Absorption Coefficient and Light Irradiance for UP LSC

UP LSCs with PFV dye, PFV copolymer dye, and Rhodamine 6G at their respective optimum dye concentration were selected to study their degradation rate. The peak absorption coefficient and light irradiance of the LSC were plotted against the cumulative solar energy received by the LSC as shown in Figure 6.20 and Figure 6.21. From the result, PFV dye and PFV copolymer dye has small degradation in its peak absorption coefficient. However, the Rhodamine 6G has a drastic reduction in its peak absorption coefficient after the first cycle of sunlight exposure. After that, the peak absorption coefficient has a very low value and becomes relatively stable in the subsequent days.

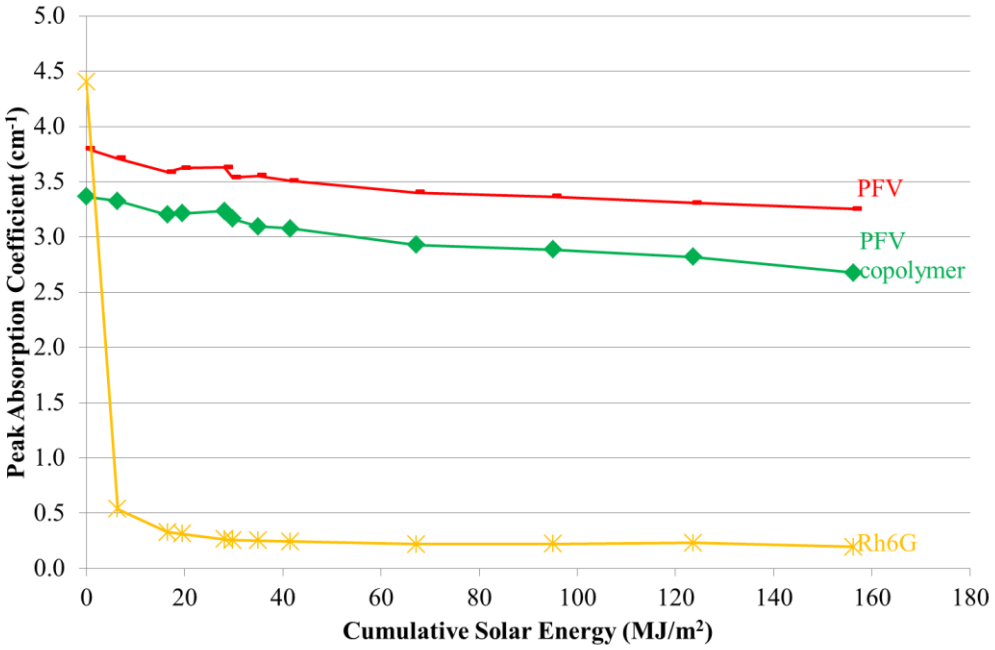

Figure 6.20 Degradation of peak absorption coefficient for UP LSC with optimum dye concentration

Similarly, degradation of light irradiance for UP LSC follows the degradation of its peak absorption coefficient. Rhodamine 6G dye degrades rapidly after the first cycle of sunlight exposure and then becomes stable in the subsequent days. Both PFV dye and PFV copolymer dye show varying light irradiance because of the light source intensity variation and their low light irradiance that is affected very much by the electrical noise from the spectrometer. They have better photo-stability than the Rhodamine 6G because their light irradiances do not change much towards the end of the experiment. However, the PFV dye has very low dye emission. This result again shows that the PFV copolymer dye has good photo-stability under the sun.

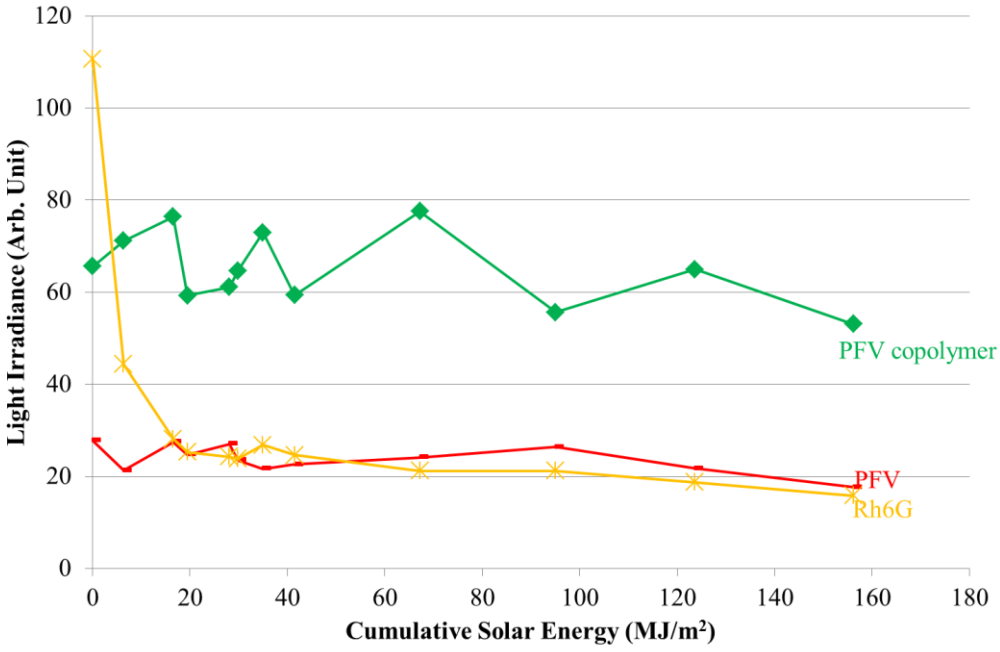

Figure 6.21 Degradation of light irradiance for UP LSC with optimum dye concentration

6.3.3 Degradation of Absorption Coefficient and Light Irradiance for Epoxy LSC

Epoxy LSCs with PFV dye, PFV copolymer dye, and Rhodamine 6G at their respective optimum dye concentration were selected to study their degradation rate. The peak absorption coefficient and light irradiance of the LSC were plotted against the cumulative solar energy received by the LSC as shown in Figure 6.22 and Figure 6.23. Overall, PFV dye and PFV copolymer dye have smaller degradation in their peak absorption coefficient than Rhodamine 6G.

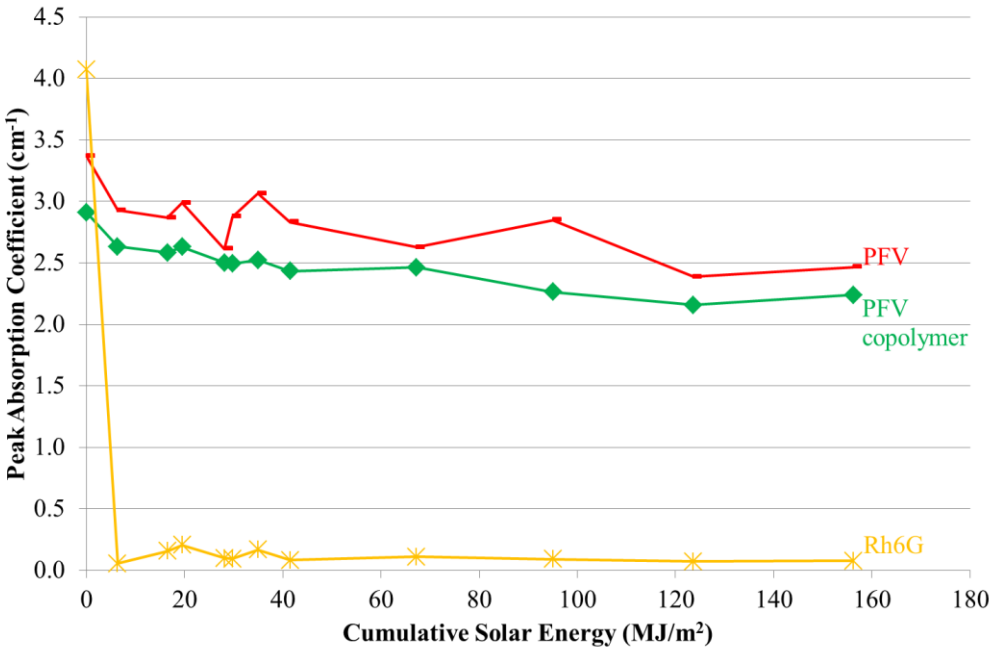

Figure 6.22 Degradation of peak absorption coefficient for epoxy LSC with optimum dye concentration

From Figure 6.23, it is noticed that the light irradiance of epoxy LSC with PFV dye or PFV copolymer dye do not show significant degradation even

at the end of this experiment. The result shows that the light irradiances of these LSCs are almost unaffected by the degradation of dyes in the epoxy matrices. The light irradiance from the epoxy LSC is mostly contributed by scattering of light by the large amount of micro-voids inside the LSC instead of the dye emission. The micro-voids in epoxy LSC do not degrade under the sun, so their scattering intensities do not degrade as well.

The light irradiance of epoxy LSC with another dye, Rhodamine 6G with very small amount of micro-voids degraded rapidly after exposing to sunlight. It is mostly contributed by the dye emission and the contribution from the micro-voids scattering is not significant. Therefore, the degradation of the dye emission causes a significant drop in the light irradiance of LSC.

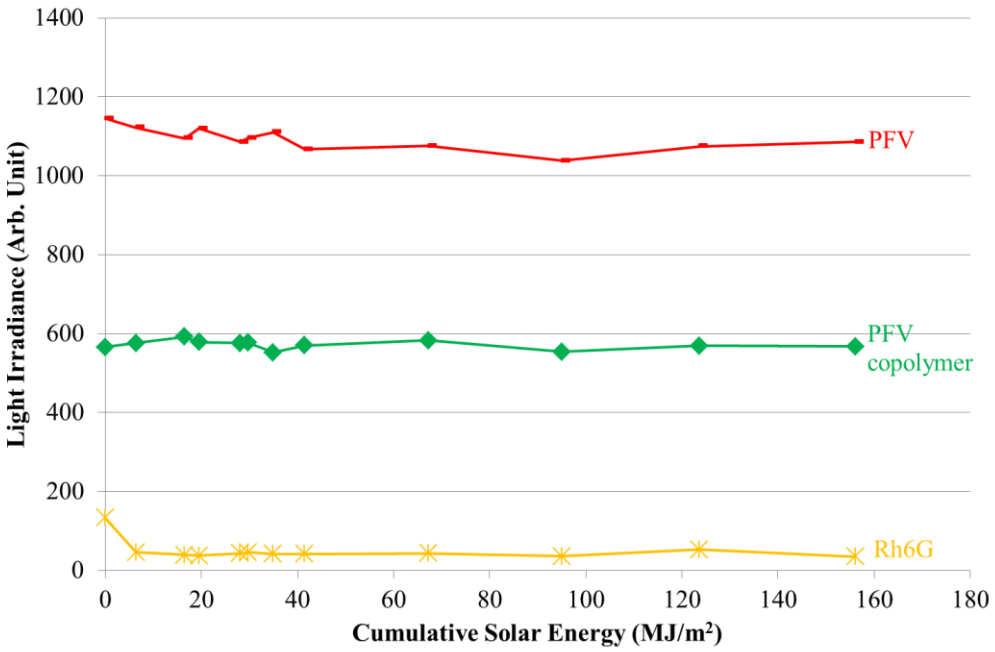

Figure 6.23 Degradation of light irradiance for epoxy LSC with optimum dye concentration

6.4 Summary

Epoxy is a good host matrix for LSCs because the micro-voids that are formed inside can scatter a substantial amount of the incident light toward the solar cell at the edge. From the result, epoxy LSC with micro-voids has the highest short circuit current density and power conversion efficiency compared to LSCs with other matrices. The maximum LSC power conversion efficiency of 9.34% was achieved by attaching two 35mm × 7.5mm Gallium Arsenide (GaAs) solar cells to two sides of a 35mm × 12mm × 7.5mm epoxy LSC (with PFV dye) that has very high micro-voids concentration. Furthermore, the epoxy LSC with micro-voids also shows greater photo-stability than other LSC without micro-voids because the micro-voids do not degrade under the sun. The micro-voids in epoxy LSC can be regarded as scatterers doped into the LSC with the aid of PFV dye by controlling the stirring duration during its casting process. The use of LSC with micro-voids is not only limited to standalone LSC, it can also be coupled to ordinary dye-doped LSC at the edge next to the mirror or in the middle to serve as light coupling element to the planar waveguide (LSC).

CHAPTER 7

CONCLUSION

This chapter concludes and highlights all the key findings in the thesis. Besides, the future work is proposed in this chapter as well. The proposed future work is to investigate the formation of micro-voids and all possible parameters that can be used to control the micro-voids concentration.

The polymerizable naphthalimide dye that is synthesized in the laboratory - 4-butylamino-N-allyl-1,8-naphthalimide - has low dye emission irradiance in PMMA LSC but it helps to improve the dye emission irradiance when it is copolymerized with Rhodamine 6G dye in the ratio of 2:1. This multiple dye PMMA LSC has 4.45% higher dye emission irradiance than PMMA LSC with Rhodamine 6G dye.

The commercially available PFV copolymer dye that is previously used in LED has the potential to be used in PMMA LSC too. It has the highest dye emission irradiance in PMMA LSC among all other luminescent dyes that are studied here.

The performance of different commercially available polymer host matrices for LSC - PMMA, unsaturated polyester and epoxy - is studied and evaluated by doping them with PFV dye, PFV copolymer dye or Rhodamine 6G dye. The results show that epoxy is a good host matrix for LSC with the

formation of large amount of micro-voids in it. Micro-voids scatter the incident light towards the edges of the LSC. Therefore, light irradiance of the epoxy LSC with micro-voids is found to be higher than other LSCs made by other host matrices even though the same dye is used. Furthermore, the epoxy LSC with the largest amount of micro-voids has the highest light irradiance because more light is trapped and scattered to the edge of LSC which is attached to solar cell.

The epoxy LSC with very high micro-voids concentration has higher short circuit current density and power conversion efficiency as compared with LSCs with other matrices. The epoxy LSC with 1.000mg/cm^3 PFV dye gives the highest short circuit current density when the mono-crystalline silicon solar cell is attached to its side. The maximum power conversion efficiency of 9.45% is achieved when two Gallium Arsenide (GaAs) solar cells, each of them having a dimension of 35mm x 7.5mm are attached to both sides of it.

Besides, the photo-degradation of LSC is also determined to find out which LSC has the longest lifetime. Generally, the peak absorption coefficient and light irradiance of all dyes degrade rapidly after the first cycle of sunlight exposure. However, it becomes stable in the subsequent days. Overall, the photo-stability of all luminescent dyes being studied here is higher than that of the reference dye - Rhodamine 6G regardless of the polymer matrix material after exposing to sunlight for 30 days.

The epoxy LSC has the highest photo-stability as compared with LSCs made by PMMA or unsaturated polyester. The micro-voids that are formed in it do not degrade under the sun. Therefore, it is very suitable to be used as a LSC matrix material where the micro-voids act as highly photo-stable scatterers to enhance the light irradiance.

7.1 Future work

In this study, the performances of different LSCs are assessed. Each of the LSCs consists of one of the different polymer matrices and doped with one of the different new organic luminescent dyes. One of the main findings of this research is the discovery of the formation of micro-voids in epoxy matrix that aid to scatter the incident light. The micro-voids scattering increases the overall performance of LSC.

Current study focuses on the examination of the micro-voids using optical microscope as well as measurement of the micro-voids sizes and concentration. It is noticed that higher micro-voids concentration contributed to higher LSC light irradiance. Therefore, it is believed that the performance of LSC with micro-voids can be maximized if the micro-voids concentration can be tuned precisely where just the right amount of micro-voids is introduced into the LSC.

The proposed future work starts with the design of an experiment to control the micro-voids concentration. A few parameters can be taken into account to control the micro-voids concentration, such as the surface tension and viscosity of the polymer in liquid state which affect the micro-voids dissolution in it (Kontopoulou & Vlachopoulos 1999). Besides, the initiator amount, stirring duration and temperature should be studied also to control the reaction rate that can affect the micro-voids concentration.

After that, a set of LSCs will be casted with various different micro-voids concentration. All their light irradiances will be measured and the LSC with optimum micro-voids concentration can be identified in this stage. This information is important to maximize the performance of LSC with micro-voids.

REFERENCES

Andjelkovic, D.D., Culkin, D.A. & Loza, R., 2009. Unsaturated Polyester Resins Derived from Renewable Resources. *Composites & Polycon, American Composites Manufacturers Association, Tampa, Florida USA*.

Arbeloa, F.L. et al., 2010. Fluorescence Anisotropy to Study the Preferential Orientation of Fluorophores in Ordered Bi-Dimensional Systems: Rhodamine 6G/Laponite Layered Films. In C. D. Geddes, ed. *Reviews in Fluorescence 2008*. Reviews in Fluorescence 2008. Springer New York, pp. 1–35.

Ashby, M.F. & Johnson, K., 2010. *Materials and Design: The Art and Science of Material Selection in Product Design*, Butterworth-Heinemann.

Bakr, N.A., Mansour, A.F. & Hammam, M., 1999. Optical and thermal spectroscopic studies of luminescent dye doped poly(methyl methacrylate) as solar concentrator. *Journal of Applied Polymer Science*, 74(14), pp.3316–3323.

Ballato, J., Foulger, S.H. & Smith, J., 2004. Optical properties of perfluorocyclobutyl polymers. II. Theoretical and experimental attenuation. *Journal of the Optical Society of America B*, 21(5), pp.958–967.

Barnham, K. et al., 2000. Quantum-dot concentrator and thermodynamic model for the global redshift. *Applied Physics Letters*, 76, p.1197.

Batchelder, J.S., 1982. *The luminescent solar concentrator*. Ph.D. Thesis. California Inst. of Tech., Pasadena.

Bhatnagar, M.S., 1993. Epoxy Resins from 1980 to Date. Part 1. *Polymer-Plastics Technology and Engineering*, 32(1-2), pp.53–113.

Bindhu, C.V. & Harilal, S.S., 2001. Effect of the Excitation Source on the Quantum-Yield Measurements of Rhodamine B Laser Dye Studied Using Thermal-Lens Technique. *Analytical Sciences*, 17(1), pp.141–144.

Bohren, C.F. & Huffman, D.R., 2008. *Absorption and Scattering of Light by Small Particles*, John Wiley & Sons.

Bojinov, V. & Konstantinova, T., 2002. Synthesis of polymerizable 1,8-naphthalimide dyes containing hindered amine fragment. *Dyes and Pigments*, 54(3), pp.239–245.

Bomm, J. et al., 2011. Fabrication and full characterization of state-of-the-art quantum dot luminescent solar concentrators. *Solar Energy Materials and Solar Cells*, 95(8), pp.2087–2094.

Bomm, J. et al., 2010. Fabrication and spectroscopic studies on highly luminescent CdSe/CdS nanorod polymer composites. *Beilstein Journal of Nanotechnology*, 1, pp.94–100.

Bouché, C.-M. et al., 1996. Side-chain electroluminescent polymers. *Synthetic Metals*, 81(2–3), pp.191–195.

Burroughes, J.H. et al., 1990. Light-emitting diodes based on conjugated polymers. *nature*, 347(6293), pp.539–541.

Chandra, S. et al., 2012. Enhanced quantum dot emission for luminescent solar concentrators using plasmonic interaction. *Solar Energy Materials and Solar Cells*, 98, pp.385–390.

Cosnard, F. & Wintgens, V., 1998. A new fluoroionophore derived from 4-amino-N-methyl-1,8-naphthalimide. *Tetrahedron Letters*, 39(18), pp.2751–2754.

Currie, M.J. et al., 2008. High-Efficiency Organic Solar Concentrators for Photovoltaics. *Science*, 321(5886), pp.226–228.

Daram, B., Al-Rawi, K.R. & Hussin, S.H.A., 2011. Improve the Performance Efficiency of Solar Cell by Using Epoxy Plates Doped with Rhodamine 6G Dye. *Indian Journal of Science and Technology*, 4(12), pp.1726–1731.

Debije, M., Broer, D. & Bastiaansen, C., 2007. Effect of dye alignment on the output of a luminescent solar concentrator. In *In Proc. 22nd Eur. Photovolt. Solar Energy Conf. Exhib.* Milan, Italy, pp. 87–89.

Debije, M.G. et al., 2009. The effect of a scattering layer on the edge output of a luminescent solar concentrator. *Solar Energy Materials and Solar Cells*, 93(8), pp.1345–1350.

Drake, J.M. et al., 1982. Organic dyes in PMMA in a planar luminescent solar collector: a performance evaluation. *Applied Optics*, 21(16), pp.2945–2952.

Du, H. et al., 2002. Optical Properties of Colloidal PbSe Nanocrystals. *Nano Letters*, 2(11), pp.1321–1324.

Earp, A.A. et al., 2004. Maximising the light output of a Luminescent Solar Concentrator. *Solar Energy*, 76(6), pp.655–667.

Field, H., 1997. Solar cell spectral response measurement errors related to spectral band width and chopped light waveform. In *, Conference Record of the Twenty-Sixth IEEE Photovoltaic Specialists Conference, 1997*. , Conference Record of the Twenty-Sixth IEEE Photovoltaic Specialists Conference, 1997. pp. 471–474.

Filatov, Y. et al., 2003. Spectral Properties of the Dye Activated Polymers with Added Fine Scattering Particles. *Solid State Phenomena*, 94, pp.299–304.

Fink, J.K., 2005. Unsaturated Polyester Resins. In *Reactive Polymers Fundamentals and Applications*. Norwich, NY: William Andrew Publishing, pp. 1–67.

Friedman, P.S., 1981. Luminescent Solar Concentrators. *Optical Engineering*, 20(6), pp.206887–206887.

Gallagher, S.J. et al., 2007. Quantum dot solar concentrator: Device optimisation using spectroscopic techniques. *Solar Energy*, 81(4), pp.540–547.

Goetzberger, A., 1978. Fluorescent solar energy collectors: Operating conditions with diffuse light. *Applied physics*, 16(4), pp.399–404.

Goetzberger, A. & Greube, W., 1977. Solar energy conversion with fluorescent collectors. *Applied physics*, 14(2), pp.123–139.

Goetzberger, A. & Schirmer, O., 1979. Second stage concentration with tapers for fluorescent solar collectors. *Applied physics*, 19(1), pp.53–58.

Grabchev, I. et al., 2000. Synthesis and properties of fluorescent 1,8-naphthalimide dyes for application in liquid crystal displays. *Journal of Materials Chemistry*, 10(6), pp.1291–1296.

Grabchev, I., Bojinov, V. & Petkov, C., 2001. Synthesis and photophysical properties of polymerizable 1,8-naphthalimide dyes and their copolymers with styrene. *Dyes and Pigments*, 51(1), pp.1–8.

Green, M.A. et al., 2012. Solar cell efficiency tables (version 39). *Progress in Photovoltaics: Research and Applications*, 20(1), pp.12–20.

Griffini, G. et al., 2013. Photo-degradation of a perylene-based organic luminescent solar concentrator: Molecular aspects and device implications. *Solar Energy Materials and Solar Cells*, 111, pp.41–48.

Gustafsson, G. et al., 1992. Flexible light-emitting diodes made from soluble conducting polymers. *Nature*, 357(6378), pp.477–479.

Haq, M.I.U., 2007. Applications of unsaturated polyester resins. *Russian Journal of Applied Chemistry*, 80(7), pp.1256–1269.

Hermann, A.M., 1982. Luminescent solar concentrators—A review. *Solar Energy*, 29(4), pp.323–329.

Hwang, D.-H. et al., 2003. Syntheses and light-emitting properties of poly(9,9-di-n-octylfluorenyl-2,7-vinylene) and PPV copolymers. *Journal of Materials Chemistry*, 13(7), pp.1540–1545.

Hyldahl, M.G., Bailey, S.T. & Wittmershaus, B.P., 2009. Photo-stability and performance of CdSe/ZnS quantum dots in luminescent solar concentrators. *Solar Energy*, 83(4), pp.566–573.

Jeżowska-Trzebiatowska, B. et al., 1986. Neodymium-chromium doped phosphate glasses as luminescent solar concentrators. *Solar energy materials*, 13(4), pp.267–277.

Jin, S.-H. et al., 2003. Synthesis and Electroluminescence Properties of Poly(9,9-di-n-octylfluorenyl-2,7-vinylene) Derivatives for Light-Emitting Display†. *Macromolecules*, 36(11), pp.3841–3847.

Jiu, H. et al., 2006. Fluorescence enhancement of europium complex co-doped with terbium complex in a poly (methyl methacrylate) matrix. *Journal of non-crystalline solids*, 352(3), pp.197–202.

Kastelijn, M.J., Bastiaansen, C.W.M. & Debije, M.G., 2009. Influence of waveguide material on light emission in luminescent solar concentrators. *Optical Materials*, 31(11), pp.1720–1722.

Kennedy, M. et al., 2009. Improving the optical efficiency and concentration of a single-plate quantum dot solar concentrator using near infra-red emitting quantum dots. *Solar Energy*, 83(7), pp.978–981.

Kinderman, R. et al., 2007. IV performance and stability study of dyes for luminescent plate concentrators. *Journal of solar energy engineering*, 129(3), pp.277–282.

Konstantinova, T.N., Meallier, P. & Grabchev, I., 1993. The synthesis of some 1,8-naphthalic anhydride derivatives as dyes for polymeric materials. *Dyes and Pigments*, 22(3), pp.191–198.

Kontopoulou, M. & Vlachopoulos, J., 1999. Bubble dissolution in molten polymers and its role in rotational molding. *Polymer Engineering & Science*, 39(7), pp.1189–1198.

Kurian, A. et al., 2002. Studies on fluorescence efficiency and photodegradation of rhodamine 6G doped PMMA using a dual beam thermal lens technique. *Laser Chemistry*, 20(2-4), pp.99–110.

Latorre, R.M. et al., 2002. Epoxy impregnation without hardener: to decrease yellowing, to delay casting, and to aid bubble removal. *Journal of the International Society for Plastination*, 17, pp.17–22.

Lim, Y.S., Lo, C.K. & Teh, G.B., 2012. Unsaturated polyester resin blended with MMA as potential host matrix for luminescent solar concentrator. *Renewable Energy*, 45(0), pp.156–162.

Machida, K. et al., 2000. Preparation and application of lanthanide complex incorporated ormosil composite phosphor films. *Journal of Luminescence*, 87, pp.1257–1259.

Mansour, A.F. et al., 2005. Laser dyes doped with poly(ST-Co-MMA) as fluorescent solar collectors and their field performance. *Polymer Testing*, 24(4), pp.519–525.

Meredith, D., 1983. The Luminescent Solar Concentrator: An Illuminating Solution for Solar Energy. *Engineering and Science*, 46(3), pp.10–12.

Mićić, O.I. et al., 1997. Size-Dependent Spectroscopy of InP Quantum Dots. *The Journal of Physical Chemistry B*, 101(25), pp.4904–4912.

Morgado, J. et al., 1998. 4-AcNI—a new polymer for light-emitting diodes. *Synthetic Metals*, 95(2), pp.113–117.

Panah, H.S. et al., 2010. Synthesis and characterization of new fluorescent polymerizable dyes based on naphthalimide. *Iranian Polymer Journal*, 19(7), pp.491–500.

Pavia, D., Lampman, G. & Kriz, G., 2000. *Introduction to Spectroscopy* 3rd ed., Brooks/Cole Pub Co.

Peeters, S., UGent. Faculteit Ingenieurswetenschappen en Architectuur (TW) & Neyts, K., 2011. *Reabsorption losses in Luminescent Solar Concentrators*. s.n.

Peng, X. et al., 1997. Epitaxial growth of highly luminescent CdSe/CdS core/shell nanocrystals with photostability and electronic accessibility. *Journal of the American Chemical Society*, 119(30), pp.7019–7029.

Rainhart, L.G. & Schimmel Jr., W.P., 1975. Effect of outdoor aging on acrylic sheet. *Solar Energy*, 17(4), pp.259–264.

Rau, U., Einsele, F. & Glaeser, G.C., 2005. Efficiency limits of photovoltaic fluorescent collectors. *Applied Physics Letters*, 87(17), pp.171101–171101–3.

Reda, S.M., 2008. Synthesis and optical properties of CdS quantum dots embedded in silica matrix thin films and their applications as luminescent solar concentrators. *Acta Materialia*, 56(2), pp.259–264.

Reisfeld, R. & Kalisky, Y., 1981. Nd3+ and Yb3+ germanate and tellurite glasses for fluorescent solar energy collectors. *Chemical Physics Letters*, 80(1), pp.178–183.

Richards, B.S. & McIntosh, K.R., 2006. Ray-tracing simulations of luminescent solar concentrators containing multiple luminescent species. In *Proceedings of the 21st European Photovoltaic Solar Energy Conference*. pp. 185–188.

Rowan, B. et al., 2007. Quantum dot solar concentrators: an investigation of various geometries. , p.66490A–66490A.

Rowan, B.C., Wilson, L.R. & Richards, B.S., 2008. Advanced Material Concepts for Luminescent Solar Concentrators. *IEEE Journal of Selected Topics in Quantum Electronics*, 14(5), pp.1312–1322.

Sadek, E.M. et al., 2011. POLY (METHYL METHACRYLATE)/CARBON NANOPARTICLES CAST COMPOSITES. *Journal of Applied Sciences Research*, 7(4).

Sah, R.E., Baur, G. & Kelker, H., 1980. Influence of the solvent matrix on the overlapping of the absorption and emission bands of solute fluorescent dyes. *Applied physics*, 23(4), pp.369–372.

Samini, B. et al., 2009. Nanophotonics for Applications in Solar Cell Concentrators.

Sanguineti, A. et al., 2013. High Stokes shift perylene dyes for luminescent solar concentrators. *Chemical Communications*, 49(16), pp.1618–1620.

Sark, W.G.J.H.M. van et al., 2008. Luminescent Solar Concentrators - A review of recent results. *Optics Express*, 16(26), pp.21773–21792.

Scheibe, G., 1937. Über die Veränderlichkeit der Absorptionsspektren in Lösungen und die Nebenvalenzen als ihre Ursache. *Angewandte Chemie*, 50(11), pp.212–219.

Seybold, G. & Wagenblast, G., 1989. New perylene and violanthrone dyestuffs for fluorescent collectors. *Dyes and Pigments*, 11(4), pp.303–317.

Sholin, V., Olson, J.D. & Carter, S.A., 2007. Semiconducting polymers and quantum dots in luminescent solar concentrators for solar energy harvesting. *Journal of Applied Physics*, 101(12), p.123114.

Slooff, L.H. et al., 2008. A luminescent solar concentrator with 7.1% power conversion efficiency. *physica status solidi (RRL) – Rapid Research Letters*, 2(6), pp.257–259.

Soti, R. et al., 1996. Photon transport in luminescent solar concentrators. *Journal of luminescence*, 68(2), pp.105–114.

Teh, G.B. et al., 2009. Efficacy of utilization of microemulsion technique to produce photoluminescent nanoparticles. In Young Scientists of Asia Conclave 2009. Bangalore, TWAS –ROCASA, India.

Tian, H., He, Y. & Chang, C.P., 2000. Synthesis and spectral properties of novel laser copolymers based on modified rhodamine 6G and 1, 8-naphthalimide. *J. Mater. Chem.*, 10(9), pp.2049–2055.

Weber, W.H. & Lambe, J., 1976. Luminescent greenhouse collector for solar radiation. *Applied Optics*, 15(10), p.2299.

Werts, M.H.V. et al., 1997. Fluorescein and eosin as sensitizing chromophores in near-infrared luminescent ytterbium (III), neodymium (III) and erbium (III) chelates. *Chemical physics letters*, 276(3), pp.196–201.

Wilson, L.R., 2010. *Luminescent solar concentrators : a study of optical properties, re-absorption and device optimisation*. Thesis. Heriot-Watt University.

Wolarz, E., Moryson, H. & Bauman, D., 1992. Dichroic fluorescent dyes for "guest-host" liquid crystal displays. *Displays*, 13(4), pp.171–178.

Wu, W. et al., 2010. Hybrid solar concentrator with zero self-absorption loss. *Solar Energy*, 84(12), pp.2140–2145.

Wu, X. et al., 2004. High-quality poly[2-methoxy-5-(2′-ethylhexyloxy)-p-phenylenevinylene] synthesized by a solid–liquid two-phase reaction: Characterizations and electroluminescence properties. *Journal of Polymer Science Part A: Polymer Chemistry*, 42(12), pp.3049–3054.

Würthner, F., Kaiser, T.E. & Saha-Möller, C.R., 2011. J-Aggregates: From Serendipitous Discovery to Supramolecular Engineering of Functional Dye Materials. *Angewandte Chemie International Edition*, 50(15), pp.3376–3410.

Zheng, M., Bai, F. & Zhu, D., 1999. Photoluminescence of poly(1,4-phenylenevinylene) derivatives in solution and film. *Polymers for Advanced Technologies*, 10(7), pp.476–480.

Zhu, W. et al., 1998. Luminescent properties of copolymeric dyad compounds containing 1,8-naphthalimide and 1,3,4-oxadiazole. *Synthetic Metals*, 96(2), pp.151–154.

APPENDIX A

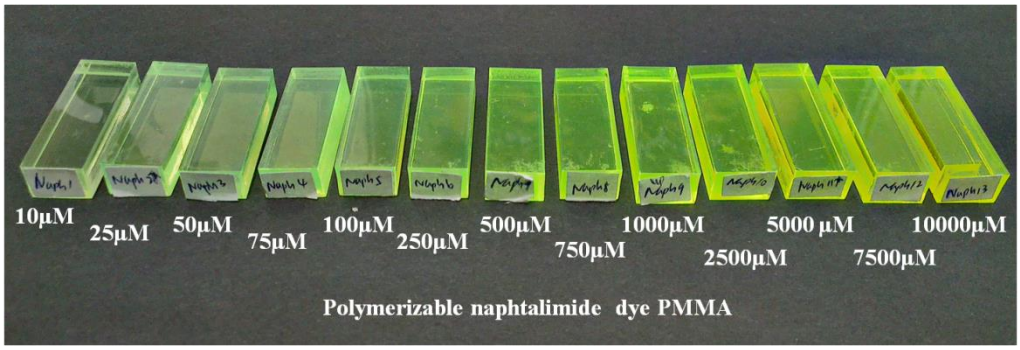

PMMA LSC with polymerizable naphthalimide dye

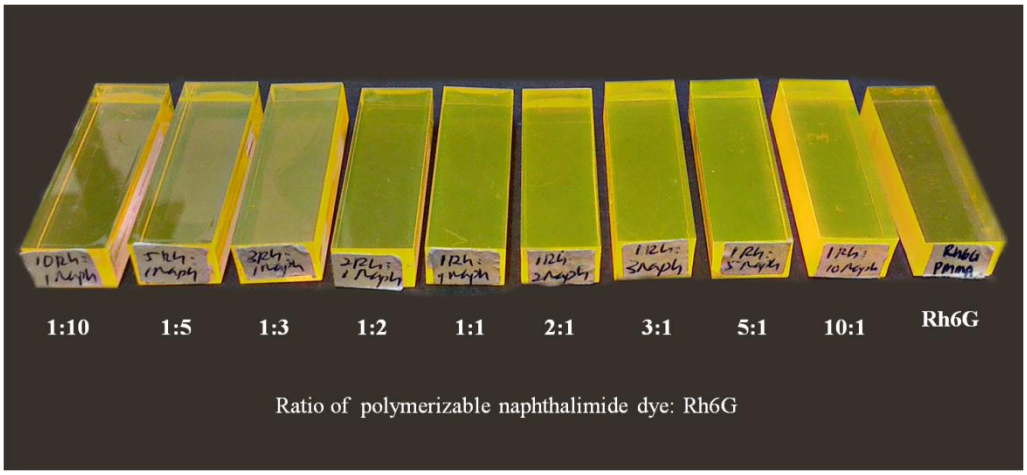

Multiple-dye PMMA LSC with polymerizable naphthalimide dye and Rhodamine 6G in different ratio

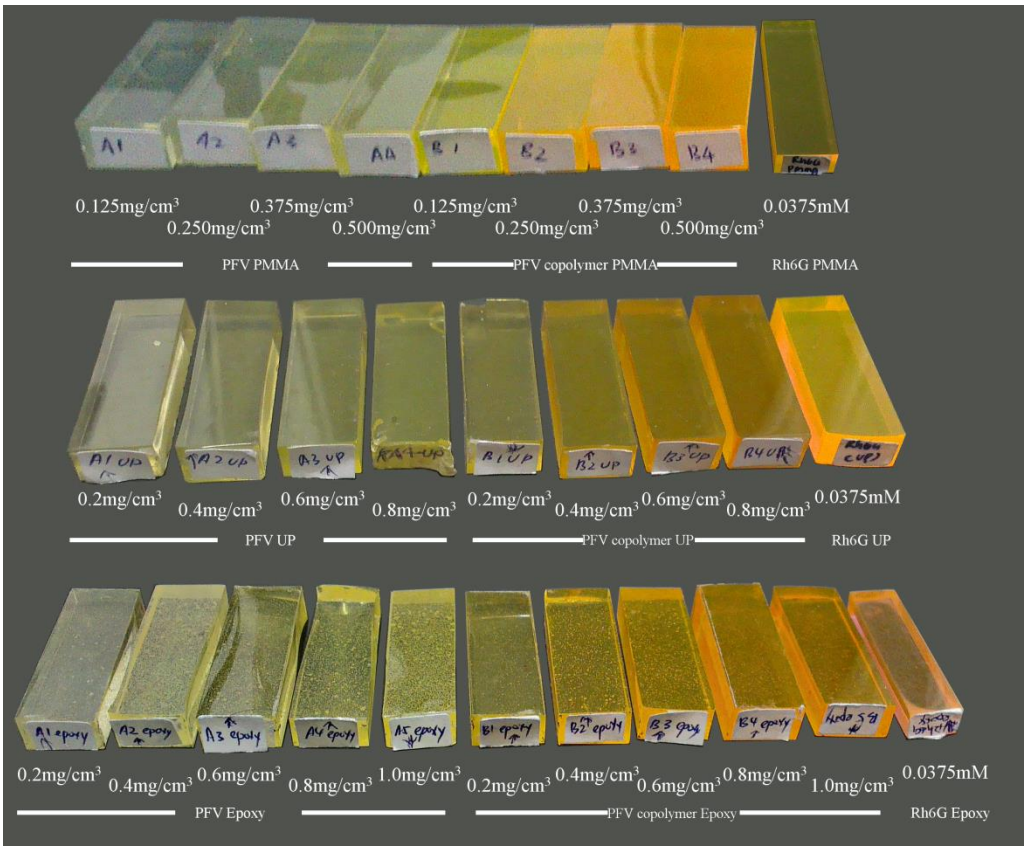

PFV, PFV copolymer and Rh6G dye in three polymer matrices: PMMA, unsaturated polyester and epoxy

APPENDIX B

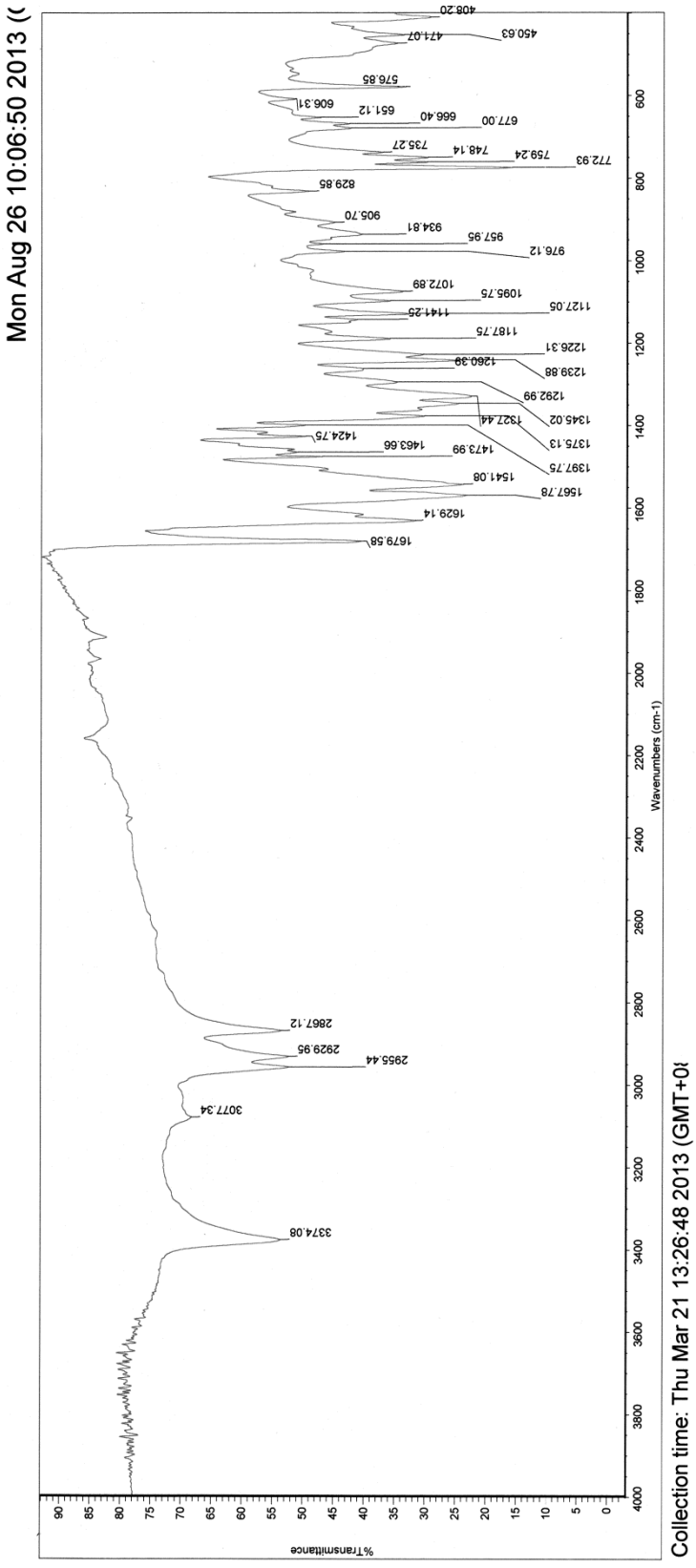
Mon Aug 26 10:06:50 2013 (
Collection time: Thu Mar 21 13:26:48 2013 (GMT+0
%Transmittance
Wavenumbers (cm-1)
3374.08
3077.34
2955.44
2929.95
2867.12
1679.58
1629.14
1567.78
1541.08
1473.99
1463.66
1424.75
1397.75
1375.13
1345.02
1327.44
1292.99
1260.38
1239.88
1226.31
1187.75
1141.25
1127.05
1095.75
1072.89
976.12
957.95
934.81
905.70
829.85
772.93
759.24
748.14
735.27
677.00
666.40
651.12
606.31
576.85
471.07
450.63
408.20

Mon Aug 26 10:06:03 2013 (GMT+08:00)
FIND PEAKS:
Spectrum: Naphthalimide
Region: 4000.00 400.00
Absolute threshold: 70.361
Sensitivity: 55
Peak list:

Position:	408.20	Intensity:	29.323
Position:	450.63	Intensity:	33.665
Position:	471.07	Intensity:	34.787
Position:	576.85	Intensity:	33.386
Position:	606.31	Intensity:	51.487
Position:	651.12	Intensity:	47.272
Position:	666.40	Intensity:	42.612
Position:	677.00	Intensity:	42.410
Position:	735.27	Intensity:	37.149
Position:	748.14	Intensity:	29.725
Position:	759.24	Intensity:	29.811
Position:	772.93	Intensity:	15.901
Position:	829.85	Intensity:	49.270
Position:	905.70	Intensity:	45.077
Position:	934.81	Intensity:	40.665
Position:	957.95	Intensity:	46.935
Position:	976.12	Intensity:	43.541
Position:	1072.89	Intensity:	33.872
Position:	1095.75	Intensity:	35.909
Position:	1127.05	Intensity:	32.729
Position:	1141.25	Intensity:	41.386
Position:	1187.75	Intensity:	35.908
Position:	1226.31	Intensity:	30.505
Position:	1239.88	Intensity:	25.061
Position:	1260.39	Intensity:	40.349
Position:	1292.99	Intensity:	34.800
Position:	1327.44	Intensity:	22.624
Position:	1345.02	Intensity:	24.719
Position:	1375.13	Intensity:	30.265
Position:	1397.75	Intensity:	49.891
Position:	1424.75	Intensity:	49.696
Position:	1463.66	Intensity:	51.140
Position:	1473.99	Intensity:	47.015
Position:	1541.08	Intensity:	23.857
Position:	1567.78	Intensity:	23.526
Position:	1629.14	Intensity:	31.742
Position:	1679.58	Intensity:	40.803
Position:	2867.12	Intensity:	53.706
Position:	2929.95	Intensity:	52.494
Position:	2955.44	Intensity:	52.483
Position:	3077.34	Intensity:	68.341
Position:	3374.08	Intensity:	53.776

APPENDIX C

Qualitative Analysis Report

Data Filename	FES_KEE_19072013_DYE_Direct_Pos2.d	**Sample Name**	Dye
Sample Type	Sample	**Position**	Vial 1
Instrument Name	Instrument 1	**User Name**	
Acq Method	100pg_res_ms(DIRECT RUN).m	**Acquired Time**	7/19/2013 4:43:56 PM
IRM Calibration Status	Success	**DA Method**	TIC.m
Comment			

User Chromatograms

Fragmentor Voltage 100 **Collision Energy** 0 **Ionization Mode** ESI

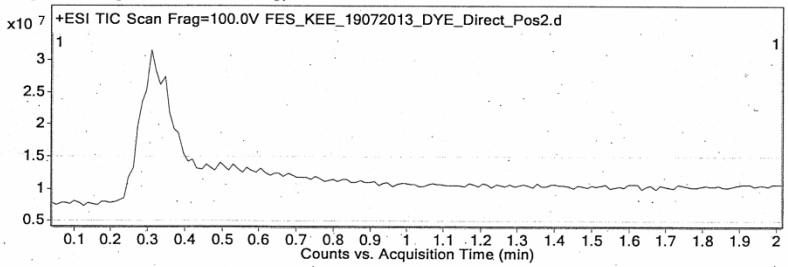

User Spectra

Fragmentor Voltage 100 **Collision Energy** 0 **Ionization Mode** ESI

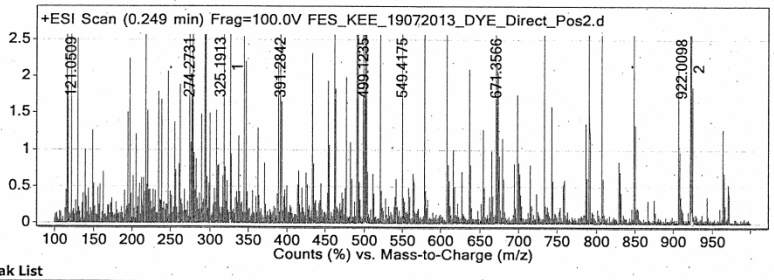

Peak List

m/z	z	Abund
116.1072		54434.4
121.0509		141514.7
274.2731		11926.4
294.2057		30734.7
325.1913	1	207657.8
326.1944	1	40758.2
499.1235		36664.2
501.1204		24790.2
922.0098	1	130484.8
923.0124	1	23173.8

Fragmentor Voltage 100 **Collision Energy** 0 **Ionization Mode** ESI

Sample Name	Dye	**Position**	Vial 1	**Instrument Name**	Instrument 1	**User Name**	
Inj Vol	-1	**InjPosition**		**SampleType**	Sample	**IRM Calibration Status**	Success
Data Filename	FES_KEE_19072013_DYE	**ACQ Method**	100pg_res_ms(DIRECT	**Comment**		**Acquired Time**	7/19/2013 4:43:56 F

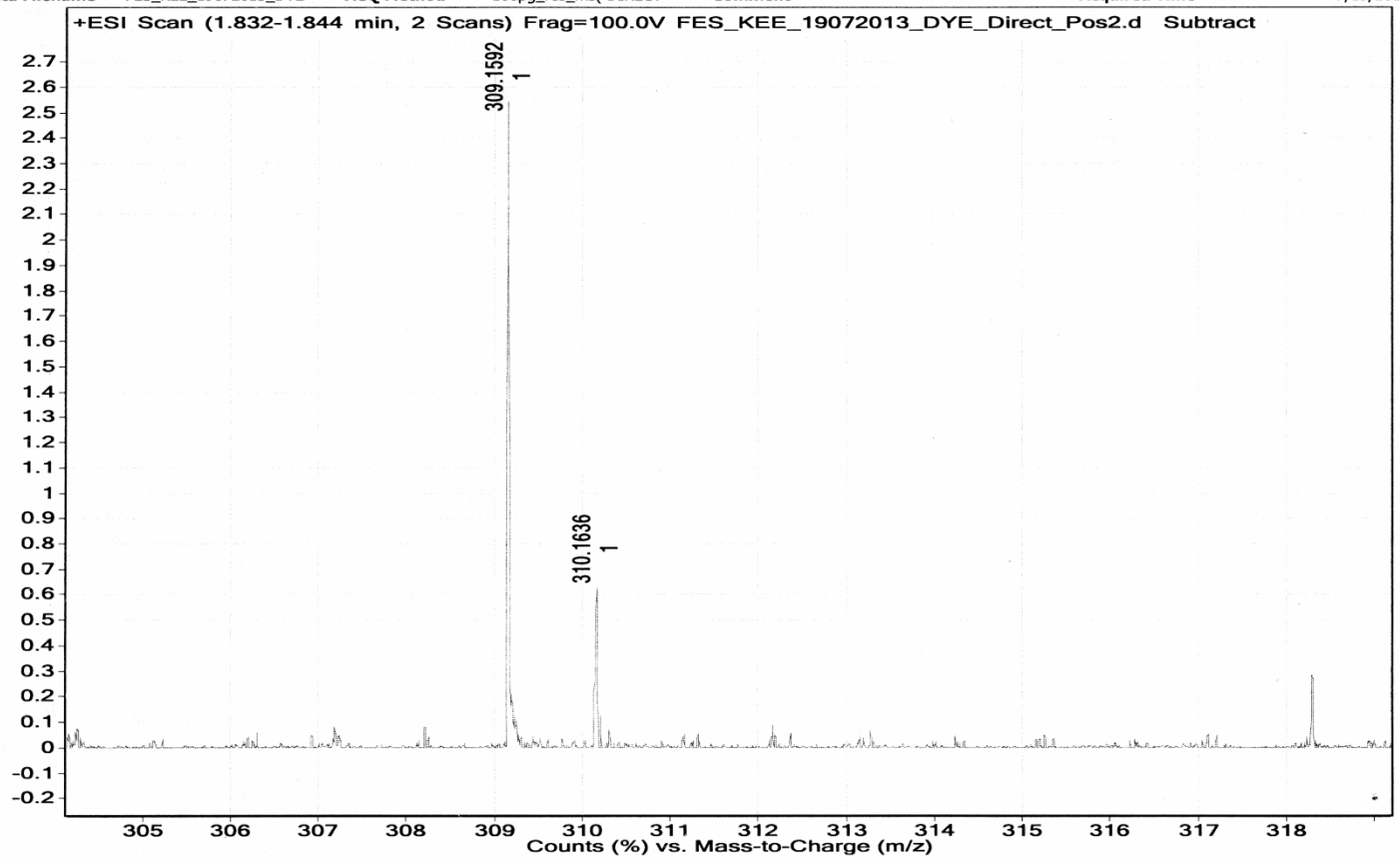

Spectrum Identification Results: + Scan (1.832-1.844 min) Sub (FES_KEE_19072013_DYE_Direct_Pos2.d)

Best	Formula	Score	Mass	Mass (MFG)	Diff (ppm)	Diff (abs. ppm)	Diff (mDa)	ID Source	Score (DB)	Score (MFG)
☑	C19 H20 N2 O2	80.69	308.1519	308.1525	1.86	1.86	0.57	MFG		80.69

Specie	Ion Formula	m/z	Height	Score (MFG)	Score (MFG, MS)	Score (MFG, MS/MS)	Score (MFG, mass)	Score (MFG, abund)	Score (MFG, iso. spacing)
(M	C19 H21 N2 O2	309.1598	5277	80.69	80.69		97.67	85.05	41.52

m/z	m/z (Calc)	Diff (ppm)	Diff (mDa)	Height	Height (Calc)	Height %	Height % (Calc)	Height Sum %	Height Sum% (Calc)
	309.1598	1.91	0.6	5380	5498.7	100	100	80.5	82.2
	310.1629	-2.2	-0.7	1306.3	1187.6	24.3	21.6	19.5	17.8